

1. LEG 192 SUMMARY¹

Shipboard Scientific Party²

ABSTRACT

With a surface area of 1.6×10^6 km² and a crustal volume of $4\text{--}5 \times 10^7$ km³, the Ontong Java Plateau is the world's largest volcanic oceanic plateau and may represent the largest magmatic event on Earth in the last 200 m.y. During Ocean Drilling Program (ODP) Leg 192 we recovered igneous rock and sediment cores in five widely separated sites in previously unsampled areas across the plateau. Primary objectives of the leg were to determine (1) the age and duration of emplacement of the plateau, (2) the compositional range of magmas, and (3) the environment and style of eruption.

Acoustic basement at the four sites on the main or high plateau consists of pillow and/or massive basalt flows with rare, thin sedimentary interbeds. Biostratigraphic evidence suggests that basement ages at Sites 1183, 1186, and 1187 are Aptian. At Site 1185, two groups of basalt are present; the lower group appears to be Aptian, whereas the age of the upper group is estimated only loosely as latest Cenomanian to Albian. These preliminary results, together with data from Deep Sea Drilling Project (DSDP) Site 289 and ODP Site 807, suggest that the great bulk of the high plateau formed in a single episode in the early Aptian. More recent volcanic events, including the ~90-Ma event recorded at Site 803 and in the eastern Solomon Islands, appear to have been volumetrically minor on the high plateau and confined mainly to its margins. One of these late-stage events may have been recorded in our fifth site, Site 1184, on the plateau's eastern lobe or salient, where we cored 338 m of a basaltic volcanoclastic sequence that yielded a rare and poorly preserved middle Eocene nannofossil assemblage. However, such a young age is difficult to reconcile with the steep paleomagnetic inclination, which implies that the sequence is much older.

The basalts at Sites 1183 and 1186 and those making up the lower group of lava flows at Site 1185 are moderately evolved, low-K tholeiites

¹Examples of how to reference the whole or part of this volume.

²Shipboard Scientific Party addresses.

with closely similar compositions. They belong to the remarkably homogeneous Kwaimbaita magma type found at Site 807 and in the eastern Solomons. Thus, much of the high plateau's upper crust seems to consist of Kwaimbaita-type basalt. The Eocene volcanoclastic rocks of Site 1184 also have a Kwaimbaita-like bulk composition. No flows of Singgalo-type basalt, which overlies Kwaimbaita-type lavas at Site 807 and on the island of Malaita, were encountered. An exciting discovery of Leg 192 was that basement at Site 1187 and the upper group of flows at Site 1185 are composed of a high-MgO (8–10 wt%), incompatible-element-poor (e.g., $\text{TiO}_2 = 0.72\text{--}0.77$ wt%; $\text{Zr} = 36\text{--}43$ ppm) type of basalt not found previously on the plateau. These rocks appear to represent very high total fractions of partial melting of their mantle source, and their presence in >100-m-thick lava piles at two sites 146 km apart suggests that such basalt is voluminous on the eastern edge of the high plateau.

Although the volcanoclastic sequence cored in Hole 1184A was emplaced in a shallow-marine or even subaerial environment, emplacement of lavas at all four high-plateau sites was entirely submarine. The shallowest estimated Aptian water depth for basement is at least 800 m at Site 1183 on the broad dome of the plateau; estimated paleodepths for Sites 1185, 1186, and 1187 are much greater. Together with previous evidence, our results suggest that most of the Ontong Java Plateau formed well below sea level. The only evidence that a small portion of the high plateau was ever at shallow depth is two thin intervals of Aptian vitric tuff above basement in Hole 1183A and possibly a vitric tuff just above basement at DSDP Site 289. The submarine emplacement of most of the plateau probably limited its paleoenvironmental impacts; to date, no major extinction events can be correlated with massive Aptian volcanism on the plateau.

INTRODUCTION

Volcanic oceanic plateaus are formed by immense volumes of magma emplaced in pre-existing oceanic lithosphere or at spreading centers. Nearly all plateaus in the oceans today were formed in the Cretaceous period and may reflect a major mode of mass and energy transfer from the Earth's interior to its surface that was different from the ocean ridge-dominated mode of the Cenozoic (e.g., Stein and Hofmann, 1994; McNutt et al., 1996). Since the mid-1980s, oceanic plateaus have been recognized as the counterparts of continental flood basalt provinces and associated thick volcanic sequences at many passive continental margins, collectively termed large igneous provinces (LIPs) by Coffin and Eldholm (1994). In the last decade, these features have been ascribed by many workers to the initial plume-head stage of hotspot development (e.g., Richards et al., 1991; Saunders et al., 1992). Alternative, nonplume models have been proposed (e.g., Smith, 1993; Anderson, 1996) but have thus far not received widespread support. The plume-head model predicts that LIPs are formed from ocean-island-like mantle in massive eruptive outpourings lasting only a few million years or less (e.g., Campbell, 1998). For many continental LIPs and at least some volcanic passive margins, eruption probably did indeed occur rapidly, but continental lithospheric contamination usually has overprinted the sublithospheric mantle-source signature. Many oceanic LIPs formed in locations remote from any continental lithosphere, but comparable data on eruption ages and source composition are lacking

because very few basement sites have yet been sampled. Because of the thick sediments that blanket oceanic plateaus, drilling is generally the only way to sample basement crust effectively.

The climatic, oceanographic, and associated biospheric effects of plateau emplacement are poorly known but appear to have been very significant in some cases (e.g., Coffin and Eldholm, 1994; Jones et al., 1994; Kerr, 1998; Tarduno et al., 1998; Larson and Erba, 1999). After emplacement, plateaus appear to have important effects on subduction patterns, plate motions, continental growth, and crustal evolution. Large oceanic plateaus, in particular, tend to resist subduction and thus may form an important early stage in the growth of continents (e.g., Kroenke, 1974; Cloos, 1993; Tejada et al., 1996; Albarède, 1998; Polat et al., 1999).

The Ontong Java Plateau in the western Pacific (Figs. F1, F2) is the largest volcanic oceanic plateau in the world, with a crustal volume of $\sim 5 \times 10^7 \text{ km}^3$ (Mahoney, 1987; Coffin and Eldholm, 1993). If the great bulk of this plateau formed in a single, geologically brief magmatic episode, then the rate at which it was emplaced would have rivaled the magma production rate of the entire global mid-ocean-ridge system at the time. The plateau would then represent the largest igneous event of the last 200 m.y. (Tarduno et al., 1991; Mahoney et al., 1993).

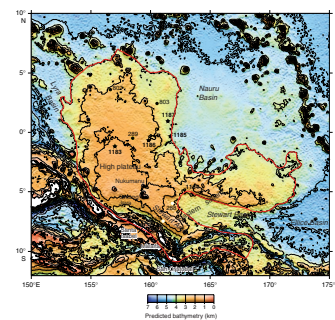
The goal of Leg 192 was to sample the igneous basement of the Ontong Java Plateau at four widely spaced sites, one of which was to be drilled at least 150 m and three at least 100 m into basement. Shipboard and shore-based studies of the rocks recovered would provide insights into the age and duration of magmatism, the compositional range of the mantle sources, and the processes of magmatic evolution. We also hoped to evaluate the environment and style of eruption and the association of plateau emplacement with changes in paleoceanographic and paleoclimatic conditions. During the leg, we drilled five sites and recovered substantial amounts of igneous basement at four.

BACKGROUND

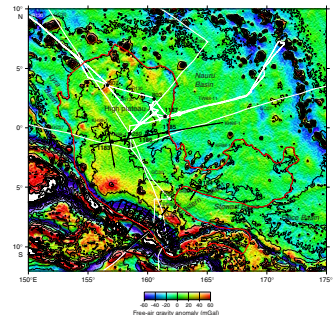
Previous Basement Sampling

Although sampled in only a few locations, the basement of the Ontong Java Plateau was already the best sampled of any Pacific plateau before Leg 192, with drill holes (see Fig. F1) at Deep Sea Drilling Project (DSDP) Site 289 (9 m basaltic basement penetration) and Ocean Drilling Program (ODP) Sites 803 (26 m) and 807 (149 m). In contrast to other Pacific plateaus, slivers of the southern edge of the Ontong Java Plateau are exposed above sea level in the eastern Solomon Islands. The principal outcrops are on the islands of Malaita and Santa Isabel where, respectively, 3.5- and ~2-km-thick basement crustal sections have been sampled recently (Tejada et al., 1996, in press; Parkinson et al., 1996; Petterson et al., 1997; R. Arculus, pers. comm., 2000). On the island of San Cristobal (also called Makira) a thick pile of lava flows also is exposed (e.g., Birkhold-VanDyke et al., 1996), whereas on Ramos, Ulawa, and possibly Choiseul smaller basement sections are present (e.g., Coleman, 1965; Petterson et al., 1999).

F1. Predicted bathymetry of the Ontong Java Plateau, p. 36.



F2. Satellite-derived free-air gravity field of Ontong Java Plateau region, p. 37.



Physical Features and Gross Structure of the Plateau

The Ontong Java Plateau covers an area $>1.6 \times 10^6$ km² (roughly the size of Alaska or six times that of the United Kingdom) and consists of two parts: the main or high plateau in the west and north and the eastern lobe or salient in the east and south (Fig. F1) (Kroenke, 1972). The plateau is bounded by the Lyra Basin to the northwest, the East Mariana Basin to the north, the Nauru Basin to the northeast, and the Ellice Basin to the southeast. Along its southern and southwestern boundaries, the plateau has collided with the Solomon Islands arc and now sits at the junction of the Pacific and Australian plates. The plateau surface rises to depths of ~1700 m below sea level in the central region of the high plateau but elsewhere generally lies at water depths of between 2 and 3 km. Much of the high plateau's surface is relatively smooth, although several large seamounts have been built on it. In many areas, the basement crust is covered with pelagic sediments >1 km thick. The eastern lobe consists of a large but unnamed northern ridge and the Stewart Arch, which are separated by the ~300-km-wide Stewart Basin. At its southeastern end, the Stewart Basin merges with the Ellice Basin (Kroenke and Mahoney, 1996). Physiography around the margins of the plateau is complicated. In the north and northeast, numerous horst-and-graben structures appear to predate much of the sediment cover (e.g., Kroenke, 1972; Berger et al., 1992). Faulting and deformation along the Ontong Java Plateau's southern and southwestern margins are associated with the plateau's collision with the Solomon arc (e.g., Petterson et al., 1997). An extensive fold belt, the Malaita Anticlinorium, embraces the island of Malaita and the northern half of Santa Isabel.

Crustal thickness on much of the high plateau is considerable, even in comparison to other plateaus. Seismic and combined seismic and gravity evidence indicates that crustal thickness is generally in the 25- to 35-km range (e.g., Furumoto et al., 1976; Hussong et al., 1979; Miura et al., 1996; Gladczenko et al., 1997; Richardson et al., 2000). Over much of the high plateau, the depth to the top of Layer 3A (i.e., to the base of the seismically defined upper crust) is 10–16 km (see review of Neal et al., 1997). Lower crustal seismic wave velocities suggest a granulite-grade gabbroic lower crust, whereas sub-Moho *P*-wave velocities of 8.4–8.6 km/s detected in the northwest and southwest portions of the plateau may indicate the presence of eclogite at depth (Saunders et al., 1996; Neal et al., 1997). The maximum extent of Ontong Java-related volcanism may go well beyond the plateau proper, as the Early Cretaceous lava flows filling the Nauru Basin and similar flows in the East Mariana and Pigafetta basins to the north appear likely to be related closely to the plateau (e.g., Castillo et al., 1994; Neal et al., 1997; Gladczenko et al., 1997). Beneath the plateau, Rayleigh wave tomographic data indicate a low-velocity root extending as deep as 300 km (Richardson et al., 2000).

Tectonic Setting and Age of Emplacement

The original plate-tectonic setting of the Ontong Java Plateau is open to some question because well-defined magnetic lineations have not been found on the plateau. However, block-faulting structures along the eastern margin of the high plateau, interpreted as roughly north-northeast-trending fracture zones, led to proposals that the plateau formed at a west-northwest-trending ridge (Hussong et al., 1979) and

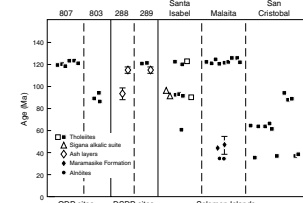
possibly at a triple junction (Winterer, 1976; Hilde et al., 1977). A reconnaissance isotopic study of Ontong Java basement lava flows suggested a hotspot connection and that the plateau may have formed at a ridge-centered or near-ridge hotspot (Mahoney, 1987). Subsequent geochemical work indicated that plateau basement lavas were formed from a hotspot-type mantle source by large percentages of partial melting (estimated at 15%–30%), consistent with the plateau having formed on relatively thin and young lithosphere (Mahoney et al., 1993; Tejada et al., 1996; Neal et al., 1997). From bathymetry and satellite-derived gravity fabric, Winterer and Nakanishi (1995) inferred that a north-northeast-trending spreading axis ran through the plateau, whereas Neal et al. (1997) argued that the north-northeast-trending fabric represents fracture-zone orientation. M-series magnetic lineations adjacent to the plateau in the Nauru and Lyra basins run east-northeast to west-southwest. Coffin and Gahagan (1995) reviewed the available geophysical evidence and concluded that it weakly favors emplacement of most of the plateau in an off-ridge location.

Richards et al. (1991), Tarduno et al. (1991), Mahoney and Spencer (1991), and Phinney et al. (1999) all favored the starting-plume head of the Louisville hotspot (now at ~50°S) as the source of the Ontong Java Plateau. However, 0- to 70-Ma lava flows dredged from sites along the Louisville Ridge, the plume-tail seamount chain formed by the hotspot, are isotopically distinct from Ontong Java basalt (Mahoney et al., 1993). Moreover, a recent plate reconstruction suggests that the plateau formed 8°–15° north of this hotspot's current location (Neal et al., 1997).

As noted above, the plume-head model predicts that plateaus are emplaced in a massive eruptive pulse lasting only a few million years or less. Surprisingly, however, ⁴⁰Ar–³⁹Ar ages of Ontong Java Plateau lava flows in the Solomon Islands and the pre-Leg 192 drill sites revealed a sharply bimodal distribution (Fig. F3), with ages of 122 ± 3 and 90 ± 4 Ma (total ranges). Thus, most of the plateau may have formed in two relatively brief episodes (Mahoney et al., 1993; Tejada et al., 1996, in press; Parkinson et al., 1996). Because sampling over the plateau's huge area was very limited, the relative importance of these two episodes remained unclear. However, Tejada et al. (1996) argued that the 122-Ma event was significantly larger than the 90-Ma event. On the basis of abundant 90-Ma lavas (and some dikes) in Santa Isabel and Cenomanian–Coniacian ash layers at DSDP Site 288, they suggested that the 90-Ma episode may have been focused on the eastern salient; shortly thereafter, 90-Ma basalts were also found to be abundant on San Cristobal (Birkhold-VanDyke et al., 1996). An alternative possibility, however, was that further sampling (and dating) could show that eruptions on the plateau actually occurred over a span of 30 m.y. or more (e.g., Tejada et al., 1996; Birkhold-VanDyke et al., 1996; Ito and Clift, 1998).

Between 124 and 100 Ma, the plateau appears to have been positioned close to the Pacific plate Euler pole, so that it would have moved little relative to the inferred hotspot source (see Neal et al., 1997). At ~100 Ma, plate motion changed from a northwestward to a more northward trajectory, which continued until ~85 Ma. At ~90 Ma the southeastern corner of the plateau may have been situated rather close to the 122-Ma position of the central high plateau. Following the 90-Ma eruptive episode, rifting and seafloor spreading may have occurred for several million years within the plateau's eastern salient, forming the Stewart Basin in conjunction with spreading in the Ellice Basin to the east (Kroenke and Mahoney, 1996; Neal et al., 1997). An ⁴⁰Ar–³⁹Ar age of

F3. Summary of pre-Leg 192 age data for Ontong Java Plateau, p. 38.



83 Ma was determined by Duncan (1985) for an ocean ridge–type basalt from the eastern Ellice Basin.

Relatively localized Tertiary volcanism is recorded in Malaita in the 44-Ma alkalic lavas of the Maramasike Formation (Tejada et al., 1996; Petterson et al., 1997). Malaita is also peppered with small intrusions of 34-Ma alnöites (e.g., Davis, 1977; Nixon and Neal, 1987). In San Cristobal, a sequence of tholeiitic basalts with ages of ~61 and ~36 Ma overlie the ~90-Ma basalt and are compositionally similar to it (Birkhold-VanDyke et al., 1996). The causes of these later magmatic events are uncertain.

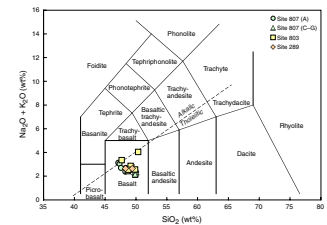
After a long period of northward and northwestward motion, the Ontong Java Plateau collided with the old Solomon arc during the early Neogene (~27 Ma), initially in a diachronous “soft docking” without significant deformation. Following a reversal of subduction direction, the intense deformation of the Malaita Anticlinorium began in the late Miocene (~6 Ma) and intensified in the Pliocene (4–2 Ma) (see Petterson et al., 1997). The bulk of the plateau appears to be more or less unobductible (Cloos, 1993; Abbott and Mooney, 1995), but the post-Miocene underthrusting of a portion of the lower Ontong Java Plateau between Santa Isabel and San Cristobal is evident from recent seismic surveys (Mann et al., 1996; Phinney et al., 1999).

Results from Previous Sampling of Cretaceous Igneous Basement

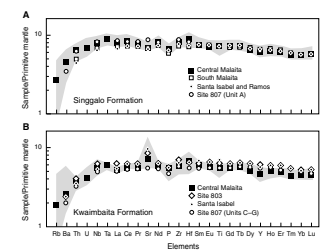
Ontong Java Plateau basement at all previously drilled sites and in the Solomon islands of Malaita, Santa Isabel, Ulawa, Ramos, and San Cristobal consists of pillowed or massive flows of basalt averaging ~10 m in thickness. Dikes are rare in the island exposures, and, hence, the eruptive vents for most of the lava flows may be rather distant. All of the basalt flows appear to have been emplaced well below sea level and are overlain by bathyal or abyssal pelagic marine sediments (see Neal et al., 1997, and references therein). However, all of the locations studied before Leg 192, except Site 289, were at the margins of the plateau; thus it remained possible that the central regions of the high plateau and eastern lobe were formed under shallow-marine or even subaerial conditions. Basement of the 122-Ma age group comprises lava flows from Sites 289 and 807, Malaita, Ramos, and part of Santa Isabel, whereas the 90-Ma flows are found at Site 803, in Santa Isabel, and in San Cristobal (Fig. F3) (Mahoney et al., 1993; Tejada et al., 1996, in press; Parkinson et al., 1996; Birkhold-VanDyke et al., 1996). Also, volcanic ash layers of late Cenomanian to Coniacian age (i.e., in roughly the ~95- to 87-Ma range) are present at DSDP Site 288 (which did not reach basement) on the southern edge of the high plateau (Andrews, Packham, et al., 1975). A glass-shard-rich interval in Aptian limestone at Site 288 and several late Aptian ash layers above basement at Site 289 (Andrews, Packham, et al., 1975) may indicate fairly prolonged shallow or subaerial volcanism in some areas on the crest of the plateau following eruptions at 122 Ma (early Aptian).

Lava flows drilled at all pre-Leg 192 sites are composed of unmetamorphosed, moderately evolved, low-K tholeiite (Fig. F4). They have relatively flat primitive-mantle-normalized incompatible-element patterns (intermediate between those of normal ocean-ridge basalt and most oceanic island or continental tholeiites) (Fig. F5) and a narrow range of ocean-island-like Nd-Sr-Pb isotopic ratios (Fig. F6). Major and trace element modeling indicates that the basalts represent high-degree partial melts (Mahoney et al., 1993; Tejada et al., 1996; Neal et al.,

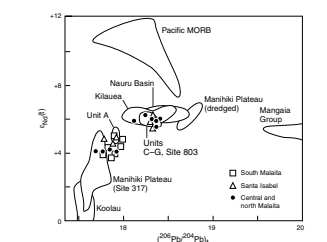
F4. Total alkalis vs. silica diagram for Ontong Java Plateau sites, p. 39.



F5. Primitive mantle-normalized incompatible-element averages for basalts, p. 40.



F6. Initial $\epsilon_{Nd}(t)$ vs. $(^{206}Pb/^{204}Pb)_t$ data, p. 41.



1997). Two geochemically and stratigraphically distinct groups of 122-Ma lava flows are apparent in the thick basement section on Malaita (Tejada et al., 1996, in press) and in the much thinner one at Site 807 (Mahoney et al., 1993). Lava flows forming the upper 46 m of the basement section (Unit A) at Site 807 are isotopically and chemically closely similar to those of the Singgalo Formation, which comprises the upper 750 m of flows in central Malaita (Tejada et al., in press). Similar lavas are also present in Santa Isabel and southern Malaita. The lower basalt units at Site 807 (Units C–G) and the single flow encountered at Site 289 resemble the flows forming the lower 2.7 km of the volcanic pile on Malaita, termed the Kwaimbaita Formation, with which they tentatively have been correlated. The 90-Ma lava flows of Site 803, Santa Isabel, and most of those of San Cristobal are isotopically similar to the 122-Ma Kwaimbaita Formation basalt. Thus, an isotopically ocean-island-type mantle source containing (at least) two distinct components was involved in the generation of crust at the northern and southern margins of the plateau at 122 Ma. Furthermore, the mantle source of most 90-Ma lava flows was similar to that of the Kwaimbaita Formation, the stratigraphically lower of the two 122-Ma basalt groups.

SCIENTIFIC OBJECTIVES

Age and Duration of Emplacement

Hypotheses that involve mantle plumes in the formation of large igneous provinces include rapid-eruption, age-progressive, and episodic growth models.

1. Rapid-emplacment models are of two main types. The plume-head or plume-impact model (e.g., Richards et al., 1991; Saunders et al., 1992; Campbell, 1998) predicts that large oceanic plateaus are formed by widespread basaltic flood eruptions as the inflated head of a rising new mantle plume approaches the base of the lithosphere. An alternative model devised specifically for continental and continental-margin flood basalt provinces (White and McKenzie, 1989), sometimes called the plume-incubation model (e.g., Saunders et al., 1992), considers flood volcanism to result from cataclysmic pressure-release melting when a rift propagates above the enlarged top of a more or less steady-state mantle plume that has accumulated gradually (perhaps over several tens of millions of years) beneath thick, slow-moving continental lithosphere. Both types of model predict that the great bulk of magmatism occurs in only a few (probably <5) million years.
2. In contrast, an age-progressive, Icelandic style of construction in which oceanic plateaus are formed over much longer intervals (tens of millions of years) remains a distinct possibility for many plateaus (e.g., Mahoney and Spencer, 1991; Coffin and Gahagan, 1995; Ito and Clift, 1998).
3. Alternatively, plateau growth may occur in two or more discrete pulses of activity, dependent on mantle plume dynamics or the interplay between episodes of lithospheric extension and mantle melting (Bercovici and Mahoney, 1994; Larson and Kincaid, 1996; Neal et al., 2000; Ito and Taira, 2000).

As the world's largest oceanic plateau, the Ontong Java Plateau provides an important test case. Its great crustal volume implies partial melting of at least $1.5\text{--}4.0 \times 10^8 \text{ km}^3$ of mantle, which virtually necessitates involvement of the lower mantle if the bulk of the plateau was formed in the 122-Ma event (e.g., Coffin and Eldholm, 1994). Melting on such a scale is not happening in the Earth's mantle today, and this consideration has helped fuel suggestions of fundamental differences between Cretaceous and Cenozoic mantle convection. However, if the plateau accreted more slowly over several tens of millions of years (like the much smaller Iceland Plateau) or in two or more discrete pulses, then this partial melting requirement is eased considerably, but simple plume-head models either would need to be modified significantly or would not apply. The few basement locations sampled before Leg 192 demonstrated that both 122- and 90-Ma lava flows are present in widely separated areas, but the importance of the 90-Ma episode remained unclear. In many places, 90-Ma lava flows may simply form a relatively thin carapace over a thick 122-Ma volcanic pile.

Range and Diversity of Magmatism

Laboratory and numerical modeling suggests that starting-plume heads should be strongly zoned because of entrainment of large amounts of ambient, nonplume mantle during their rise to the base of the lithosphere (e.g., Campbell, 1998). Thus, even if a plume's source region (usually assumed to be at the base of, or deep within, the mantle) is compositionally homogeneous, significant isotopic and trace element variability is nevertheless predicted in magmas erupted from different parts of the plume head or at different times. Major element compositions are predicted to vary as well, with magmas erupted above the hottest (axial) parts of the plume head having picritic (e.g., Campbell, 1998) or possibly even komatiitic (Storey et al., 1991) affinities, and more ordinary basaltic magma predicted above cooler, more distal regions. In this regard, the two most remarkable features of the Ontong Java Plateau basement samples available before Leg 192 were (1) the limited overall range of chemical and isotopic variation in the 122-Ma lava flows and (2) that the 90- and 122-Ma flows are so chemically and isotopically similar to each other. The isotopic and incompatible element results could indicate that the world's largest plateau had a much more homogeneous source (both relative to the scale of melting and in time) than predicted by plume-head models. Furthermore, the combined major and trace element data imply that storage and homogenization in large reservoirs was a dominant process in the evolution of the magmas.

Eruptive Environment and Style

Plume-head models predict as much as 1–3 km of dynamic uplift associated with the arrival of a large starting-plume head at the base of the lithosphere (e.g., Hill, 1991; Neal et al., 1997). The associated constructional volcanism also creates a much thicker crust than normal oceanic crust. The combination of these effects is predicted to elevate parts of a plateau's surface to shallow water depths or even cause portions to emerge above sea level. Indeed, significant portions of several plateaus are known to have been initially shallow or subaerial (e.g., Richards et al., 1991; Coffin, Frey, Wallace, et al., 2000). However, although most of the Ontong Java Plateau stands 2–3 km above the sur-

rounding seafloor today, basement lava flows from all locations studied before Leg 192 were emplaced beneath fairly deep water, probably below the calcite compensation depth (CCD) in some cases (Neal et al., 1997; Ito and Clift, 1998; Michael, 1999). The reasons for this behavior and whether it is typical of the plateau as a whole were unknown, but critical for understanding how plateaus are constructed and for testing the plume-head model. Moreover, whether or not parts of the Ontong Java Plateau were shallow at the time of volcanism has important implications for how its emplacement affected large-scale climatic, oceanographic, and biospheric conditions. If significant amounts of magma were erupted in shallow water or subaerially, the flux of climate-modifying volatile species (particularly SO₂, Cl, and F) to the atmosphere would have been much greater than if the bulk of plateau volcanism occurred at greater water depths.

The physical volcanology of large-scale submarine lava flows is poorly known, as are the nature and scale of hydrothermal fluid fluxes associated with plateau magmatism. Knowledge of the physical volcanology of lava flows is important for understanding eruption mechanisms and how the volcanic pile accumulated, whereas data on hydrothermal activity are critical for understanding the environmental effects of plateau formation. Flows making up continental flood basalt provinces are typically 10–30 m thick and, in some cases, have been traced for distances of several hundred kilometers (e.g., Hooper, 1997). Areas distant from eruptive sources tend to be made up of simple flows, whereas compound flows are more indicative of relative proximity to eruptive vents. Previous sampling of the Ontong Java Plateau basement revealed that flow thickness varies from <1 m to 60 m, although most of the flows are in the 4- to 12-m range (e.g., Neal et al., 1997). The flows are dominantly simple, consistent with the locations of most pre-Leg 192 basement sites at the margins of the plateau and presumably far from their eruptive vents. Very little interlava ash has been found. With regard to hydrothermal activity, pre-Leg 192 Ontong Java basement sites show almost no evidence of anything but low-temperature seawater-mediated alteration in either the lava flows or overlying sediments (e.g., Babbs, 1997). This lack of higher-temperature hydrothermal alteration again is consistent with the inferred distance from eruptive vent systems. Major hydrothermal systems would be expected to be centered around major eruptive loci, postulated by Tejada et al. (1996) to be the comparatively shallow regions of the high plateau and eastern lobe.

DRILLING STRATEGY

Despite the considerable geodynamic significance of LIPs, relatively little is known about the composition and origin of large oceanic plateaus. The Ontong Java Plateau's enormous size and thick blanket of marine sediments constitute particularly formidable obstacles to representative sampling of basement crust. A widely agreed-upon strategy for plateau basement sampling involves a reconnaissance phase of drilling several holes ~100 m into basement in key areas, followed by a small number of much deeper holes selected on the basis of results from reconnaissance drilling (e.g., Dick et al., 1996). On the two largest plateaus, Ontong Java and Kerguelen–Broken Ridge, the deeper drill holes would consist of one or two holes penetrating ~1 km of basement and one hole with >2 km of basement penetration. Leg 192 was designed to

complete the reconnaissance phase of Ontong Java drilling that began with Sites 289, 803, and 807 and was complemented by recent field-based work in the Solomon Islands. We selected four sites that would cover as much as possible (in a 2-month cruise) of the history of major, but previously unsampled, parts of the plateau. Because basement penetration was the main objective, we planned to drill through (i.e., not core) the upper parts of the sedimentary section at all sites.

Site 1183 lies near the crest of the high plateau; Site 1184 is on the northern ridge of the eastern salient; and Site 1185 sits at the edge of the eastern flank of the high plateau, near where it adjoins the Nauru Basin (see Fig. F1). The fourth site (proposed Site OJ-7) was an eastern-salient site located atop the Stewart Arch to the north-northeast of Malaita, in waters claimed by the Solomon Islands. However, ODP was unable to obtain approval for drilling this site before or during the cruise. At sea, guided by our results from Sites 1183 and 1185, we chose an alternative site, Site 1186. This site is roughly midway between Sites 1183 and 1185, thereby forming a four-site basement transect (including DSDP Site 289) from the crest to the eastern edge of the main plateau. After penetrating 65.4 m of Kwaimbaita-type basalt flows at Site 1186 (i.e., the same magma type we found at Site 1183 and in the lower 92 m of basement at Site 1185; see “Principal Results,” p. 10), we decided that the time remaining in the cruise would best be used by drilling a fifth site rather than attempting to deepen Site 1186. On the basis of our results at Site 1185, in particular, we selected Site 1187, on the eastern edge of the plateau north of Site 1185 and southeast of Site 803. Details of each of the five sites drilled during Leg 192 are given in Table T1.

Objectives at all sites were similar. Igneous basement penetration was the priority in order to address the primary questions of the age of the plateau and the compositional range of the mantle source. We also hoped for good recovery because it would permit assessment of the character and mode of emplacement of basement rocks and allow us to better address the question of whether volcanism was submarine or subaerial. Ideally, we also would obtain some information on how far from their eruptive vents the basement rocks were emplaced. Wireline logging of basement was planned at two sites (one of which was the proposed OJ-7 site) in order to obtain additional information on lava flow morphology and volcanic stratigraphy. We planned to core much of the lower portion of the sedimentary cover at each site because the age of the sedimentary rocks immediately overlying basement, their environment of deposition, and the early crustal subsidence history are all important for understanding the origin and environmental impact of the plateau. Moreover, coring of the lower sedimentary section would allow us to ascertain the ages of some of the sequence boundaries observed in the seismic reflection record.

PRINCIPAL RESULTS

Site 1183

Site 1183 is located near the crest of the main edifice of the Ontong Java Plateau (Figs. F1, F2). We chose this site because it is in the shallowest region of the high plateau, where the seismically defined upper-crustal layer is thickest but the sediment cover is relatively thin (see Neal et al., 1997, and references therein). The original basement depth

T1. Hole summary, p. 74.

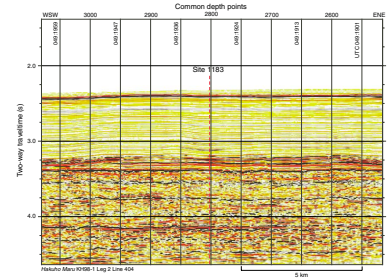
of the high plateau may have been at its shallowest in this region, and eruptive activity may have been at its most vigorous. We thought it possible that the compositional range of basement lava flows in this central area may have been greater than in previously studied areas located much closer to the margins of the plateau (Malaita, Santa Isabel, and ODP Sites 803 and 807). Also, a distinctive sediment package appears above basement on the multichannel seismic reflection line across this area (Fig. F7), and we thought that this package might correspond to much shallower water deposits than those found elsewhere on the high plateau.

The sedimentary succession (cored from 328.0 to 452.7 meters below the seafloor [mbsf] and from 752.0 mbsf to basement at 1130.4 mbsf; Table T1) is dominated by nannofossil foraminifer chalk and limestone. We divided the sequence into three lithologic units and seven subunits (Fig. F8). Unit I consists of ooze and chalk, with the transition between the two (at 337.6 mbsf) defining the boundary between Subunits IA and IB. However, because we did not core the upper part of the succession, only a single core of ooze (Subunit IA) was recovered. *P*-wave velocities in the ooze and chalk sections of Unit I increase downward from a mean of 1700 m/s to a mean of 2240 m/s. Oligocene chalk cored from 752.0 to 838.6 mbsf contains abundant volcanic ash layers and is designated Subunit IC.

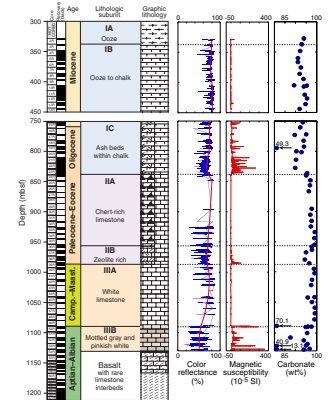
Unit II is Paleocene to middle Eocene limestone. Conspicuous bands of chert between 838.6 and 958.3 mbsf characterize Subunit IIA, and the presence of zeolite-rich bands (probably altered ash layers) and less pronounced chert bands below 958.3 mbsf define Subunit IIB. The base of Unit II is placed at the lowest significant zeolite-rich horizon (986.6 mbsf), which coincides approximately with the base of the Cenozoic. Bulk density increases sharply in the lowest part of Subunit IIB, and both the water content and porosity decrease. A marked *P*-wave velocity increase occurs at the boundary between the chert-rich limestone of Subunit IIA (generally <2500 m/s) and the zeolite-rich limestone of Subunit IIB (generally >3000 m/s); the highest velocities of 3500–4400 m/s are at the bottom of the unit. Cretaceous limestone Unit III is subdivided on the basis of color, with the change from a white Subunit IIIA to a mottled gray and pinkish white Subunit IIIB at 1088.8 mbsf, corresponding approximately to a hiatus and condensation of the Cenomanian through upper Coniacian portion of the sequence. Subunit IIIB, directly above basement, contains microfossils (*Eporolithis floralis* and *Leupoldina cabri*) restricted to a short interval straddling the boundary between the early and late Aptian.

The lowest 2 m of Subunit IIIB contains two intervals of vitric tuff, the lowermost of which is separated from the underlying basalts by a 25-cm-thick limestone bed. The main component of the tuff intervals is basaltic ash consisting of partly glassy to tachylitic fragments with abundant plagioclase microlites. Texturally, many of the fragments are similar to aphanitic pillow margins in the underlying basalts. Most fragments are nonvesicular, but some have vesicles or scalloped margins. Altered brown glass shards are also present; most are blocky and nonvesicular, but some are moderately vesicular. The tuff is composed of at least eight normally graded beds, several of which have scoured bases. The uppermost layer grades up through parallel-laminated to cross-laminated beds, indicating deposition by turbidity currents or reworking by currents. The minor, moderately vesicular basaltic glass shards in these tuff beds indicate formation by relatively shallow submarine eruptions, whereas the partly glassy basaltic ash that constitutes the

F7. MCS reflection profile across Site 1183, p. 42.



F8. Site 1183 log, p. 43.



dominant component could have been derived from shallow-water to subaerial hydroclastic eruptions or by erosion of a volcanic edifice somewhere in this summit region of the main Ontong Java Plateau. These beds, and possibly a vitric tuff of similar age just above basement basalt at DSDP Site 289 (Andrews, Packham, et al., 1975) are the only evidence to date for any shallow-water or subaerial emplacement on the entire high plateau.

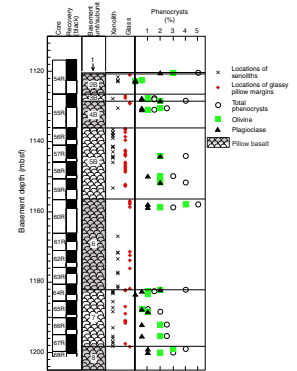
We cored 80.7 m of basaltic basement, from 1130.4 to 1211.1 mbsf, recovering a total of 44.2 m (Table T1) at a low average penetration rate of 1.2 m/hr. We divided the basalt into eight units (Fig. F9), ranging in thickness from 0.36 to 25.70 m, on the basis of the presence of thin interbeds of recrystallized limestone and/or hyaloclastite. Microfossils in the interbeds indicate an age no older than early Aptian. All eight units contain pillow basalt, defined by quenched glassy rims, grain-size variations from aphanitic near pillow margins to fine grained in the interiors, and vesicle patterns. Some of the glassy rims appear to be unaltered even though they are laced with calcite veins. The glass is preserved best in Units 4–7. Except near pillow margins, where small (1–2 mm), elongate vesicles are present, the basalt is essentially nonvesicular, implying a paleodepth >800 m (Moore and Schilling, 1973). Most of it is sparsely olivine ± plagioclase phyric, with a quenched to subophitic groundmass consisting of plagioclase, clinopyroxene, titanomagnetite, glassy mesostasis, and a trace of sulfide. The abundance of olivine phenocrysts increases slightly with depth in the succession, reaching a maximum of ~4%.

Shipboard major and trace element analyses show that the basalt flows at Site 1183 are tholeiitic and very similar in composition to those forming the >2.7-km-thick Kwaimbaita Formation on Malaita, nearly 1000 km to the south (Figs. F10, F11, F12, F13). Kwaimbaita-type basalt also has been sampled 533 km to the north of Site 1183 at Site 807 (Units C–G), in the single flow penetrated at Site 289, 183 km to the northeast, and at Sites 1185 and 1186 (see “Site 1185,” p. 17, and “Site 1186,” p. 21). The upper group of basalt flows in Malaita, the ~750-m-thick Singgalo Formation, is compositionally distinct from the Kwaimbaita Formation (Figs. F11, F12, F13); Singgalo-type basalt also is found in Santa Isabel and forms the upper 46 m of flows (Unit A) at Site 807. Its complete absence from Sites 289 and 1183 suggests that basalt of this composition may not be present on the broad crest of the plateau.

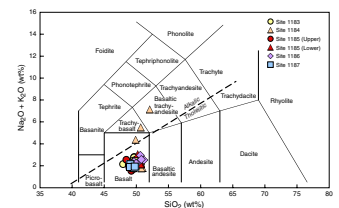
Cumulate gabbroic xenoliths and plagioclase megacrysts are present in Units 2–7 at Site 1183 (Fig. F14). They are round to subround and ≤3 cm in diameter. Clinopyroxene in the xenoliths is partially to totally resorbed, whereas the plagioclase shows only minimal signs of reaction with its basaltic host. Interestingly, similar xenoliths and megacrysts have been found in lava flows of the Kwaimbaita Formation on Malaita (Tejada et al., in press) and in the Units C–G flows at Site 807, as well as at Sites 1185 and 1186.

Pervasive low-temperature interaction of the basaltic basement with seawater-derived fluids under anoxic to suboxic conditions has resulted in alteration ranging from <5% to 20% of the rock. Olivine phenocrysts are completely replaced by smectite (probably saponite with subordinate nontronite and celadonite), Fe oxyhydroxide and, more rarely, calcite. Groundmass glass has been partly to completely replaced by the same secondary minerals, with minor amounts of pyrite. A second stage of alteration is marked by the development of black halos, ranging from 2 to 50 mm in thickness. They are seen in hand specimen along sur-

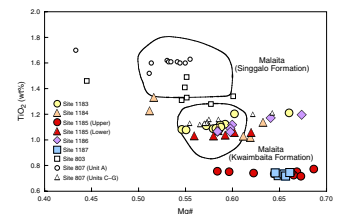
F9. Lithologic log of basement units, Hole 1183A, p. 44.



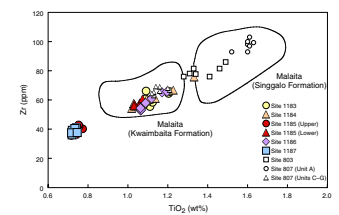
F10. Total alkalis vs. silica diagram for all Leg 192 sites, p. 45.



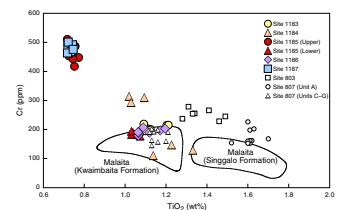
F11. TiO₂ vs. Mg# for basement rocks, p. 46.



F12. Zr vs. TiO₂ for basement rocks, p. 47.



F13. Cr vs. TiO₂ for basement rocks, p. 48.



faces previously exposed to seawater and, less commonly, along the margins of veins and are characteristic of an alteration process initiated during cooling of the lava and completed within 1–2 m.y. (e.g., Honnorez, 1981). Pyrite is associated with the black halos and scattered in the groundmass as far as several centimeters beyond the black alteration front. A third stage of alteration, olive halos containing Fe oxyhydroxide and brown smectite, is common in the upper part of the hole and decreases downhole. This stage of alteration corresponds to halmyrolysis or submarine weathering, which takes place at bottom seawater temperature (i.e., ~2°C) in highly oxidizing conditions and with large water:rock ratio.

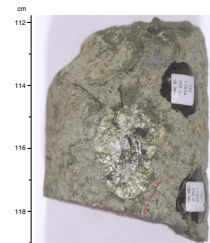
Veins are relatively abundant (~20 veins/m) in the basaltic basement. Most result from symmetrical infilling of open cracks with minor or no replacement of the wall rock, and the vast majority contain the following succession of secondary minerals from vein wall to center: smectite and/or celadonite, Fe oxyhydroxide or pyrite, and calcite. Rare, small grains of native copper are present in veins in the upper part of the basement. Veins in the lower part of the basement sequence contain chalcedony and quartz as the final phases precipitated.

The natural remanent magnetization (NRM) of the Miocene ooze and chalk is weak, only slightly above the noise level of the pass-through magnetometer. The Oligocene to Aptian chalk and limestone, with ash layers rich in magnetic minerals, are more strongly magnetized. The NRM of the basalt is strong, but much of the material is broken into small pieces, and reliable magnetic directions are difficult to obtain. However, from detailed sampling of the larger intact pieces, we were able to characterize the intensity and direction of stable remanence. For each core we defined magnetic polarity intervals from consistent values of magnetization and calculated a mean paleoinclination. The combination of polarity intervals and biostratigraphic data yields a magnetic stratigraphy for much of the cored interval below 770 mbsf, including the Cretaceous/Paleogene boundary. All basalt samples measured have normal polarity, consistent with formation of basement during the Aptian. Conversion of paleoinclinations to paleolatitudes, combined with age information, allowed us to construct a drift path for Site 1183 for times between ~120 Ma and the present (Fig. F15). The oldest sedimentary rocks indicate a paleolatitude of 25°–30°S. These values are slightly higher than those determined for basement lava flows at ODP Site 807 (Mayer and Tarduno, 1993) but slightly lower than obtained by Hammond et al. (1975) for basal sedimentary rocks and basement at DSDP Site 289. Results for Sites 1185, 1186, and 1187 are within error of those for Site 1183 (see “Site 1185,” p. 17, “Site 1186,” p. 21, and “Site 1187,” p. 24). Values for all of these sites are significantly less than both the predicted ~40°S early Aptian paleolatitude of the central plateau in the plate reconstruction of Neal et al. (1997) and the ~50°S latitude of the Louisville hotspot today.

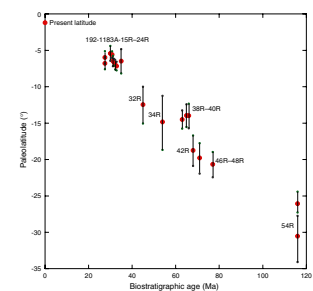
The major results of drilling at Site 1183 are summarized below:

1. Depositional setting of the sedimentary sequence was primarily deep, oxygenated (pervasively bioturbated and no organic-carbon preservation), and quiet (no significant currents or re-deposition events after the Aptian).
2. Calcareous microfossil assemblages in ~800 m of uppermost lower Aptian through upper middle Miocene sediments and sedimentary rocks are for the most part poorly preserved. However, planktonic foraminifers and calcareous nannofossils reveal 12

F14. Plagioclase-rich xenolith on core’s outer surface, p. 49.



F15. Paleolatitude data, p. 50.



- unconformities, of which the most significant are in the Albian (spanning ~10 m.y.) and terminal Albian to late Coniacian (~13 m.y.).
3. The preserved sediment was deposited above the CCD, and generally above the foraminifer lysocline. However, the regional pattern of the terminal Albian to late Coniacian condensation or hiatus is consistent with a progressive relative rise of the CCD through the Aptian and Albian to a level above the summit of the plateau, followed by a rapid descent of the CCD during the Campanian and early Maastrichtian. These trends may represent the posteruption subsidence history of the plateau coupled with oscillations in the Pacific CCD.
 4. Input of volcanic ash into the sedimentary succession is concentrated in two main periods: Paleocene to early Eocene and late Eocene to Oligocene. The latter episode is probably related to the Melanesian arc. The middle Eocene chalk is chert rich and corresponds to a lull in the input of volcanic ash.
 5. Emplacement of basaltic lava flows was entirely submarine at this site and ceased no later than the middle Aptian. The non-vesicular nature of the flows and the microfossil evidence suggest minimum paleodepths of >800 m. Microfossils at Site 807 indicate that basalt emplacement there ended about the same time or slightly earlier. Sedimentary interbeds in the upper levels of basement at both sites yielded microfossils no older than early Aptian. Two thin intervals of vitric tuff in the Aptian limestone at Site 1183 and a vitric tuff just above basement at DSDP Site 289 provide the only evidence that at least a small portion of the high plateau was shallow (possibly in the form of a few isolated summit volcanoes).
 6. The Site 1183 basalt flows are petrographically and chemically similar to those of the Kwaimbaita Formation, the lower of the two basalt formations defined on Malaita, and to the lower basalt units (Units C–G) at Site 807, despite the considerable distances separating Site 1183 from Malaita (~1000 km) and Site 807 (533 km). Very similar basalt is present in Hole 1186A and in the lower basement units at Site 1185 (see “[Site 1185](#),” p. 17, and “[Site 1186](#),” p. 21).

Site 1184

Site 1184 lies on the unnamed northern ridge of the eastern lobe or salient of the Ontong Java Plateau (Figs. [F1](#), [F2](#)). The eastern lobe had not been drilled before Leg 192. As with the dome of the high or main plateau (see “[Site 1183](#),” p. 10), we thought that this site near the summit of the ridge might be in an area that originally was at relatively shallow water depths. The relationship of the eastern lobe to the high plateau is unknown. It could be contemporaneous with the high plateau or be the trace of the postulated plume tail following the emplacement of the high plateau and, specifically, may be the main locus of 90-Ma eruptions (Tejada et al., 1996). Also, the eastern lobe appears to have been rifted into northern and southern portions that were separated by nearly 300 km of seafloor spreading in the Stewart Basin (Kroenke and Mahoney, 1996). The southern portion, Stewart Arch, is the proposed conjugate feature to the northern ridge. Eruptive products of this poorly understood rifting event may have been preserved along both the northern and southern rift-facing sides of the salient. Furthermore,

this part of the plateau passed over the calculated position of the Samoan hotspot ~35–40 Ma (Yan and Kroenke, 1993), and volcanic evidence of this passage might be present.

In the seismic reflection record for this site (Fig. F16), a sedimentary megasequence laps onto the upper surface of a large fault block. Reflection character of the block differs from that of basaltic basement on the main plateau (e.g., Site 1183; Fig. F7). Parallel to subparallel, high-frequency, slightly dipping reflections of limited and variable continuity persist to depths as great as 1.0 s of two-way (*P*-wave) traveltime beneath the surface of the fault block.

We cored lower Miocene pelagic calcareous ooze and chalk (Unit I) from 134.4 mbsf to the top of the fault block at 201.1 mbsf and volcanoclastic rocks (Unit II) from 201.1 mbsf to the base of the hole at 538.8 mbsf. A 1-cm-thick ferromanganese oxide crust represents the contact between the two units. Paleontological data suggest that deposition of the volcanoclastic succession occurred during the middle Eocene (principally nannofossil Zone NP16) and that deposition of the calcareous ooze began during the earliest Miocene. Little, if any, sedimentary record of events during the late Eocene or Oligocene is preserved.

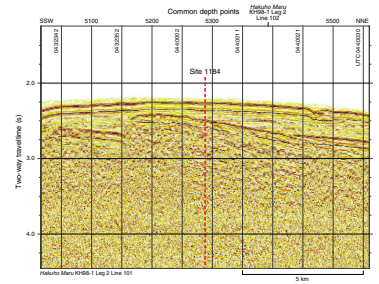
Unit I is dominated by nannofossil foraminifer ooze with as much as 10% siliceous microfossils; volcanic ash is a minor component. Paleodepths appear to have been bathyal. Grain densities generally lie between 2.3 and 2.6 g/cm³, with a mean of 2.5 g/cm³; porosity averages 66.1%, and the mean bulk density is 1.5 g/cm³. The ooze is weakly magnetic and was badly disturbed by drilling; consequently, we were unable to obtain reliable paleomagnetic data.

The volcanoclastic sequence of Unit II consists of coarse lithic vitric tuff, lapilli tuff, and lapillistone, most of which have a massive texture. Several thin beds of fine ash are also present, but we recovered no pelagic or neritic interbeds. Grain densities in Unit II are significantly more variable than those in Unit I, with a mean of 2.4 g/cm³; bulk densities maintain a nearly constant value of ~1.9 g/cm³, and porosities cluster between 31% and 37%. This unit exhibits normal-polarity magnetization and what appears to be a continuous record of paleosecular variation. The mean inclination (–54°) is much steeper than the expected Eocene inclination and indicates a paleolatitude (35°S) significantly different from that expected for this area in the Eocene (~15°–20°S). Tectonic rotation of the volcanoclastic beds may have taken place after the magnetic remanence was acquired, but it is unlikely that a sufficiently large amount of rotation in the direction required has occurred.

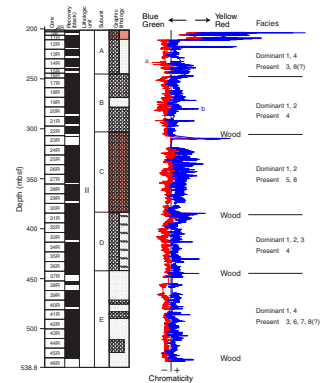
We divided Unit II into five subunits on the basis of changes in grain size, sorting, and sedimentary structures (Fig. F17; Table T2). Wood fragments (Fig. F18) and organic-rich layers were found at the boundaries between four of the subunits (B, C, D, and E) and at the base of the cored part of Subunit IIE, perhaps indicating lulls in volcanic activity. Subunit IID contains numerous thin-bedded intervals with inclined bedding. At ~305 mbsf, where a sharp increase in lapilli size marks the boundary between Subunits IIB and IIC, magnetic susceptibility and *P*-wave velocity increase abruptly, and mean thermal conductivity decreases slightly. Below 380 mbsf, where a reduction in lapilli size marks the top of Subunit IID, both magnetic susceptibility and velocity decrease and mean thermal conductivity increases slightly.

All five subunits of Unit II consist predominantly of coarse ash to lapilli-size glass and volcanic lithic fragments (Fig. F19), with less abundant accretionary and armored lapilli, set in a fine ash matrix (Figs. F20, F21). In most of the sequence, glass fragments are more abundant than

F16. Seismic reflection record, p. 51.

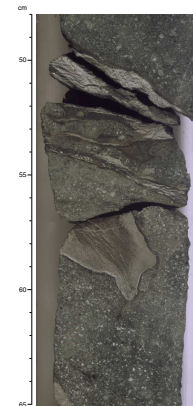


F17. Summary of lithologic characteristics, p. 52.

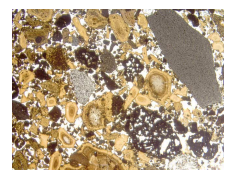


T2. Volcanoclastic facies, p. 75.

F18. Wood fragments in lithic vitric tuff, p. 53.



F19. Lithic and vitric clast types in a lithic vitric tuff, p. 54.



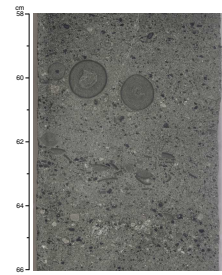
lithic fragments. However, both the abundance of lithic fragments relative to glass and the proportion of red, oxidized lithic fragments are greatest in the lapilli tuff and lapillistone of Subunit IIC. Oxidation of lapilli probably accounts for the distinctively high magnetic susceptibility of Subunit IIC, and the presence of both hematite and magnetite has been confirmed by X-ray diffraction analysis.

Glass shards in Unit II volcanoclastic rocks range from <0.1 to ~10 mm and are predominantly subangular, blocky, and nonvesicular. Slightly to highly vesicular glass shards are relatively rare. Tachylite clasts are found throughout Unit II and form the main component of the upper and lower parts of Subunit IIC. Lithic fragments are mainly subround and subequant to subelongate and principally comprise non-vesicular and vesicular basalt (generally <10 mm), ranging from partly glassy to microcrystalline and fine grained, with rare fragments of diabase (≤ 20 mm). Rip-up clasts of tuff (≤ 65 mm) are also common. Plagioclase and clinopyroxene grains are present as phenocrysts in basaltic lithic fragments and as discrete clasts; as clasts, they are generally anhedral, showing signs of mechanical transport and/or fracturing. Accretionary (Fig. F20) and armored lapilli (≤ 15 mm) are present in all the subunits and are sometimes concentrated in bands.

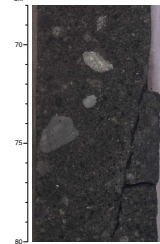
We interpret the accretionary and armored lapilli, together with abundant blocky glass shards, to indicate that these deposits were formed by explosive hydroclastic eruptions in a shallow-water to emergent eruptive setting (Fig. F22). The presence of nannofossils in finer grained intervals of tuff suggests primary deposition or reworking in a marine environment, and wood fragments and organic-rich layers indicate proximity to a vegetated island. Several features indicate that a component of the volcanoclastic material was derived from subaerial eruptions. These include the presence of vesicular tachylite lapilli throughout the volcanoclastic sequence, two intervals of well-sorted lapillistone (consisting almost entirely of nonvesicular tachylite at the top and bottom of Subunit IIC), and the abundant red, oxidized lithic fragments in Subunit IIC.

The entire 337.7-m volcanoclastic sequence cored from Hole 1184A is altered to varying extents, and the uppermost 8 m is completely altered to pale brown Fe oxyhydroxide, indicative of weathering in an oxidizing (subaerial?) environment. Except for plagioclase and clinopyroxene, almost all of the volcanic components and matrix are heavily altered to smectite, analcime, celadonite, calcite, zeolites, pyrite, and Fe oxyhydroxide. Unaltered glass is present in several cores (most commonly below ~470 mbsf); individual shards are typically rimmed by brown smectite (Fig. F23). From rim to center, the most commonly observed assemblage of secondary minerals in individual glass fragments follows the progression: smectite; analcime and/or other zeolites; rare calcite. The cement between individual clasts is predominantly composed of the same minerals as those replacing glass. Rare pleochroic, blue-green celadonite is also tentatively identified in the cement, filling vesicles in glass and partly replacing individual glassy fragments. The zeolites identified by X-ray diffraction are gmelinite, chabazite, levyne, mordenite, and natrolite, an assemblage rarely found in submarine basalt but common in subaerial environments. Several generations of white, hairline to >5-mm-wide veins cut the cores; these veins are filled with analcime \pm other zeolites \pm calcite and lined with minor smectite and/or celadonite. Halos in the groundmass adjacent to veins are rare, diffuse, and poorly developed; if present, they typically extend <1 cm

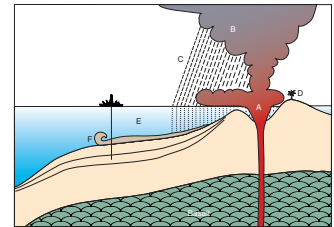
F20. Accretionary lapilli, p. 55.



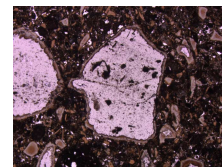
F21. Coarse angular clasts in lapilli tuff, p. 56.



F22. Eruptive setting of volcanoclastic rocks at Site 1184, p. 57.



F23. Photomicrograph of lithic vitric tuff, p. 58.



into the wall rock and contain smectite and bluish celadonite or brown Fe oxyhydroxide.

Despite the apparent middle Eocene biostratigraphic age of the volcanoclastic rocks, their chemical compositions are similar to those of the 122-Ma Kwaimbaita-type basalt flows and many of the 90-Ma lavas, such as those at Site 803 (Figs. F11, F12, F13). If the biostratigraphic age is correct, then this result would suggest that a fertile portion of the distinctive Kwaimbaita-type mantle source remained beneath this part of the eastern salient for 50–80 m.y. In light of shipboard inductively coupled plasma–atomic emission spectrometry (ICP-AES) analyses, it now seems unlikely that the Samoan hotspot provided much, if any, material for volcanism at Site 1184, although it potentially could have provided a source of heat for melting.

The major results of drilling at Site 1184 are summarized below:

1. Nannofossil evidence suggests a middle Eocene age for the volcanoclastic sequence drilled; much of the sequence appears to have been deposited within Zone NP16. However, the steep paleomagnetic inclination (-54°) implies a much greater age. If the volcanism is indeed middle Eocene, it could be contemporaneous with the major change in Pacific plate motion at ~ 43 Ma (e.g., Duncan and Clague, 1985). The volcanoclastic sequence would be much younger than the main phase of construction of the Ontong Java Plateau but similar in age to the 44-Ma alkalic Maramasike Formation in Malaita (Tejada et al., 1996). However, shipboard elemental data show that the volcanoclastic rocks at Site 1184 are composed of tholeiitic basalt clasts, the bulk composition of which resembles that of the widespread 122-Ma Kwaimbaita-type basalt or the similar basalts erupted at 90 Ma. A contribution of Samoan hotspot mantle in Eocene magmatism at Site 1184 appears unlikely.
2. The abundance of blocky glass shards implies that the volcanoclastic deposit was formed by hydroclastic eruptions, through the interaction of magma with shallow water. The abundant accretionary lapilli support this conclusion because they form only in steam-rich, subaerial eruption columns.
3. The virtual absence of lapilli larger than 20 mm suggests that the tuffs could not have accumulated close to the center of eruption. Deposition on the margin of a shoaling submarine volcano provides the most likely explanation for the volcanoclastic sequence.
4. Deep subaerial weathering at the top of the volcanoclastic section coupled with a zeolite assemblage typically formed in non-marine environments indicates that this part of the eastern salient was above sea level initially. Proximity to land also is suggested by wood fragments found in organic-rich ash layers in the volcanoclastic sequence. However, the presence of nannofossils shows that at least some of the tuff was deposited, or redeposited, in seawater.

Site 1185

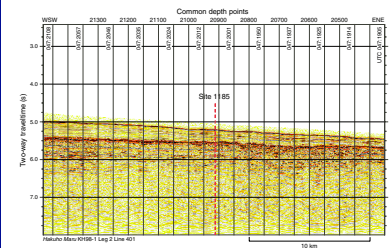
Site 1185 is on the eastern edge of the main or high Ontong Java Plateau, at the northern side of an enormous submarine canyon system (informally termed the Grand Canyon or Kroenke Canyon) that extends from Ontong Java and Nukumanu atolls into the Nauru Basin

(Fig. F1). This part of the plateau is far from sites where basaltic basement crust was sampled previously, the closest being ODP Site 803 (334 km to the north-northwest) and DSDP Site 289 (351 km to the west). We chose this site for two principal reasons. Firstly, the portion of basement volcanic stratigraphy that we could sample by drilling was likely to be different in this part of the plateau from that in more centrally located areas. In particular, only relatively few far-traveled lava flows may have reached the edge of the plateau, and it might be possible to sample deeper stratigraphic levels here than atop the plateau. Secondly, the 26 m of lava flows penetrated at ODP Site 803 (the only other basement site on the eastern side of the high plateau) belongs to the 90-Ma eruptive event (Mahoney et al., 1993). Basement at other sites drilled on the high plateau (Sites 289, 807, and 1183) formed at ~122 Ma. We thought it possible that 90-Ma basement might also be found at Site 1185; indeed, seismic reflection data (Fig. F24) reveal intrabasement reflections in this part of the plateau, suggesting that a carapace of 90-Ma lava flows might overlie 122-Ma basalt. If so, drilling at Site 1185 would provide further insight into the extent, composition, and mantle sources of the poorly understood 90-Ma event, documented previously at Site 803 and far to the south in lava sequences on the islands of Santa Isabel (Tejada et al., 1996; Parkinson et al., 1996) and San Cristobal (Birkhold-VanDyke et al., 1996) and in ash layers at DSDP Site 288 (Andrews, Packham, et al., 1975).

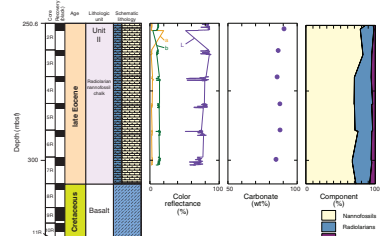
We drilled two holes at Site 1185 (Table T1), the first of which was a pilot hole to determine the depth to basement and the length of casing necessary to attach to a reentry cone at the second hole. In Hole 1185A, we started coring sediments at 250.6 mbsf, contacted basaltic basement at 308.5 mbsf, and cored basement rocks to 328.7 mbsf. In Hole 1185B (20 m west of Hole 1185A), we started coring at 308.0 mbsf, contacted basaltic basement at 309.5 mbsf, and cored basement to 526.1 mbsf. We recovered 14.1 m of the 57.9-m sedimentary section cored in Hole 1185A (Fig. F25). The dominant lithology is middle to upper Eocene radiolarian nannofossil chalk, which gradually darkens downward from white to light gray. Maximum bulk density is 1.6 g/cm³. The most distinctive features of the chalk are its abundant siliceous microfossils and a highly variable abundance (in places, a virtual absence) of planktonic foraminifers, suggesting that deposition was often below the foraminifer lysocline. Foraminifers preserved in the chalk indicate a middle to upper Eocene unconformity that may be associated with a (relative) rise in the CCD. Eocene siliceous chalk has been found at other DSDP and ODP sites on the Ontong Java Plateau.

The basement sequence consists of pillow basalt and massive basalt flows. We did not recover the sediment-basalt contact in either Hole 1185A or 1185B, but rare intercalations of limestone are present between lava flows and in fissures within the basalt. The limestone is composed of micritic calcite with very rare and poorly preserved nannofossils, foraminifers, and radiolarians that provide only rough age control but reveal that limestones of two ages are present. Extremely rare nannofossils in limestone within the upper 15 m of basement indicate a latest Cenomanian to Albian (possibly late Albian) age, whereas recrystallized planktonic foraminifers in thermally metamorphosed limestone 126 m below the top of basement suggest a late Aptian age. This difference in age between the upper and lower parts of the basement section corresponds to differences in basalt petrography, composition, and alteration. The entire basement sequence exhibits normal magnetic polarity, compatible with this range of ages. Paleo-

F24. MCS reflection profile across Site 1185, p. 59.



F25. Site 1185 log, p. 60.



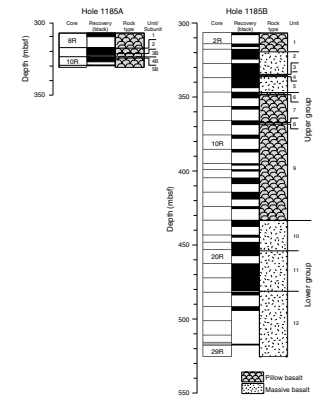
latitudes derived from paleoinclination data are similar, within error, to those for Site 1183. The ~50-m.y. hiatus between the lower sediments and basement suggests that this site may have been below the CCD for much of the time from the Cenomanian to middle Eocene.

In Hole 1185A, we cored 16.7 m of pillow basalt (312.0 to 328.7 mbsf; 67% average recovery). The pillows have glassy rims, spherulitic chilled margins, and fine-grained interiors. We divided the basalt into five units (Fig. F26) on the basis of apparent limestone interbeds, some of which may be only interpillow fill. The 216.6 m of basaltic basement penetrated in Hole 1185B (309.5 to 526.1 mbsf; 42% average recovery) exceeds the previous maximum on the plateau of 149 m of lava flows penetrated at Site 807 (Kroenke, Berger, Janecek, et al., 1991). We divided the basement section of Hole 1185B into 12 units ranging in thickness from 1 to 65 m. Units 1, 3, 4, and 6–9 were identified as pillow basalt on the basis of glassy rims and grain-size variations, and Units 2 and 5 are more massive lava flows with pillowed tops and bases. Units 1–9 are separated by thick (as much as 70 cm) intervals of hyaloclastite breccia composed of pillow-rim fragments cemented by carbonate and clay. Units 10–12 are massive flows. The flow tops of Units 10 and 12 are marked by carbonate- and clay-cemented breccia; the top of Unit 11 was not recovered but was inferred from the presence of vesicles, a pronounced change in alteration, and a marked increase in drilling rate over an interval of ~3 m.

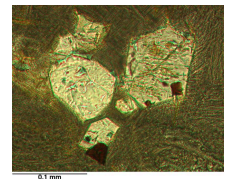
The basalt from Hole 1185A and in Units 1–9 of Hole 1185B is sparsely to moderately olivine phyric and generally highly veined. Olivine, the only common phenocryst phase, varies from fresh, in the glassy and aphanitic rims of pillows, to completely replaced by smectite, Fe oxyhydroxide, or calcite. Tiny octahedral crystals of chrome spinel are present, often as inclusions in the olivine phenocrysts (Fig. F27). Aphanitic pillow margins display a prominent spherulitic texture (Fig. F28) that grades into variolitic texture in fine-grained pillow interiors. The massive units also have variolitic texture and are less heavily veined. Units 10–12 in Hole 1185B contain small, sparse phenocrysts of plagioclase and clinopyroxene in addition to olivine. These rocks are similar in appearance to the basalt flows at Sites 1183 and 1186 and, like them, contain plagioclase-rich xenoliths. Shipboard ICP-AES analyses show that Units 10–12 are also very similar in composition to basalt from Holes 1183A and 1186A (Figs. F10, F11, F12, F13). For example, all have $\text{TiO}_2 \approx 1.1$ wt%, $\text{Cr} \approx 200$ ppm, and $\text{Zr} \approx 60$ ppm and appear to belong to the widespread Kwaimbaita magma type. In contrast, samples of the overlying basalt flows and those in Hole 1185A have the lowest concentrations of incompatible elements ($\text{TiO}_2 \approx 0.7$ wt%; $\text{Zr} \approx 38$ ppm; Fig. F12) and the most primitive, magnesium-rich compositions (MgO 8–10 wt%; $\text{Cr} \approx 460$ ppm) yet found in basalt from the plateau (Figs. F11, F13). This combination of elemental characteristics appears to indicate that their parental magmas formed by even higher total fractions of partial melting than other Ontong Java Plateau basalts (see “Results from Previous Sampling of Cretaceous Igneous Basement,” p. 6, in “Background”).

Bulk densities are higher (>2.4 g/cm³) in Units 2, 5, 10, and 11 than in Units 3 and 6–9 (<2.3 g/cm³). Both grain and bulk density decrease downhole in Units 4–9, corresponding to a change from massive to highly veined pillow basalt, and bulk density increases with the change from veined to massive basalt from Unit 9 to Units 10–12. *P*-wave

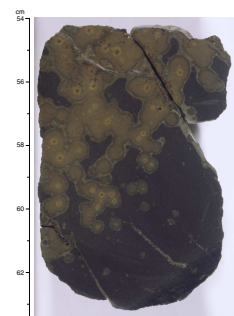
F26. Lithologic log of basement units, Site 1185, p. 61.



F27. Phenocrysts and crystals in pillow margin, p. 62.



F28. Spherulitic texture in an aphanitic pillow margin, p. 63.



velocities are generally >5000 m/s in the dense basalt of Units 2 and 10–12 and generally <5000 m/s in the veined basalt of Units 3 and 6–9.

Seawater-derived fluids have interacted pervasively at low temperatures with the basaltic basement, and we can divide the basement section into two groups of flows with different alteration characteristics. One group consists of all the basement units of Hole 1185A and Units 1–9 of Hole 1185B. Alteration in these units occurred under highly oxidizing conditions and with high water:rock ratios, as indicated by light and dark yellow-brown colors near glassy and aphanitic pillow margins; these colors fade to gray-brown and dark gray in coarser grained pillow interiors. The yellow-brown colors are a result of the complete replacement of olivine and pervasive alteration of groundmass by smectite (saponite and nontronite) and Fe oxyhydroxide. Although olivine phenocrysts are commonly completely replaced, rare unaltered olivine is present in aphanitic, dark gray to black areas interpreted as pillow rims. These characteristics are significantly different from the style of alteration in basalt at Site 1183.

A very different type of alteration has affected Units 10–12 at Hole 1185B. The top of Unit 10 marks a dramatic change in alteration character, and the brecciated top of this unit consists of pervasively altered angular basalt fragments. Such severe alteration is likely to be the result of exposure of very permeable basaltic seafloor to bottom seawater for an extended period of time (several million years). Groundmass alteration in Units 10–12 is characterized by pervasive celadonite. Unaltered glass is much rarer in these units than in Units 1–9, but this may be a consequence of the greater flow thickness rather than the level of glass alteration. Broad (centimeter scale) green-gray halos surround veins; wider reduction fronts consisting of scattered pyrite grains in the groundmass extend a few millimeters to a few centimeters beyond these halos. Smaller (millimeter scale) olive halos similar to those from Hole 1183A also are developed near veins, both within green-gray halos and where green-gray halos are absent.

Veins throughout the basement sequence predominantly contain calcite, zeolites (phillipsite), smectite, Fe oxyhydroxide, and rare celadonite and pyrite. Some veins were probably produced by sediment filling open fractures in the basalt; these veins are <5 mm to a few centimeters wide, are filled with pink carbonate and Fe oxyhydroxide, and contain recrystallized foraminifers. They are present both near the boundaries and within the interiors of basaltic units.

The major results of drilling at Site 1185 are summarized below:

1. The 60 m of white to light-gray radiolarian nannofossil chalk immediately above basement is of middle to late Eocene age. The most distinctive feature is the abundance of siliceous microfossils and, in places, a nearly complete absence of planktonic foraminifers, suggesting that many of the sediments were deposited below the foraminifer lysocline. Recovered foraminifers indicate a middle/upper Eocene unconformity within the unit that may be associated with a rise in the CCD.
2. A hiatus on the order of 50 m.y. separates the sedimentary succession from the basaltic basement.
3. Extremely rare calcareous nannofossils recovered from limestone between basalt flows in the upper 15 m of basement indicate an Albian to latest Cenomanian age. Recrystallized planktonic foraminifers found within thermally altered limestone 126 m

below the sediment-basement contact in Hole 1185B tentatively suggest a late Aptian age.

4. The basaltic lava flows in Hole 1185B can be divided into two major groups. The upper group appears to have been erupted sometime between the latest Cenomanian and Albian; the lower group is Aptian in age.
5. The two basalt groups have distinct chemical compositions. The older group is very similar to the basalt from Holes 1183A and 1186A and appears to represent the abundant Kwaimbaita magma type. The younger group has much lower concentrations of incompatible elements and includes the most primitive (magnesian) basalt yet found on the plateau.
6. Different styles of alteration in the two groups of basement lava flows suggest that the older group was in contact with seawater for a long period before the eruption of the younger group. This observation is consistent with the paleontological evidence that suggests a >15-m.y. hiatus between the two groups.

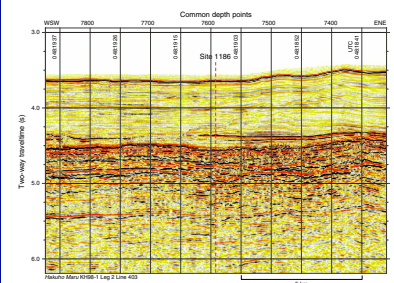
Site 1186

The plan for Leg 192 included a site on Stewart Arch within the territorial waters of the Solomon Islands (proposed Site OJ-7; see Fig. F1). However, ODP and the U.S. State Department were unable to obtain clearance for this site before the cruise. By midcruise, it was evident that clearance would not be forthcoming in time (if at all) to drill the site. We therefore chose Site 1186, on the eastern slope of the main Ontong Java Plateau, 206 km west of Site 1185, 319 km east of Site 1183, and 149 km east-southeast of DSDP Site 289 (Figs. F1, F2). The very different volcanic stratigraphy at Sites 1183 and 1185, particularly our discovery of high-Mg, low-Ti basalt of probable latest Cenomanian to Albian age at Site 1185, highlighted the importance of a site at a location intermediate between the crest and eastern edge of the main plateau.

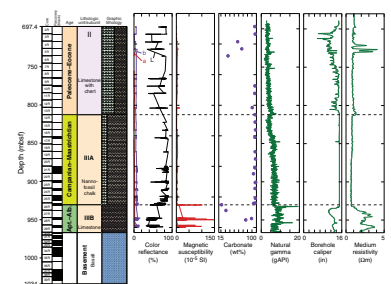
Approximately 12 km east-northeast of Site 1186 the seismic reflection data show a small body, interpreted to be an igneous intrusion or small volcanic cone, rising into the sedimentary sequence ~500 m above the surrounding acoustic basement. Extending from this body toward the drill site is a package of high-amplitude and continuous reflections (Fig. F29) that could represent a sill, lava flow, or volcanoclastic sediments. Alternatively, it could represent pelagic sediments altered by hydrothermal fluids derived from the igneous body. A secondary reason for selecting Site 1186 was to core this reflection package. If it proved to represent a sill or lava flow, it would provide information on the poorly known late-stage magmatism seen in seismic reflection records across much of the high plateau (Kroenke, 1972; Nixon, 1980) and in the 34-Ma alnöite intrusions and 44-Ma alkalic Maramasike Formation lavas on Malaita (e.g., Davis, 1977; Nixon and Neal, 1987; Tejada et al., 1996).

We began coring at 697.4 mbsf. The lithologic units recognized at this site are similar to those at other sites on the main Ontong Java Plateau, except that the Oligocene–Neogene chalk and ooze, designated as Unit I elsewhere on the plateau (and presumed to be present at Site 1186), were not cored. Recovery of Paleocene–Eocene Unit II (697.4–812.7 mbsf; see Fig. F30) was generally <5%. The rocks recovered are white limestone and chalk with faint burrow mottling and dark reddish gray to olive-brown chert interbeds. The lowest core of Unit II contains numerous thin gray beds of zeolite-rich chalk, similar to those inter-

F29. MCS reflection profile across Site 1186, p. 64.



F30. Lithologic log and selected properties, p. 65.



preted to be altered volcanic ash layers at other sites on the main plateau. No material indicative of a late-stage lava flow or sill was recovered. Despite the low overall recovery in this unit, the abundance of chert suggests that the seismic reflector package mentioned above represents a particularly chert-rich interval of sediment.

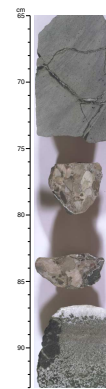
Unit III (812.7 mbsf to the contact with basaltic basement at 968.6 mbsf; Fig. F30) is Cretaceous chalk and limestone. The upper 118 m (Subunit IIIA; Campanian–Maastrichtian) consists of white to brownish white chalk, and the lower 38 m (Subunit IIIB; Aptian–Albian) is mottled light gray and dark brown limestone with minor clay beds. The division between the subunits is marked by a clay-rich band at 930.55 mbsf. As at Site 1183, this band marks a major hiatus (~13 m.y.) in carbonate deposition between the upper Albian and upper Coniacian. Other prominent hiatuses common to both Sites 1186 and 1183 are middle Albian (10 m.y.), uppermost Maastrichtian (2 m.y.), and middle Danian through middle Selandian (4 m.y.). Paleoenvironmental differences between Sites 1183 and 1186 are probably mostly a result of the greater paleodepth of Site 1186 and include a longer period of deposition in the Late Cretaceous below the foraminifer lysocline at Site 1186 (late Albian through early Maastrichtian) than at Site 1183 (late Albian through earliest Campanian).

The lowermost three beds above basement are a yellowish brown limestone overlying a bioturbated transition to a 5-cm-thick interval of dark brown ferruginous claystone, which in turn lies atop a 0.5-cm layer of breccia containing angular basaltic glass fragments. The limestone is late early Aptian in age (upper *Leupoldina cabri* Zone) and contains a small hiatus marking the absence of the planktonic foraminifer *Globigerinelloides ferreolensis* and calcareous nannofossil NC7B Zones. The 65.4 m of basement penetrated (with 59% average recovery) in Hole 1186A consists of basalt lava flows with minor interbeds of yellowish brown sandstone and one interval of reddish brown conglomerate containing rounded limestone clasts (Fig. F31). Fractures in some of the flows are filled with pale brown, partially recrystallized limestone breccia.

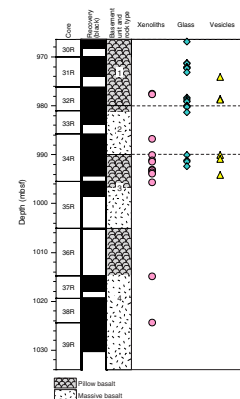
Site 1186 was the only hole logged during Leg 192. High-quality logs were acquired in igneous basement and in parts of the cored sedimentary interval. We tentatively interpret a strong seismic reflection in the sedimentary section at 4.37 s two-way traveltime (~725 mbsf; see Fig. F29) as an ~4-m-thick chert or chert-dominated interval. The Aptian–Albian limestone appears to be thinly and regularly bedded. The sharp boundary between sedimentary and igneous rock is well defined on conductivity, porosity, density, and, particularly, Formation MicroScanner logs. Using the same logs, we can distinguish between pillowed and massive intervals within igneous basement.

We divided the basement section (968.6–1034.0 mbsf) into four units on the basis of limestone and hyaloclastite interbeds and downward changes in character from massive to pillowed. The units range from 10 to >26 m in thickness (Fig. F32). Basement Unit 1 consists entirely of pillow lava, whereas Units 2–4 have massive interiors. The basalts are sparsely olivine (\pm plagioclase) phyric. All olivine is altered and usually replaced by dark green clay. The pillows have glassy rims (commonly containing some unaltered glass), aphanitic outer zones, and fine-grained interiors. In the massive flows forming most of Units 2–4, the transition from aphanitic flow tops to coarser grained interiors occurs over several meters and is marked by an intermediate zone with a patchy texture varying between fine grained and aphanitic on a scale of

F31. Limestone conglomerate between lava flows, p. 67.



F32. Lithologic log of basement units, Site 1186, p. 68.



a few millimeters. Olivine phenocrysts are concentrated in the coarser patches and are rare to absent in the aphanitic parts (Fig. F33).

Plagioclase xenocrysts (>2 mm) and, more rarely, plagioclase-rich xenoliths are present throughout the entire basalt section and are more common in the massive intervals. They are similar to the xenocrysts and xenoliths that we reported from Site 1183 and from the lower group of lava flows at Site 1185. Seven bulk-rock lava samples analyzed by shipboard ICP-AES are closely similar in chemical composition to basalt from Hole 1183A, the lower group at Hole 1185B, Units C–G at Site 807, and the Kwaimbaita Formation on the island of Malaita (Figs. F10, F11, F12, F13). The basalt flows all have normal magnetic polarity and give a 23°S paleolatitude, which agrees well with values obtained from basalt of similar age from Sites 1183 and 1185.

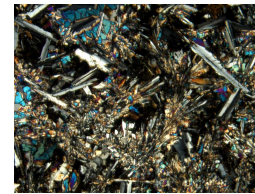
The entire section of basaltic basement cored at Site 1186 has undergone low-temperature water-rock interactions resulting in complete replacement of olivine and almost complete replacement of glassy meso-stasis. Clinopyroxene and plagioclase are generally unaltered. The overall alteration of the basalt ranges from 5% to 35% by volume, estimated visually by color distribution in hand specimen. On the whole, the alteration is similar to that in the lower group of basalt flows at Site 1185 and especially to that at Site 1183. The effects of the same three main low-temperature alteration processes are clearly seen: (1) black and dusky green halos resulted from the replacement of olivine phenocrysts and groundmass glass by celadonite, Fe oxyhydroxide, and, to a minor extent, smectite; (2) brown halos formed by the complete replacement of olivine and glass by smectite and Fe oxyhydroxide as a result of strongly oxidative alteration at high water:rock ratios; and (3) pervasive alteration under anoxic to reducing conditions and low water:rock ratios has affected the basalt in areas outside the colored halos. Smectite, pyrite, and calcite are the principal secondary minerals formed during this process.

Veins in the basement rocks are lined with smectite or celadonite and filled with calcite. Veined basalt has lower bulk density than does unveined basalt (<2.4 g/cm³ compared with >2.4 g/cm³), lower *P*-wave velocity (<5000 m/s compared with >5000 m/s), and lower magnetic susceptibility.

The major results of drilling in Hole 1186A are summarized below:

1. The sedimentary sequence closely parallels those at other sites on the main Ontong Java Plateau.
2. Biostratigraphy indicates a major hiatus (~13 m.y.) in carbonate deposition between the upper Albian and upper Coniacian, as at Site 1183. Other significant hiatuses at both sites are Albian (10 m.y.), uppermost Maastrichtian (2 m.y.), and middle Danian through middle Selandian (4 m.y.).
3. Basement at Site 1186 consists of basaltic pillow lava and massive lava flows. It is probably of similar age to basement at Site 1183; both are immediately overlain by upper lower Aptian (~118 Ma in the timescale of Gradstein et al., 1995) limestone.
4. The basalt is similar in chemical composition to basalt from Site 1183, the lower group of flows at Site 1185, Units C–G at Site 807, and the Kwaimbaita Formation on Malaita. The types and amounts of basalt alteration at Site 1186 are very similar to those at Site 1183.

F33. Plagioclase laths and clinopyroxene crystal sprays in basalt, p. 69.



5. The basalt flows have normal magnetic polarity and yield a paleolatitude of 23°S, which agrees well with that obtained from basalt of similar age from Sites 1183 and 1185.

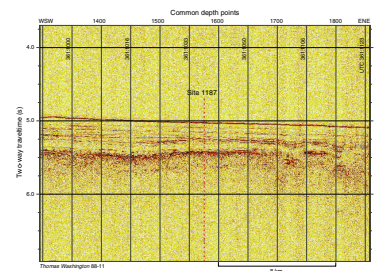
Site 1187

We decided to drill Site 1187 while coring in Hole 1186A. By the time we had penetrated ~50 m into basement at Site 1186, it was clear from shipboard ICP-AES analyses that the basalt was of the widespread, remarkably homogeneous, ~122-Ma Kwaimbaita magma type found in Hole 1183A and in the lower 92 m of basement at Site 1185. The bottom of the Kwaimbaita-type lava sequence has not been reached in any of the locations where such lavas have been encountered. This sequence is >100 m thick at Site 807 (Units C–G) (Kroenke, Berger, Janček, et al., 1991), and on the island of Malaita the Kwaimbaita Formation is >2.7 km thick (Tejada et al., in press). Furthermore, our rate of penetration in basement was low, and there was risk involved in reentering (after an imminent drill-bit change) an uncased >900-m-deep hole in chert-rich sediment. These considerations led us to favor drilling a new site to provide fundamental new information about the age, composition, and/or mantle sources of the plateau over deepening Hole 1186A.

A site somewhere between Site 1185 and Site 803 would be particularly useful because, unlike other sites on the main plateau, Sites 803 and (on the basis of shipboard biostratigraphic data) 1185 contain basalt that is younger than 122 Ma, and the lava flows in the upper 125 m of basement at Site 1185 are compositionally different from any seen elsewhere on the plateau. We therefore selected Site 1187 (Fig. F1), near Site 804 (which did not reach basement) on the eastern edge of the main plateau. Site 1187 is 194 km southeast of Site 803, 146 km north of Site 1185, and <3 km from the easternmost point where Ontong Java Plateau basement can be distinguished easily, on seismic records, from that of the Nauru Basin (Fig. F34). Our principal objectives at Site 1187 were to establish the composition, age, and eruptive environment of the basement volcanic rocks and to compare them with those of lavas sampled at Sites 803 and 1185. In particular, we wanted to determine whether basement in this region was emplaced during the ~122-Ma or later magmatic events, or both.

We encountered basaltic basement at 372.5 mbsf (Table T1), ~40 m shallower than estimated from the seismic record. We had begun coring at 365.5 mbsf and recovered only 1.47 m of the sedimentary succession above basement. The sediment recovered consists of dark brown ferruginous claystone that grades downward from burrow mottled to laminated and overlies an ~2-cm-thick chalk layer. Biostratigraphic analysis of the claystone indicates an age of late Aptian to Albian. The chalk layer, which immediately overlies basalt, contains a late Aptian foraminiferal assemblage, including the planktonic taxa *Globigerinelloides ferreolensis*, *Blowiella duboisi*, and *Blefuscuiana praetrochoidea*, and a lower-slope benthic assemblage. The calcareous nannofossils *Eprolithus floralis* and *Hayesites irregularis*, present without any Albian-restricted species, are consistent with a late Aptian age for the chalk. Washed residues of the overlying claystone very rarely contain the planktonic foraminifer *Globigerinelloides aptiensis*, indicating an age range of late Aptian to middle Albian. A single, questionable specimen of the Albian taxon *Blefuscuiana albiana* was also recovered. The clay-

F34. Seismic reflection profile across Site 1187, p. 70.



stone residues are dominated by fish-bone fragments and small ferromanganese nodules, suggesting slow accumulation below the CCD.

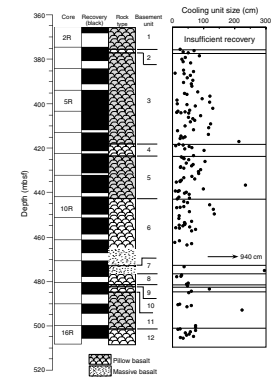
A 70-cm-thick interval of the claystone is reversely magnetized. The late Aptian to Albian biostratigraphic age of the claystone suggests that this interval may be M⁻¹r (also called “ISEA” after the site code used for its initial discovery in Italy), a short reversed-polarity subchron (~115 Ma) within the Cretaceous Normal Superchron. The underlying basalt flows all exhibit normal polarity. Paleoinclination data for the basalt indicate a paleolatitude of ~19°S, essentially the same as at Site 1186 and within error of values for Sites 1183 and 1185.

We cored 135.8 m of basaltic basement, which we divided into 12 units (ranging in thickness from 0.7 to 41.3 m; Fig. F35) on the basis of recrystallized limestone, significant (>10 cm thick) hyaloclastite interbeds, and/or downward changes in lava flow structure from massive to pillowed (e.g., the contact between Units 6 and 7). Most of the sequence consists of pillow-lava flows. The only unequivocally massive portion is the fine-grained, 9-m-thick base of Unit 6; some basalt interpreted to be from pillows >2 m thick also may be from massive flows.

The rims of the pillows contain both unaltered and altered glass. Basalt inside the rims is aphanitic, generally altered, and often contains spherulitic zones stained by Fe oxyhydroxide. In the larger pillows, the grain size coarsens gradually from aphanitic near the margins to fine grained in pillow interiors. The basalt is aphyric to moderately olivine phyric. Fresh olivine is present in some of the least-altered intervals of fine-grained basalt in pillow interiors and in the massive basalt of Unit 6. Rare, irregular miarolitic cavities (as large as 1 cm × 2 cm) are present in the interiors of pillows and in the massive portion of Unit 6. Shipboard ICP-AES analyses (Figs. F10, F11, F12, F13) show that the basalt is relatively primitive (MgO ≈ 9 wt%; Cr ≈ 485 ppm), like the upper 125 m of lava flows at Site 1185, and virtually identical to them in its unusually low concentrations of incompatible elements (e.g., Zr and Ti). The presence of these distinctive lava flows in >100-m-thick piles at two sites 146 km apart implies that substantial volumes of this type of magma were erupted on the eastern flank of the high plateau after the main plateau-forming eruptions at ~122 Ma.

Seawater-derived fluids have interacted at low temperatures with the basaltic basement, resulting in the most pervasive overall alteration observed during Leg 192. This observation is consistent with the high abundance of relatively small pillows. Alteration occurred under highly oxidizing conditions with high water:rock ratios and resulted in the development of light and dark yellow-brown colors through the complete replacement of olivine and the alteration of groundmass to smectite (saponite and nontronite) and Fe oxyhydroxide near the outer zones of pillow margins. The color grades into dark brown and dark gray in the coarser grained pillow interiors. Despite the high average level of alteration in the basalt, unaltered glass is relatively abundant at Site 1187 because of both the large number of individual pillows (i.e., more glassy margins are present per length of core) and the greater thickness of many of the glassy margins compared with those at other Leg 192 sites. Overall, the secondary mineral assemblages and visual characteristics of basalt alteration at all Leg 192 sites are remarkably similar to those seen elsewhere in nonplateau seafloor of varying ages. This similarity indicates that alteration conditions in basement on the Ontong Java Plateau were similar to those operative in typical ocean crust formed at spreading centers.

F35. Lithologic log of basement units, Site 1187, p. 71.



Veins throughout the basement sequence consist mainly of calcite, zeolites (probably phillipsite with analcime), smectite, Fe oxyhydroxide, and rare celadonite and pyrite. As at Sites 1185 and 1186, the physical properties of basement at Site 1187 strongly reflect the amount of veining and alteration in the basalts. *P*-wave velocities are high (>5300 m/s) in the dense, relatively sparsely veined basalt of Units 6 and 7 and lower (<5300 m/s) in the more abundantly veined basalt of other units. Areas of high magnetic susceptibility also correlate with the presence of dense, unveined basalt, and the mean bulk densities of sparsely veined intervals are >2.7 vs. <2.7 g/cm³ in abundantly veined intervals.

The major results of drilling in Hole 1187A are summarized below:

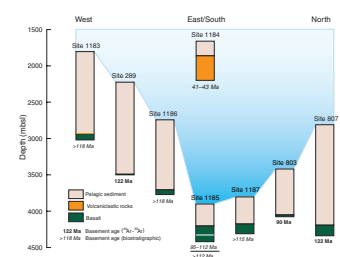
1. A late Aptian biostratigraphic age for an ~2-cm-thick chalk layer directly above basaltic basement and a late Aptian to Albian age for a ferruginous claystone overlying the chalk suggest that basalt at this site is older than the Albian to latest Cenomanian age indicated for the upper portion of basement at Site 1185.
2. Basement at Site 1187 consists mainly of basaltic pillow lavas, with minor massive flows. Despite the apparent difference in age, the chemical composition of Site 1187 basalt closely resembles that of the upper 125 m of lava flows at Site 1185. Both groups of lavas are significantly less differentiated and poorer in incompatible elements than other Ontong Java Plateau basalts. Relatively large amounts of incompatible element-poor, rather high Mg basalt appear to have been erupted along the eastern edge of the plateau. These rocks represent high total fractions of partial melting.
3. The level of basaltic alteration at Site 1187 is generally greater than at other Leg 192 sites, although fresh glass is present in many of the pillow rims and unaltered olivine is abundant in some pillow interiors and in the one massive flow. The basalt flows have normal magnetic polarity and yield a paleolatitude of ~19°S, which agrees within error with values obtained for basement at Sites 1183, 1185, and 1186. A 70-cm-thick reversed-polarity interval in the claystone overlying basement may correspond to *M*⁰-1*r*⁰ (ISEA), a short reversed-polarity subchron (~115 Ma) within the Cretaceous Normal Superchron.

DISCUSSION AND SUMMARY

Drilling/Site Overview

Four of the five sites drilled during Leg 192 are on the main or high plateau, and one is on the northern ridge of the eastern lobe or salient (Fig. F1). The four sites on the main plateau and the three previous DSDP and ODP sites that reached basaltic basement form a transect extending eastward from Site 1183 on the crest of the plateau, via Sites 289 and 1186, to Site 1185 on the extreme eastern edge of the plateau. From Site 1185, the transect runs northward along the eastern edge of the plateau to Sites 1187 and 803 and then northwestward to Site 807 on the northern flank. Figure F36 shows the stratigraphic sections drilled at all seven high-plateau igneous basement sites, arranged in order on the transect, plus the stratigraphic section at Site 1184. Eastern-salient Site 1184 lies off the transect, 586 km to the southeast of Site 1185. The diagram summarizes water depth, sediment thickness, base-

F36. Stratigraphic sections drilled, p. 72.



ment penetration, and basement rock types. Basement ages for previously drilled sites are from ^{40}Ar - ^{39}Ar dating of basalt and are estimated from biostratigraphic evidence for the Leg 192 sites. Figure F37 shows the present-day water depth to basement at each site, corrected for the effects of sediment loading. Assuming that (1) Aptian basement lies beneath a relatively thin 90-Ma lava sequence at Site 803, (2) all sites (except Site 1184) have subsided by the same amount since the Aptian, and (3) there has been no subsequent tectonic disturbance, Figure F37 should give the relative depths of each site at the time of plateau formation.

Scientific Results

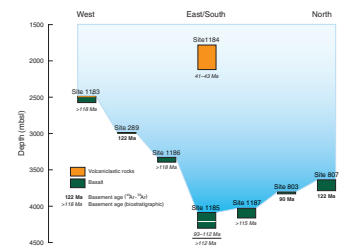
Our principal objectives for this cruise were to establish the composition, age, and eruptive environment of the basement volcanic rocks at each site. We also hoped to determine the early subsidence history from the overlying sedimentary succession at each site and to ascertain the ages of sequence boundaries observed in the seismic record. Many of these objectives were partially met through shipboard studies but will require more comprehensive shore-based work to be achieved fully.

Basement Ages

Shipboard biostratigraphic analysis brackets the age of basement at Sites 1183 and 1186 between the early and late Aptian; thus, the upper levels of basement crust at these sites belong to the 122 (± 3)-Ma phase of Ontong Java Plateau volcanism. At Site 1185, biostratigraphic age controls on basement are poor but suggest that basalt flows of two ages are present. The upper 15 m (and possibly ~125 m; i.e., the upper group of basalt units in Fig. F26) of lava flows appears to be between latest Cenomanian and Albian, possibly late Albian, in age; that is, micropaleontological data suggest they were emplaced sometime between ~93 and 112 Ma (in the timescale of Gradstein et al., 1995). The lower 92 m of Kwaimbaita-type flows (the lower group in Fig. F26) appears to be late Aptian or older. The simplest interpretation, in the absence of radiometric age data, is that the lower flows belong to the widespread ~122-Ma event and the upper ones to the 90 (± 4)-Ma event documented in lava flows at Site 803, on Santa Isabel and San Cristobal, and in ash layers at DSDP Site 288 (see Fig. F3). The nearly identical, and unusual, low-Ti, high-Mg compositions of the upper group of flows at Site 1185 and the entire lava sequence drilled in Hole 1187A suggest that all the low-Ti, high-Mg flows are related and were formed at the same time. Yet biostratigraphic data suggest that the Site 1187 flows are late Aptian or older (>115 Ma). Therefore, we have a discrepancy, the resolution of which must await ^{40}Ar - ^{39}Ar dating of basalt samples and/or refinement of the biostratigraphic age estimates.

Nevertheless, the evidence now available from Leg 192, combined with age data for Leg 30 and Leg 130 sites, indicates that an immense part of the high plateau was formed in the ~122-Ma event: the central region (Sites 289, 1183, and 1186), northern flank (Site 807), and probably much of the eastern flank (lower group of flows at Site 1185 and possibly Site 1187). Basement crust in Malaita and much of Santa Isabel also was formed in this event, and possibly the lowest part of the section exposed in San Cristobal (Neal et al., 2000). With the resolution of existing sampling and ^{40}Ar - ^{39}Ar and biostratigraphic ages, the duration of this event could have been as great as ~7 m.y., or much shorter. Im-

F37. Basement sections drilled, p. 73.



portantly, the central region of the main plateau appears to have been largely bypassed by post-122-Ma eruptive episodes. To date, evidence for these episodes has been found exclusively in locations around the eastern margins of the main plateau (Site 803, possibly Site 1187, and the upper group of basalt at Site 1185) and on the eastern salient (Santa Isabel, Malaita, San Cristobal, Site 1184, and in ash layers at Site 288, at the boundary between the eastern salient and the main plateau). Thus, the ~90-Ma episode now appears to have been volumetrically minor in relation to the ~122-Ma event, and later episodes to have been still less important. This conclusion is one of the major results of Leg 192. In sharp contrast, in the southern and central Kerguelen Plateau and Broken Ridge, substantial volumes of magma appear to have been emplaced over a period of ~30 m.y. (Pringle and Duncan, 2000).

The biostratigraphic data for the thick sequence of volcanoclastic rocks at Site 1184 suggest that at least locally significant volcanism occurred on the northern part of the plateau's eastern lobe in the middle Eocene (~41–43 Ma in the timescale of Berggren et al., 1995). On the southern part of the eastern lobe, the 44-Ma alkalic lavas of the Maramasike Formation in Malaita (Tejada et al., 1996) reach a maximum thickness of 900 m (Petterson et al., 1997). The apparent biostratigraphic age of the Site 1184 volcanoclastic rocks and the age of the Maramasike lavas are close to that of the ~43-Ma major change in Pacific plate motion (e.g., Duncan and Clague, 1985), and it is tempting to suggest that volcanism in one or both cases may have occurred in response to a change in the stress field of the plateau.

Petrology and Geochemistry of Igneous Rocks

Fundamental results of Leg 192 are that Kwaimbaita-type basalt was the only type we encountered at Sites 1183 and 1186 and that it lies below the 125 m of low-Ti, high-Mg basalt at Site 1185. Units C–G at Leg 130 Site 807 on the far northern flank of the high plateau are also of the Kwaimbaita type. Thus, Kwaimbaita-type lava flows cover an immense region of the high plateau. Furthermore, despite the considerable distances separating these sites, the total range of elemental variation is surprisingly small (Figs. **F10**, **F11**, **F12**, **F13**). Other magma types, whether ~122 Ma or younger, such as the low-Ti, high-Mg basalt discovered during Leg 192 and the Singgalo type at Site 807, in Santa Isabel, and particularly abundant in Malaita, appear to be present mainly on the margins of the plateau. No Singgalo-type basalt was recovered at any of the Leg 192 sites. We conclude that the Kwaimbaita magma type was by far the most abundant type produced, at least during construction of the upper levels of basement crust. Although shore-based isotopic work on Leg 192 basement samples is needed, the implication from the shipboard elemental data is that the magmas were derived from a very homogeneous and voluminous mantle source.

One of the most exciting discoveries of Leg 192 was the low-Ti, high-Mg basalt of Sites 1185 and 1187, along the eastern edge of the plateau. The Kwaimbaita magma type represents a high total percentage of partial melting, probably on the order of 18%–30% (Mahoney et al., 1993; Tejada et al., 1996; Neal et al., 1997). The low-Ti, high-Mg basalt requires significantly higher total amounts of partial melting. Small amounts of basalt with rather similar elemental characteristics are found along some oceanic spreading axes and in Iceland (Hemond et al., 1993; Hardarson and Fitton, 1997), but understanding how the apparently large volume of these flows on the eastern Ontong Java Plateau

originated poses a formidable challenge. An explanation of their origin and of the relationship of their mantle source region to the Kwaimbaita and Singgalo sources awaits more precise knowledge of their age, and comprehensive elemental and isotopic data from shore-based studies.

By the Eocene, the plateau had drifted thousands of kilometers from its 90- and 122-Ma positions (e.g., Yan and Kroenke, 1993). Yet, surprisingly, the mantle source of the apparently Eocene volcanism at Site 1184 was compositionally similar to the source of the Kwaimbaita-type ~122- and ~90-Ma basalts (e.g., Fig. F12). The same is true of the Paleocene and Eocene tholeiitic basalts in San Cristobal, which closely resemble the older basalt groups both elementally and isotopically (Birkhold-VanDyke et al., 1996; Neal et al., 2000). Although late-stage tholeiitic magmatism could have been caused by upwelling of mantle completely unrelated to the source that formed most of the plateau, the compositional similarity of the later tholeiitic basalts and those formed many tens of millions of years earlier argues that the sources of the later basalts were closely related to the mantle that formed the bulk of the plateau. Our working hypothesis is that the sources of such late-stage tholeiitic volcanism resided in fertile portions of the plateau's lithospheric mantle root that did not melt, or possibly were veined (i.e., refertilized) by migrating melts, at 122 (and/or 90) Ma. Such regions would be capable of melting to form tholeiitic magma if heated sufficiently, but the specific causes of melting remain obscure at present.

Basement Paleolatitude

Estimates of basement paleolatitude at Sites 1183, 1185, 1186, and 1187 are in the 20°–30°S range. This range is well to the north of the ~35°–42°S location suggested for the central high plateau between 125 and 90 Ma in the plate reconstruction of Neal et al. (1997) and even farther from the present position of the Louisville hotspot (~50°S) proposed by several workers to be the source of the plateau. The amount of true polar wander and the distance the Louisville hotspot has drifted since the Early Cretaceous (if it existed then) are unknown, but, in agreement with Nd-Pb-Sr isotopic data for pre-Leg 192 basement samples and the lack of a postplateau seamount chain corresponding to a plume tail (e.g., Neal et al., 1997; Tejada et al., in press), the paleolatitude data presently do not appear to support a Louisville hotspot origin for the Ontong Java Plateau.

Site 1184 presents a paradox in that the –54° mean magnetic inclination of the volcanoclastic sequence implies a paleolatitude of ~35°S. Assuming the middle Eocene biostratigraphic age is accurate, this value is much farther south than the expected Eocene paleolatitude of ~15°–20°S for this part of the plateau. At this site, postdepositional tilting of the sequence appears unlikely to explain a difference of this magnitude, and we currently have no satisfactory explanation for the discrepancy.

Eruptive Environment and Paleoenvironmental Impact

The volcanoclastic sequence at Site 1184 formed in shallow water but seems to represent magmatism that occurred long after the Aptian phase of plateau construction. Basement rocks at the four Leg 192 sites on the main plateau were emplaced well below sea level, as were those of Sites 289, 803, and 807, and the Ontong Java Plateau basement sections in the eastern Solomon Islands (see [“Results from Previous Sampling of Cretaceous Igneous Basement,”](#) p. 6, in “Background,” and

“Eruptive Environment and Style,” p. 8, in “Scientific Objectives”). Site 1183, on the crest of the main plateau, appears to have been by far the shallowest site originally (Fig. F37), but the virtually vesicle-free pillow lava flows there were probably erupted at a depth of at least 800 m. Indeed, the only evidence that any part of the main plateau was at least briefly shallow or emergent in the Aptian is provided by the two thin (<1 m recovered) layers of laminated vitric tuff deposited as turbidites at the base of the sedimentary sequence at Site 1183, a vitric tuff immediately above basement at Site 289 and, possibly, abundant glass shards in Aptian limestone at Site 288 (Andrews, Packham, et al., 1975). If a large proportion of Ontong Java Plateau magmas were erupted under shallow water or subaerially, then the flux of climate-modifying SO₂, Cl, and F to the atmosphere would have been considerable (e.g., Michael, 1999).

Because our results indicate that most of the plateau formed substantially below sea level, its large-scale effects on the environment and biosphere were probably limited and confined mainly to the oceans. The magnitude of hydrothermal exchanges between seawater and the plateau’s magmatic systems is unknown; all of the basement rocks recovered during Leg 192 have been affected only by low-temperature alteration processes. Overall, the types and amounts of alteration at all of the sites are similar to those found in normal (nonplateau) seafloor formed at spreading centers. The only evidence from Leg 192 sediments of relatively short-lived biological “deserts” that might be associated with the huge amount of Aptian volcanism on the plateau is in the thin, barren ferruginous claystone layers immediately above basement at Sites 1183 and 1187.

REFERENCES

- Abbott, D., and Mooney, W., 1995. The structural and geochemical evolution of the continental crust: support for the oceanic plateau model of continental growth. *Rev. Geophys. Suppl.*, U.S. Natl. Rept. to IUGG 1991–1994, 231–242.
- Albarède, F., 1998. The growth of continental crust. *Tectonophysics*, 296:1–14.
- Anderson, D.L., 1996. Enriched lithosphere and depleted plumes. *Int. Geol. Rev.*, 38:1–21.
- Andrews, J.E., Packham, G., et al., 1975. *Init. Repts., DSDP*, 30: Washington (U.S. Govt. Printing Office).
- Babbs, T.L., 1997. Geochemical and petrological investigations of the deeper portions of the Ontong Java Plateau: Malaita, Solomon Islands [Ph.D. dissert.]. Leicester Univ., U.K.
- Bercovici, D., and Mahoney, J., 1994. Double flood basalts and plume head separation at the 660-km discontinuity. *Science*, 266:1367–1369.
- Berger, W.H., Kroenke, L.W., Mayer, L.A., Backman, J., Janecek, T.R., Krissek, L., Leckie, M., Lyle, M., and Shipboard Scientific Party, 1992. The record of Ontong Java Plateau: main results of ODP Leg 130. *Geol. Soc. Am. Bull.*, 104:954–972.
- Berggren, W.A., Kent, D.V., Swisher, C.C., III, and Aubry, M.P., 1995. A revised Cenozoic geochronology and chronostratigraphy. In Berggren, W.A., Kent, D.V., Aubry, M.-P., and Hardenbol, J. (Eds.), *Geochronology, Time Scales and Global Stratigraphic Correlation*, Spec. Publ.—Soc. Econ. Paleontol. Mineral. (Soc. Sediment Geol.), 54:129–212.
- Birkhold-VanDyke, A.L., Neal, C.R., Jain, J.C., Mahoney, J.J., and Duncan, R.A., 1996. Multi-stage growth for the Ontong Java Plateau (OJP)? A progress report from San Cristobal (Makira), Solomon Islands. *Eos*, 77F:714.
- Blum, P., 1997. Physical properties handbook: a guide to the shipboard measurement of physical properties of deep-sea cores. *ODP Tech. Note*, 26 [Online]. Available from World Wide Web: <<http://www-odp.tamu.edu/publications/tnotes/tn26/INDEX.HTM>>. [Cited 2000-10-15]
- Campbell, I.H., 1998. The mantle's chemical structure: insights from the melting products of mantle plumes. In Jackson, I. (Ed.), *The Earth's Mantle: Composition, Structure, and Evolution*: Cambridge (Cambridge Univ. Press), 259–310.
- Castillo, P., Pringle, M.S., and Carlson, R.W., 1994. East Mariana Basin tholeiites: Cretaceous intraplate basalts or rift basalts related to the Ontong Java plume? *Earth Planet. Sci. Lett.*, 123:139–154.
- Cloos, M., 1993. Lithospheric buoyancy and collisional orogenesis: subduction of oceanic plateaus, continental margins, island arcs, spreading ridges, and seamounts. *Geol. Soc. Am. Bull.*, 105:715–737.
- Coffin, M.F., and Eldholm, O., 1993. Scratching the surface: estimating dimensions of large igneous provinces. *Geology*, 21:515–518.
- , 1994. Large igneous provinces: crustal structure, dimensions, and external consequences. *Rev. Geophys.*, 32:1–36.
- Coffin, M.F., Frey, F.A., Wallace, P.J., et al., 2000. *Proc. ODP, Init. Repts.*, 183 [CD-ROM]. Available from: Ocean Drilling Program, Texas A&M University, College Station, TX 77845–9547, U.S.A.
- Coffin, M.F., and Gahagan, L.M., 1995. Ontong Java and Kerguelen Plateau: Cretaceous Islands? *J. Geol. Soc. London*, 152:1047–1052.
- Coleman, P.J., 1965. Stratigraphical and structural notes on the British Solomon Islands with reference to the first geological map, 1962. *Report No. 29, British Solomon Islands Geological Record*, 2:17–33.
- Crough, S.T., 1983. The correction for sediment loading on the seafloor. *J. Geophys. Res.*, 88:6449–6454.

- Davis, G.L., 1977. The ages and uranium contents of zircon from kimberlites and associated rocks. *Extended Abstracts 2nd Intl. Kimberlite Conf.*, Santa Fe, New Mexico.
- Dick, H.J.B., Mével, C.A., et al., 1996. Report of the ODP-InterRidge-IAVCEI workshop, Oceanic Lithosphere and Scientific Drilling into the 21st Century, 26–29 May, Woods Hole, MA.
- Duncan, R.A., 1985. Radiometric ages from volcanic rocks along the New Hebrides-Samoa lineament. In Brocher, T.M. (Ed.), *Geological Investigations of the Northern Melanesian Borderland*. Circum-Pac. Coun. Energy and Miner. Resour., Earth Sci. Ser., 3:67–76.
- Duncan, R.A., and Clague, D.A., 1985. Pacific plate motion recorded by linear volcanic chains. In Nairn, A.E.M., Stehli, F.G., and Uyeda, S. (Eds.), *The Ocean Basins and Margins* (Vol. 7A): *The Pacific Ocean*: New York (Plenum), 89–121.
- Furumoto, A.S., Webb, J.P., Odegard, M.E., and Hussong, D.M., 1976. Seismic studies on the Ontong Java Plateau, 1970. *Tectonophysics*, 34:71–90.
- Gladchenko, T.P., Coffin, M., and Eldholm, O., 1997. Crustal structure of the Ontong Java Plateau: modeling of new gravity and existing seismic data. *J. Geophys. Res.*, 102:22711–22729.
- Gradstein, F.M., Agterberg, F.P., Ogg, J.G., Hardenbol, J., van Veen, P., Thierry, J., and Huang, Z., 1995. A Triassic, Jurassic and Cretaceous time scale. In Berggren, W.A., Kent, D.V., Aubry, M.P., and Hardenbol, J. (Eds.), *Geochronology, Time Scales and Global Stratigraphic Correlation*, Spec. Publ.—Econ. Paleontol. Mineral., 54:95–126.
- Hammond, S.R., Kroenke, L.W., and Theyer, F., 1975. Northward motion of the Ontong-Java Plateau between –110 and –30 m.y.: a paleomagnetic investigation of DSDP Site 289. In Andrews, J.E., Packham, G., et al., *Init. Repts. DSDP*, 30: Washington (U.S. Govt. Printing Office), 415–418.
- Hardarson, B.S., and Fitton, J.G., 1997. Mechanisms of crustal accretion in Iceland. *Geology*, 25:1043–1046.
- Hèmond, C., Arndt, N.T., Lichtenstein, U., Hofmann, A.W., Oskarsson, N., and Steinthorsson, S., 1993. The heterogeneous Iceland plume: Nd:Sm:O isotopes and trace element constraints. *J. Geophys. Res.*, 98:15833–15850.
- Hilde, T.W.C., Uyeda, S., and Kroenke, L., 1977. Evolution of the western Pacific and its margin. *Tectonophysics*, 38:145–165.
- Hill, R.I., 1991. Starting plumes and continental break-up. *Earth Planet. Sci. Lett.*, 104:398–416.
- Honnorez, J., 1981. The aging of the oceanic crust at low temperature. In Emiliani, C. (Ed.), *The Sea* (Vol. 7): *The Oceanic Lithosphere*: New York (Wiley), 525–587.
- Hooper, P.R., 1997. The Columbia River flood basalt province: current status. In Mahoney, J.J., and Coffin, M.F. (Eds.), *Large Igneous Provinces: Continental, Oceanic and Planetary Flood Volcanism*. Geophys. Monogr., Am. Geophys. Union, 100:1–28.
- Hussong, D.M., Wiperman, L.K., and Kroenke, L.W., 1979. The crustal structure of the Ontong Java and Manahiki oceanic plateaus. *J. Geophys. Res.*, 84:6003–6010.
- International Hydrographic Organization/Intergovernmental Oceanographic Commission (IHO/IOC), 1997. *General Bathymetric Chart of the Ocean (GEBCO) Digital Atlas*: London (British Oceanographic Data Centre).
- Ito, G., and Clift, P.D., 1998. Subsidence and growth of Pacific Cretaceous plateaus. *Earth Planet. Sci. Lett.*, 161:85–100.
- Ito, G., and Taira, A., 2000. Compensation of the Ontong Java Plateau by surface and subsurface loading. *J. Geophys. Res.*, 105:11171–11183.
- Jones, C.E., Jenkyns, H.C., Coe, A.L., and Hesselbo, S.P., 1994. Strontium isotopic variations in Jurassic and Cretaceous seawater. *Geochim. Cosmochim. Acta*, 58:3063–3074.
- Kerr, A.C., 1998. Oceanic plateau formation: a cause of mass extinction and black shale deposition around the Cenomanian–Turonian boundary? *J. Geol. Soc. London*, 155:619–626.

- Kroenke, L.W., 1972. Geology of the Ontong-Java Plateau. *Hawaii Inst. Geophys. Rep. HIG*, 72–75.
- Kroenke, L.W., 1974. Origin of continents through development and coalescence of oceanic flood basalt plateaus. *Eos*, 55:443.
- Kroenke, L.W., Berger, W.H., Janecek, T.R., et al., 1991. *Proc. ODP, Init. Repts.*, 130: College Station, TX (Ocean Drilling Program).
- Kroenke, L.W., and Mahoney, J.J., 1996. Rifting of the Ontong Java Plateau's eastern salient and seafloor spreading in the Ellice Basin: relation to the 90 Myr eruptive episode on the plateau. *Eos*, 77F:713.
- Larson, R.L., and Erba, E., 1999. Onset of the Mid-Cretaceous greenhouse in the Barremian–Aptian: igneous events and the biological, sedimentary and geochemical responses. *Paleoceanography*, 14:663–678.
- Larson, R.L., and Kincaid, C., 1996. Onset of Mid-Cretaceous volcanism by elevation of the 670 km thermal boundary layer. *Geology*, 24:551–554.
- Le Bas, M.J., Le Maitre, R.W., Streckeisen, A., and Zanettin, B., 1986. A chemical classification of volcanic rocks based on the total alkali-silica diagram. *J. Petrol.*, 27:745–750.
- Macdonald, G.A., and Katsura, T., 1964. Chemical composition of Hawaiian lavas. *J. Petrol.*, 5:82–133.
- Mahoney, J.J., 1987. An isotopic survey of Pacific oceanic plateaus: implications for their nature and origin. In Keating, B.H., Fryer, P., Batiza, R., and Boehlert, G.W. (Eds.), *Seamounts, Islands, and Atolls*. Geophys. Monogr., Am. Geophys. Union, 43:207–220.
- Mahoney, J.J., and Spencer, K.J., 1991. Isotopic evidence for the origin of the Manihiki and Ontong-Java oceanic plateaus. *Earth Planet. Sci. Lett.*, 104:196–210.
- Mahoney, J.J., Storey, M., Duncan, R.A., Spencer, K.J., and Pringle, M.S., 1993. Geochemistry and age of the Ontong Java Plateau. In Pringle, M.S., Sager, W.W., Sliter, W.V., and Stein, S. (Eds.), *The Mesozoic Pacific: Geology, Tectonics, and Volcanism*. Geophys. Monogr., Am. Geophys. Union, 77:233–262.
- Mann, P., Gahagan, L., Coffin, M., Shipley, T., Cowley, S., and Phinney, E. 1996. Regional tectonic effects resulting from the progressive east-to-west collision of the Ontong Java Plateau with the Melanesian arc system. *Eos*, 77F:712.
- Mayer, H., and Tarduno, J.A., 1993. Paleomagnetic investigation of the igneous sequence, Site 807, Ontong Java Plateau, and a discussion of Pacific true polar wander. In Berger, W.H., Kroenke, L.W., Mayer, L.A., et al., *Proc. ODP, Sci. Results*, 130: College Station, TX (Ocean Drilling Program), 51–59.
- McNutt, M., Austin, J., Bercovici, D., et al., 1996. Report of NSF planning workshop, Intraplate Marine Geoscience: Hot Lips and Cracked Plates, Steamboat Springs, CO.
- Michael, P.J., 1999. Implications for magmatic processes at Ontong Java Plateau from volatile and major element contents of Cretaceous basalt glasses. *Geochemistry, Geophysics, Geosystems*, 1 (Article), 1999GC000025.
- Miura, S., Shinohara, M., Takahashi, N., Araki, E., Taira, A., Suyehiro, K., Coffin, M., Shipley, T., and Mann, P., 1996. OBS crustal structure of Ontong Java Plateau converging into Solomon island arc. *Eos*, 77F:713.
- Moore, J.G., and Schilling, J.-G., 1973. Vesicles, water, and sulfur in Reykjanes Ridge basalts. *Contrib. Mineral. Petrol.*, 41:105–118.
- Neal, C.R., Birkhold, A.L., Mahoney, J.J., and Duncan, R.A., 2000. Episodic growth of the Ontong Java Plateau through a single plume event and lithospheric extension. *Proc. Geol. Soc. Am. Penrose Conf. on Volcanic Rifted Margins*: London, 62–63.
- Neal, C.R., Mahoney, J.J., Kroenke, L.W., Duncan, R.A., and Petterson, M.G., 1997. The Ontong Java Plateau. In Mahoney, J.J., and Coffin, M.F. (Eds.), *Large Igneous Provinces: Continental, Oceanic, and Planetary Flood Volcanism*. Am. Geophys. Union, Geophys. Monogr., 100:183–216.
- Nixon, P.H., 1980. Kimberlites in the South-west Pacific. *Nature*, 287:718–720.

- Nixon, P.H., and Neal, C.R., 1987. Ontong Java Plateau: deep-seated xenoliths from thick oceanic lithosphere. *In* Nixon, P.H. (Ed.), *Mantle Xenoliths*: Chichester, U.K. (John Wiley & Sons), 335–345.
- Parkinson, I.J., Arculus, R.J., and Duncan, R.A., 1996. Geochemistry of Ontong Java Plateau basalt and gabbro sequences, Santa Isabel, Solomon Islands. *Eos*, 77F:715.
- Petterson, M.G., Babbs, T., Neal, C.R., Mahoney, J.J., Saunders, A.D., Duncan, R.A., Tolia, D., Magu, R., Qopoto, C., Mahoa, H., and Natogga, D., 1999. Geological-tectonic framework of Solomon Islands, SW Pacific: crustal accretion and growth within an intra-oceanic setting. *Tectonophysics*, 301:35–60.
- Petterson, M.G., Neal, C.R., Mahoney, J.J., Kroenke, L.W., Saunders, A.D., Babbs, T.L., Duncan, R.A., Tolia, D., and McGrail, B., 1997. Structure and deformation of north and central Malaita, Solomon Islands: tectonic implications for the Ontong Java Plateau-Solomon arc collision, and for the fate of oceanic plateaus. *Tectonophysics*, 283:1–33.
- Phinney, E.J., Mann, P., Coffin, M.F., and Shipley, T.H., 1999. Sequence stratigraphy, structure, and tectonic history of the southwestern Ontong Java Plateau adjacent to the North Solomon Trench and Solomon Islands arc. *J. Geophys. Res.*, 104:20449–20466.
- Polat, A., Kerrich, R., and Wyman, D.A., 1999. Geochemical diversity in oceanic komatiites and basalts from the late Archean Wawa greenstone belts, Superior Province, Canada: trace element and Nd isotope evidence for a heterogeneous mantle. *Precambrian Res.*, 94:139–173.
- Pringle, M.S., and Duncan, R.A., 2000. Basement ages from the Southern and Central Kerguelen Plateau: initial products of the Kerguelen large igneous province. *Eos*, 81:424.
- Richards, M.A., Jones, D.L., Duncan, R.A., and DePaolo, D.J., 1991. A mantle plume initiation model for the Wrangelia and other oceanic flood basalt plateaus. *Science*, 254:263–266.
- Richardson, W.P., Okal, E., and Van der Lee, S., 2000. Rayleigh-wave tomography of the Ontong-Java Plateau. *Phys. Earth Planet. Inter.*, 118:29–51.
- Sandwell, D.T., and Smith, W.H.F., 1997. Marine gravity anomaly from Geosat and ERS-1 satellite altimetry. *J. Geophys. Res.*, 102:10039–10054.
- Saunders, A.D., Storey, M., Kent, R.W., and Norry, M.J., 1992. Consequences of plume–lithosphere interactions. *In* Storey, B.C., Alabaster, T., and Pankhurst, R.J. (Eds.), *Magmatism and the Causes of Continental Break-up*. Spec. Publ.—Geol. Soc. London, 68:41–60.
- Saunders, A.D., Tarney, J., Kerr, A.C., and Kent, R.W., 1996. The formation and fate of large oceanic igneous provinces. *Lithos*, 37:81–95.
- Smith, A.D., 1993. The continental mantle as a source for hotspot volcanism. *Terra Nova*, 5:452–460.
- Smith, W.H.F., and Sandwell, D.T., 1997. Global seafloor topography from satellite altimetry and ship depth soundings. *Science*, 277:1956–1962.
- Stein, M., and Hofmann, A.W., 1994. Mantle plumes and episodic crustal growth. *Nature*, 372:63–68.
- Stoeser, D.B., 1975. Igneous rocks from Leg 130 of the Deep Sea Drilling Project. *In* Andrews, J.E., Packham, G., et al., *Init. Repts., DSDP*, 30: Washington (U.S. Govt. Printing Office), 401–414.
- Storey, M., Mahoney, J.J., Kroenke, L., and Saunders, A.D., 1991. Are oceanic plateaus sites of komatiite formation? *Geology*, 19:376–379.
- Tarduno, J.A., Brinkman, D.B., Renne, P.R., Cottrell, R.D., Scher, H., and Castillo, P., 1998. Evidence for extreme climatic warmth from Late Cretaceous Arctic vertebrates. *Science*, 282:2241–2244.
- Tarduno, J.A., Sliter, W.V., Kroenke, L., Leckie, M., Mayer, H., Mahoney, J.J., Musgrave, R., Storey, M., and Winterer, E.L., 1991. Rapid formation of Ontong Java Plateau by Aptian mantle plume volcanism. *Science*, 254:399–403.

- Tejada, M.L., Mahoney, J.J., Neal, C.R., Duncan, R.A., and Petterson, M.G., in press. Basement geochemistry and geochronology of central Malaita, Solomon Islands, with implications for the origin and evolution of the Ontong Java Plateau. *J. Petrol.*
- Tejada, M.L.G., Mahoney, J.J., Duncan, R.A., and Hawkins, M., 1996. Age and geochemistry of basement and alkalic rocks of Malaita and Santa Isabel, Solomon Islands, southern margin of Ontong Java Plateau. *J. Petrol.*, 37:361–394.
- White, R.S., and McKenzie, D., 1989. Magmatism at rift zones: the generation of volcanic continental margins and flood basalts. *J. Geophys. Res.*, 94:7685–7729.
- Winterer, E.L., 1976. Bathymetry and regional tectonic setting of the Line Islands Chain. In Schlanger, S.O., Jackson, E.D., et al., *Init. Repts., DSDP*, 33: Washington (U.S. Govt. Printing Office), 731–747.
- Winterer, E.L., and Nakanishi, M., 1995. Evidence for a plume-augmented, abandoned spreading center on Ontong Java Plateau. *Eos*, 76F:617.
- Yan, C.Y., and Kroenke, L.W., 1993. A plate tectonic reconstruction of the southwest Pacific, 0–100 Ma. In Berger, W.H., Kroenke, L.W., Mayer, L.A., et al., *Proc. ODP, Sci. Results*, 130: College Station, TX (Ocean Drilling Program), 697–709.

Figure F1. Predicted bathymetry (after Smith and Sandwell, 1997) of the Ontong Java Plateau showing the locations of sites drilled during Leg 192 (stars). The plateau is outlined. Black dots = previous ODP and DSDP drill sites that reached basement. White dots = Site 288, which did not reach basement but bottomed in Aptian limestone, and Site OJ-7, which was proposed for Leg 192 but not drilled. The bathymetric contour interval is 1000 m (IHO/IOC, 1997).

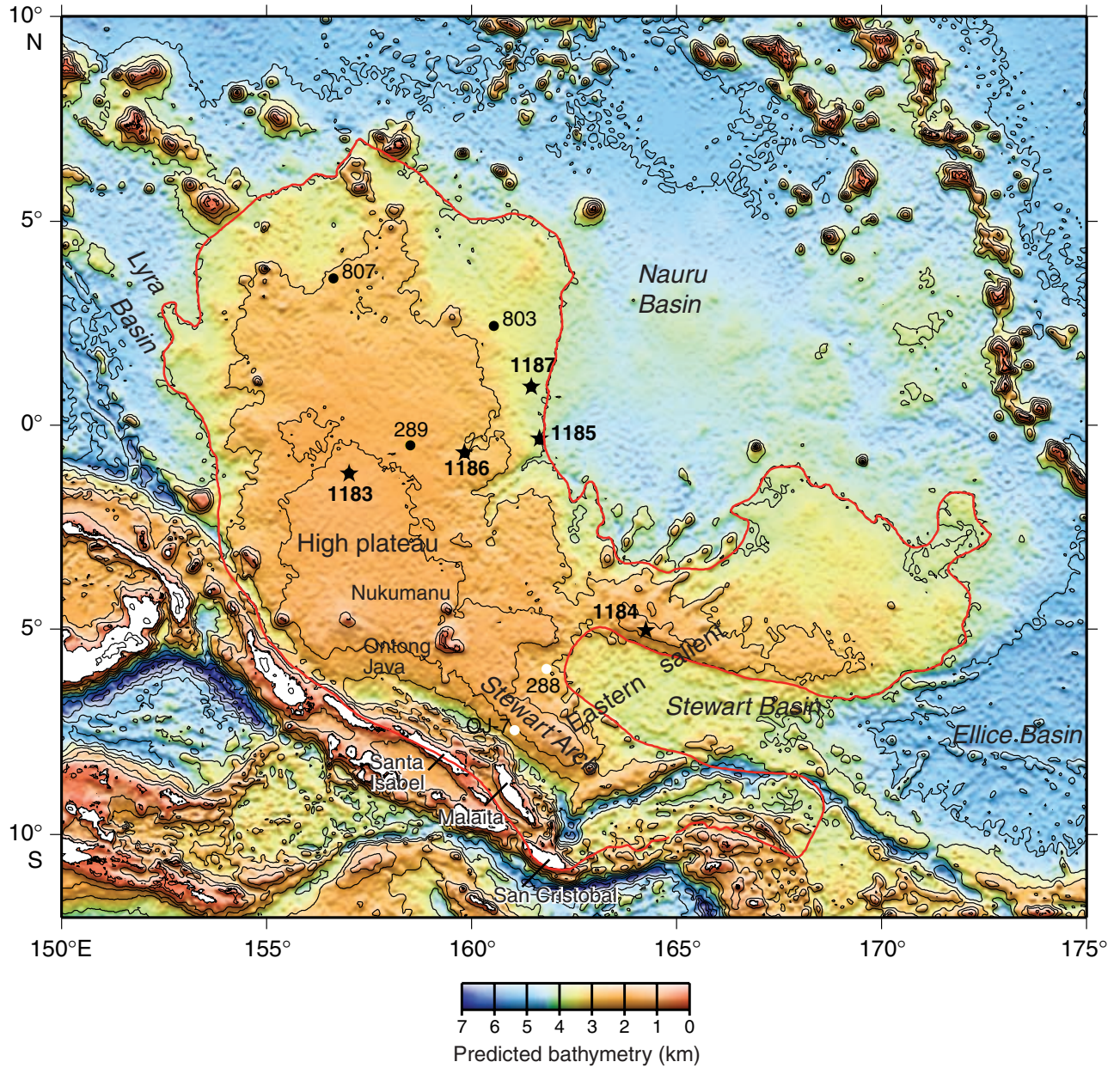


Figure F2. Satellite-derived free-air gravity field of the Ontong Java Plateau region (after Sandwell and Smith, 1997). The plateau is outlined. Stars = sites drilled during Leg 192. Black dots = previous ODP and DSDP drill sites that reached basement. White dots = Site 288, which did not reach basement but bottomed in Aptian limestone, and Site OJ-7, which was proposed for Leg 192 but not drilled. Black lines indicate multichannel seismic surveys on the plateau: *Hakuho Maru* KH98-1 Leg 2 (1998) and *Maurice Ewing* EW95-11 (1995). White lines indicate single-channel seismic surveys: *Glomar Challenger* GC07 (1969), GC30 (1973), and GC89 (1983); *Thomas Washington* TW88-11 (1988); and *JOIDES Resolution* JR130 (1990). The bathymetric contour interval is 1000 m.

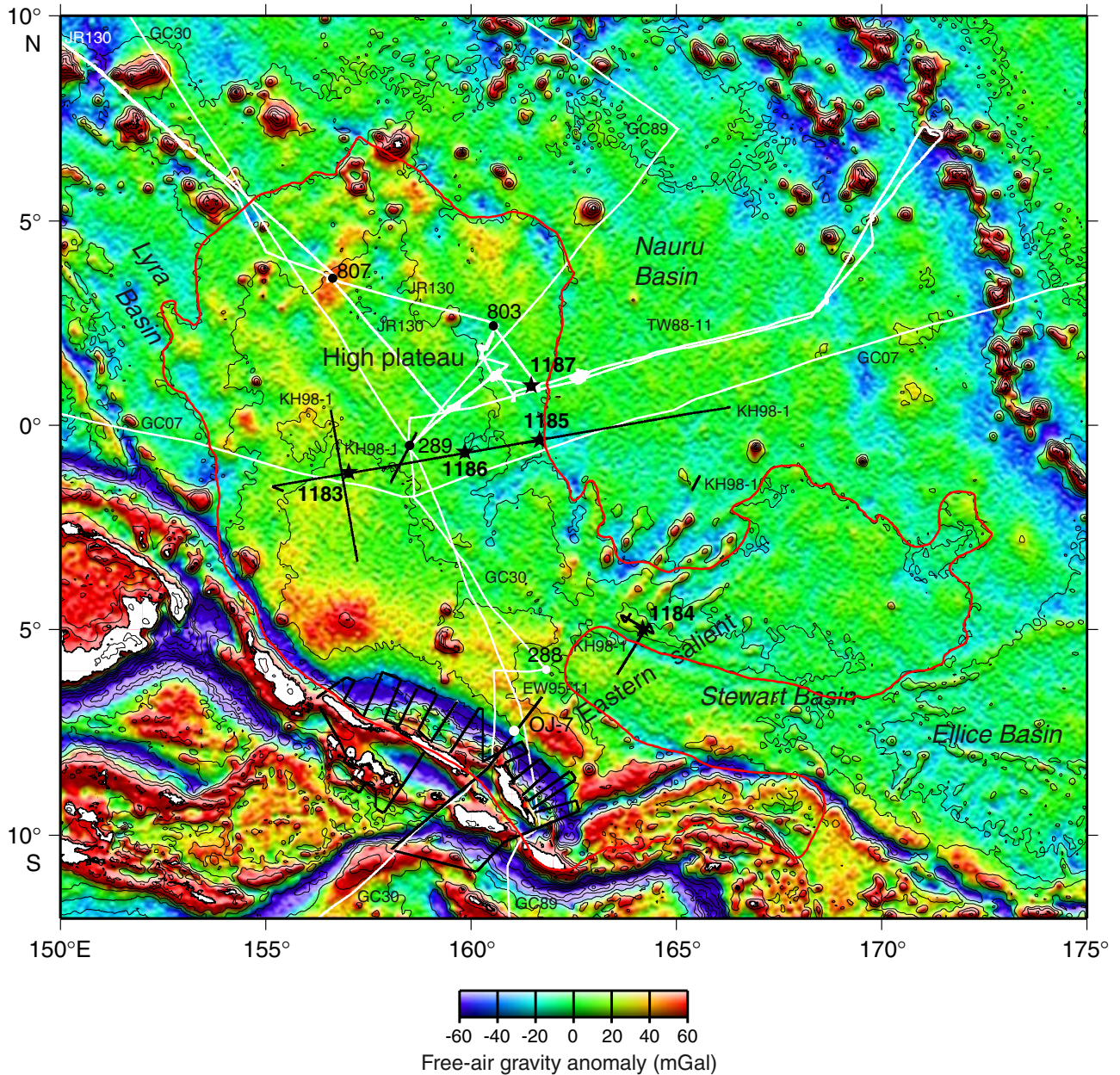


Figure F3. Summary of pre-Leg 192 age data for Ontong Java Plateau basement basalt, later lava flows and intrusions on Malaita and San Cristobal, and ash or glass-shard-rich layers within the sedimentary section at Sites 288 and 289 (Tejada et al., in press, and references therein). Ages derived from biostratigraphy are shown with error bars; the others are ^{40}Ar - ^{39}Ar plateau or, for the Malaitan alnöites, U-Pb zircon ages. Open squares = values reported by Parkinson et al. (1996).

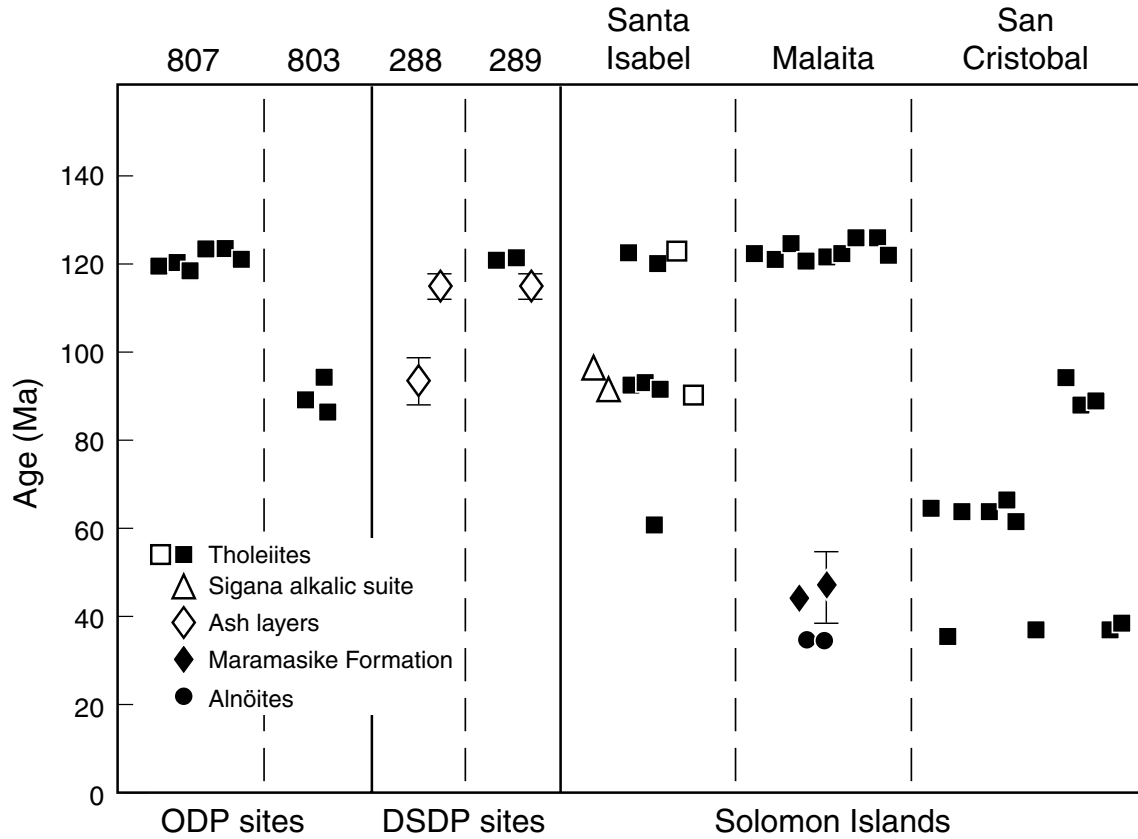


Figure F4. Total alkalis vs. silica diagram (after Le Bas, 1986) for basement rocks recovered at DSDP Site 289 and ODP Sites 803 and 807 on the Ontong Java Plateau. Data are from Stoesser (1975) and Mahoney et al. (1993). The broken line separates Hawaiian alkalic and tholeiitic basalts (Macdonald and Katsura, 1964).

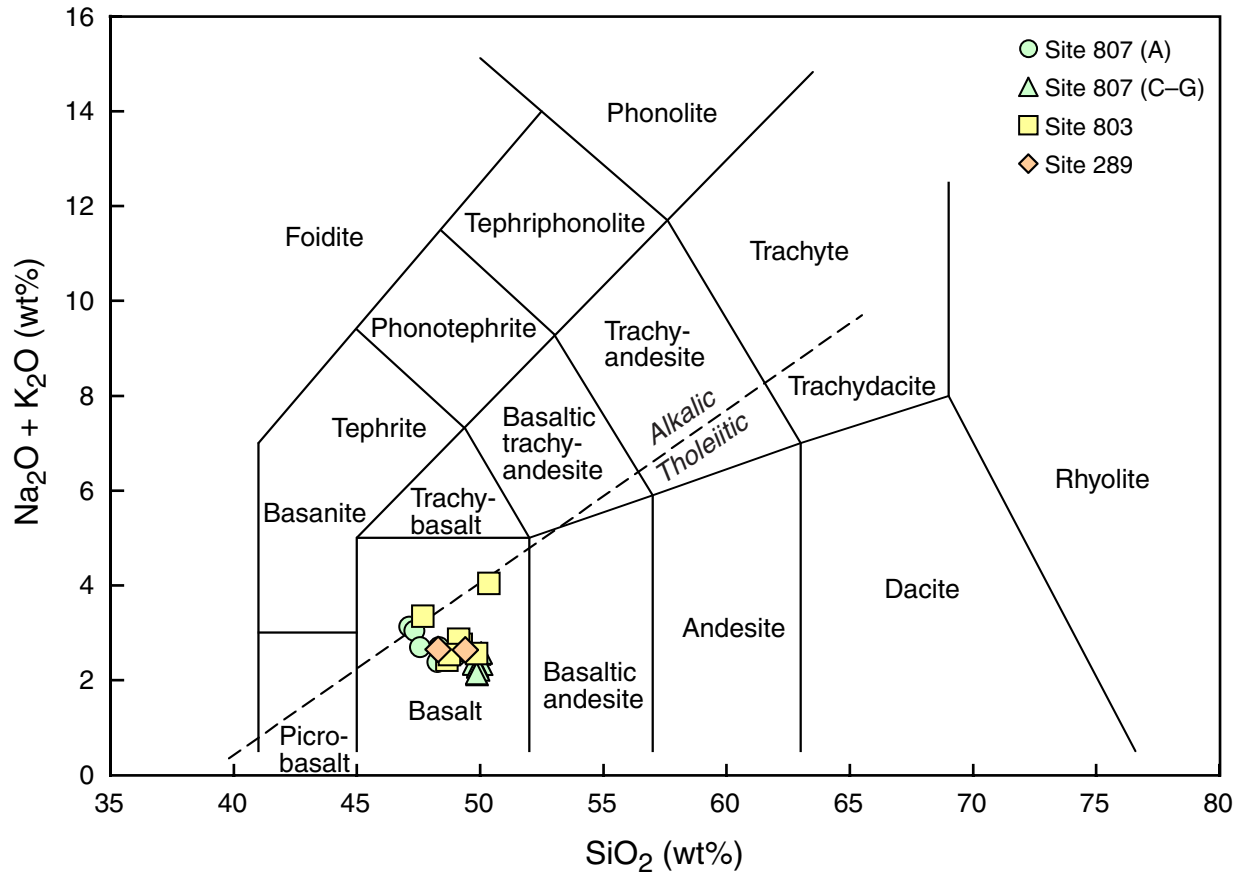


Figure F5. Primitive mantle–normalized incompatible-element averages for basalts of Malaita, Santa Isabel (plus Ramos), and ODP Sites 803 and 807. Shaded fields indicate range of values for central Malaita. Modified from Tejada et al. (in press).

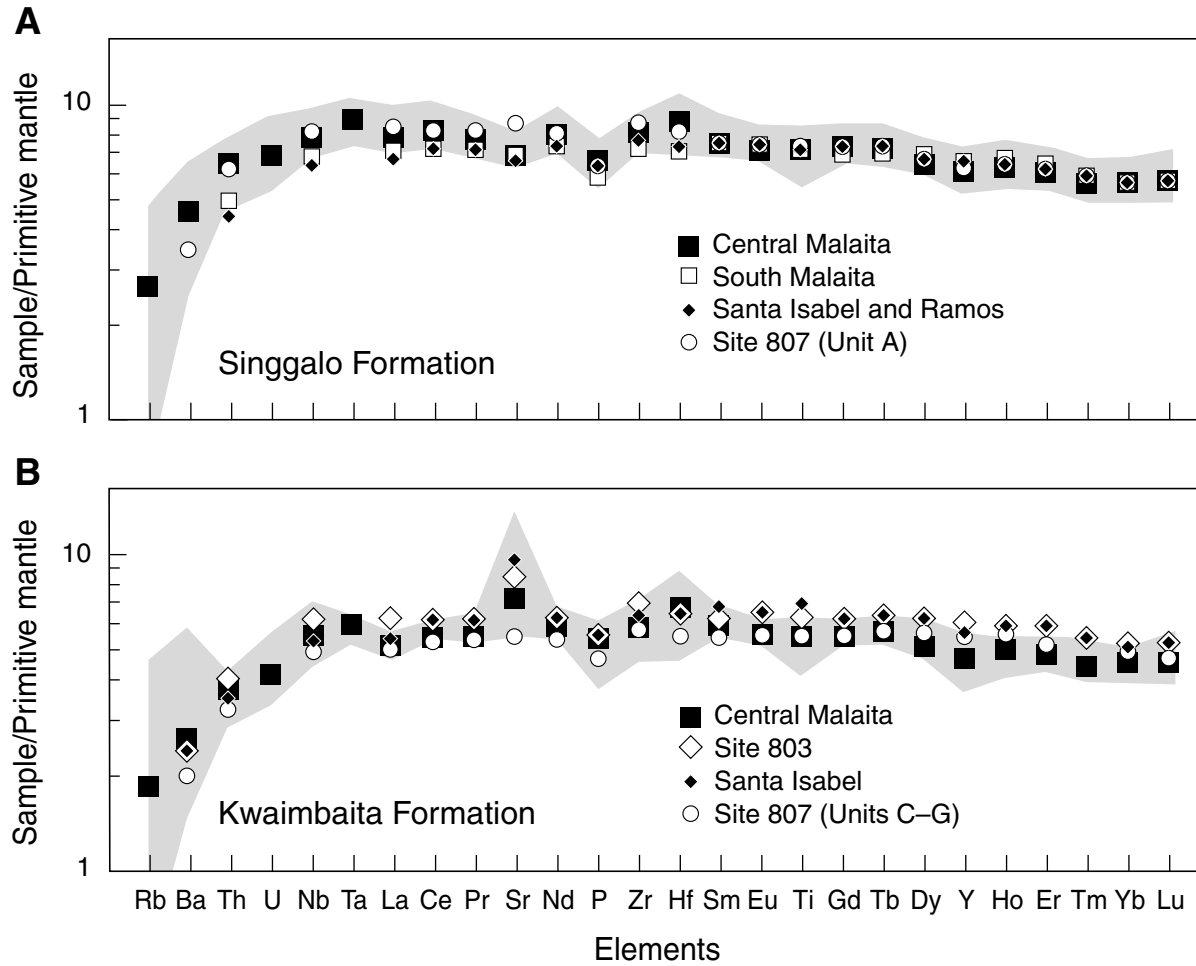


Figure F6. Initial $\epsilon_{Nd}(t)$ vs. $(^{206}Pb/^{204}Pb)_t$ data for basement lava flows of Santa Isabel and Malaita. Heavily outlined fields encompass data for ODP Site 807 basement Unit A and Sites 803 and 807, Units C–G. Data for the Site 289 basalt lie in the latter field. Data fields for the Manihiki Plateau (for dredged and DSDP Site 317 lava flows), Nauru Basin, Pacific mid-ocean-ridge basalts (MORB), the Koolau and Kilauea volcanoes of Hawaii, and the Mangaia Group islands of the South Pacific are shown by light outlines (after Tejada et al., in press).

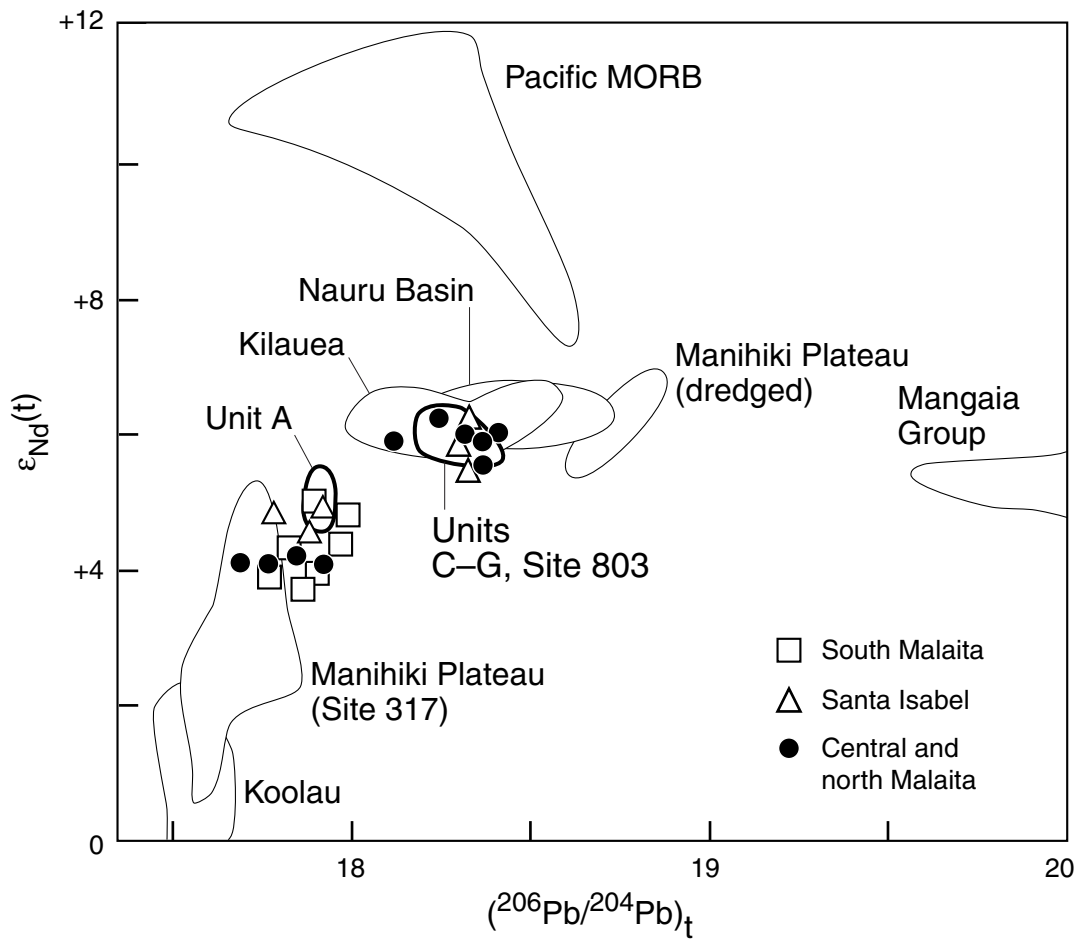


Figure F7. *Hakuho Maru* KH98-1 Leg 2, Line 404, multichannel seismic reflection profile across Site 1183 (see Fig. F2, p. 37, for location). Vertical exaggeration = ~4.2 at seafloor. UTC = Universal Time Coordinated.

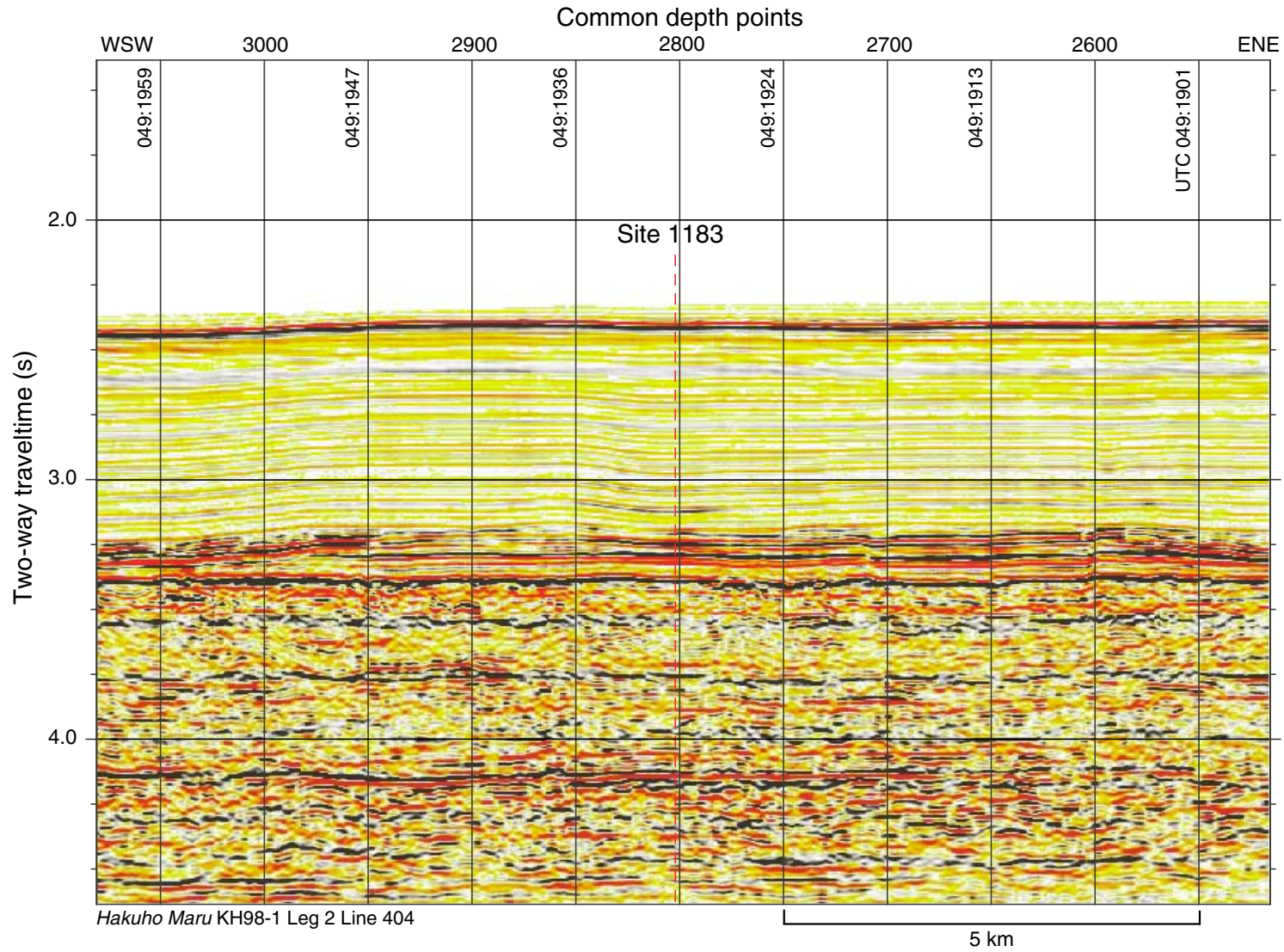


Figure F8. Site 1183 log showing core recovery, lithostratigraphic divisions, schematic lithology, color reflectance, magnetic susceptibility, and carbonate content.

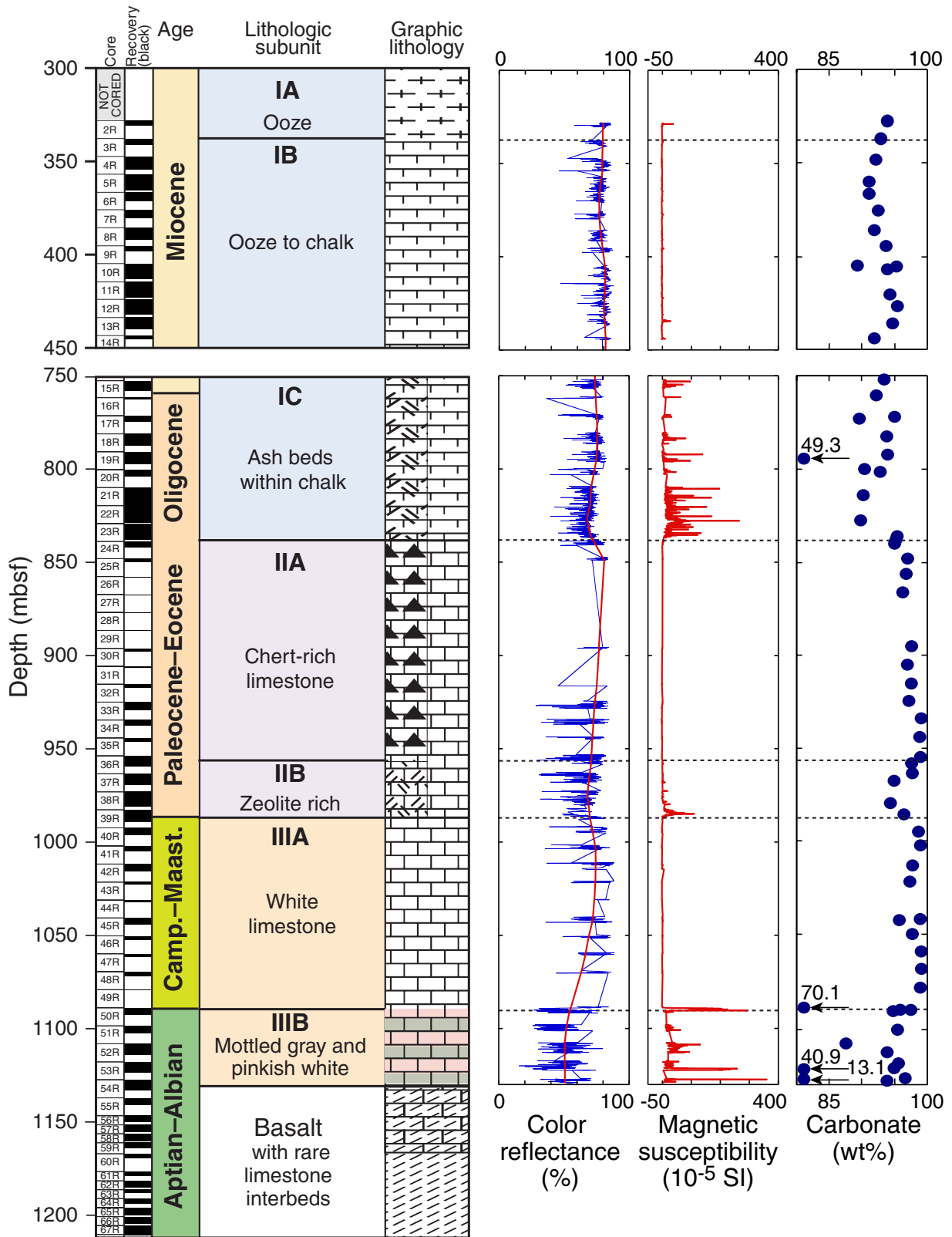


Figure F9. Lithologic log of the basement units in Hole 1183A showing the distribution of plagioclase-rich xenoliths, glassy pillow margins, and phenocrysts. Basalt units with the suffix B were delineated by the presence of thin sedimentary interbeds, which are designated as Subunit A (not shown).

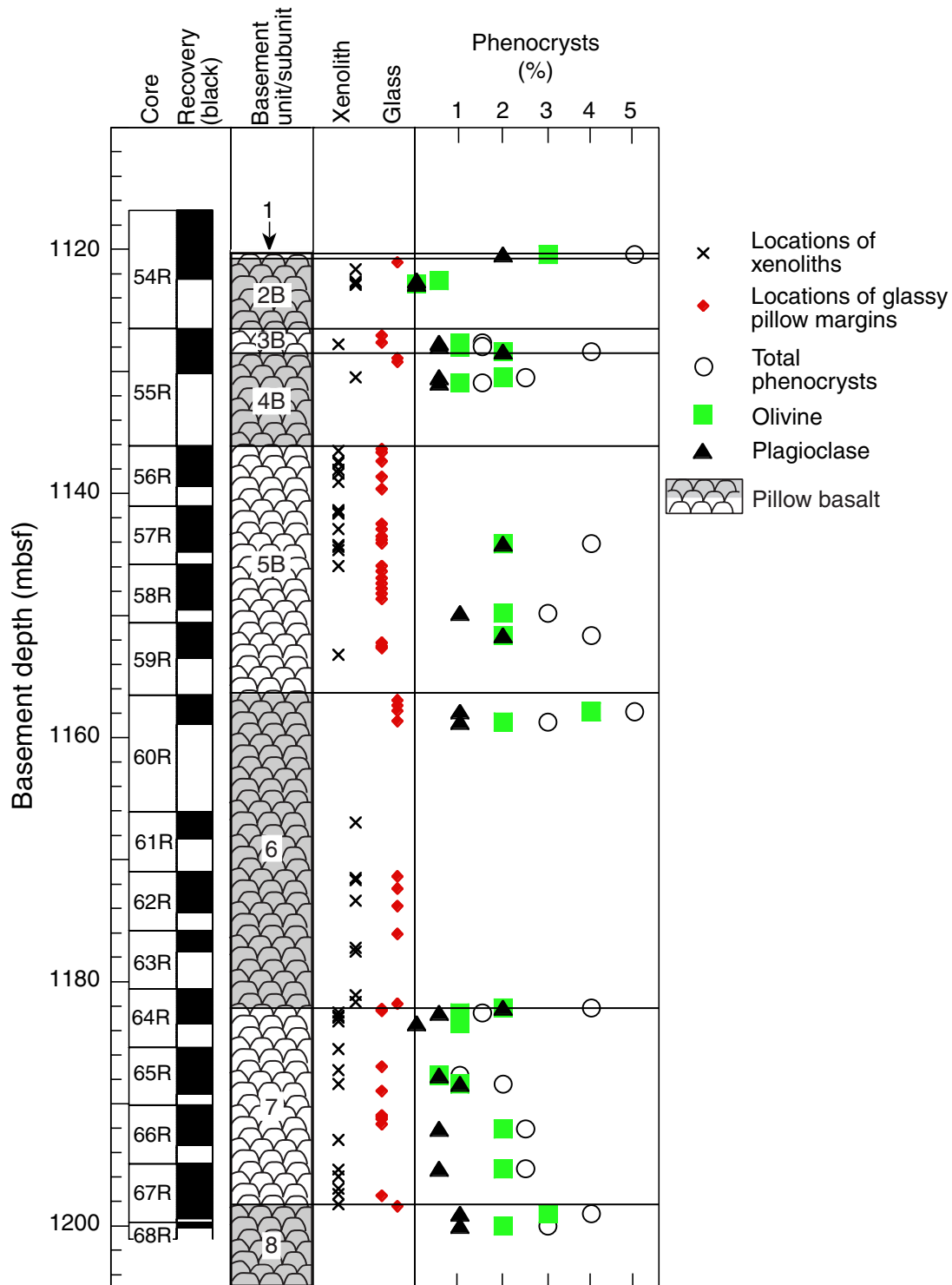


Figure F10. Total alkalis vs. silica diagram (after Le Bas, 1986) for basement rocks recovered at all Leg 192 sites. The broken line separates Hawaiian alkalic and tholeiitic basalts (Macdonald and Katsura, 1964).

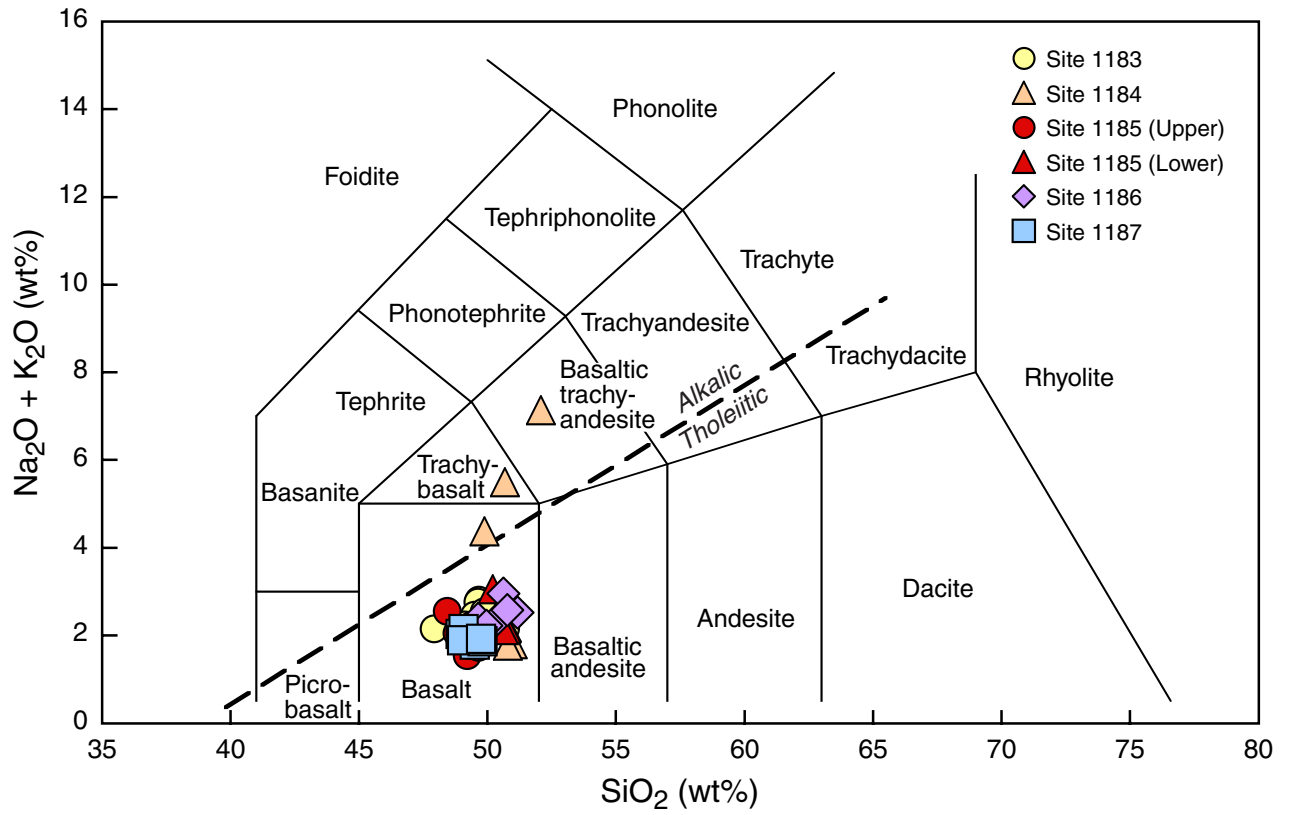


Figure F11. TiO_2 vs. Mg# for basement rocks recovered at all Leg 192 sites and ODP Sites 803 and 807. Mg# = atomic $\text{Mg}/(\text{Mg}+\text{Fe}^{2+})$. The fields for basaltic lava flows of the >2.7-km-thick Kwaimbaita Formation and the overlying ~750-m-thick Singgalo Formation on Malaita (Tejada et al., 1996, in press) are shown for comparison. Data for Sites 803 and 807 are from Mahoney et al. (1993).

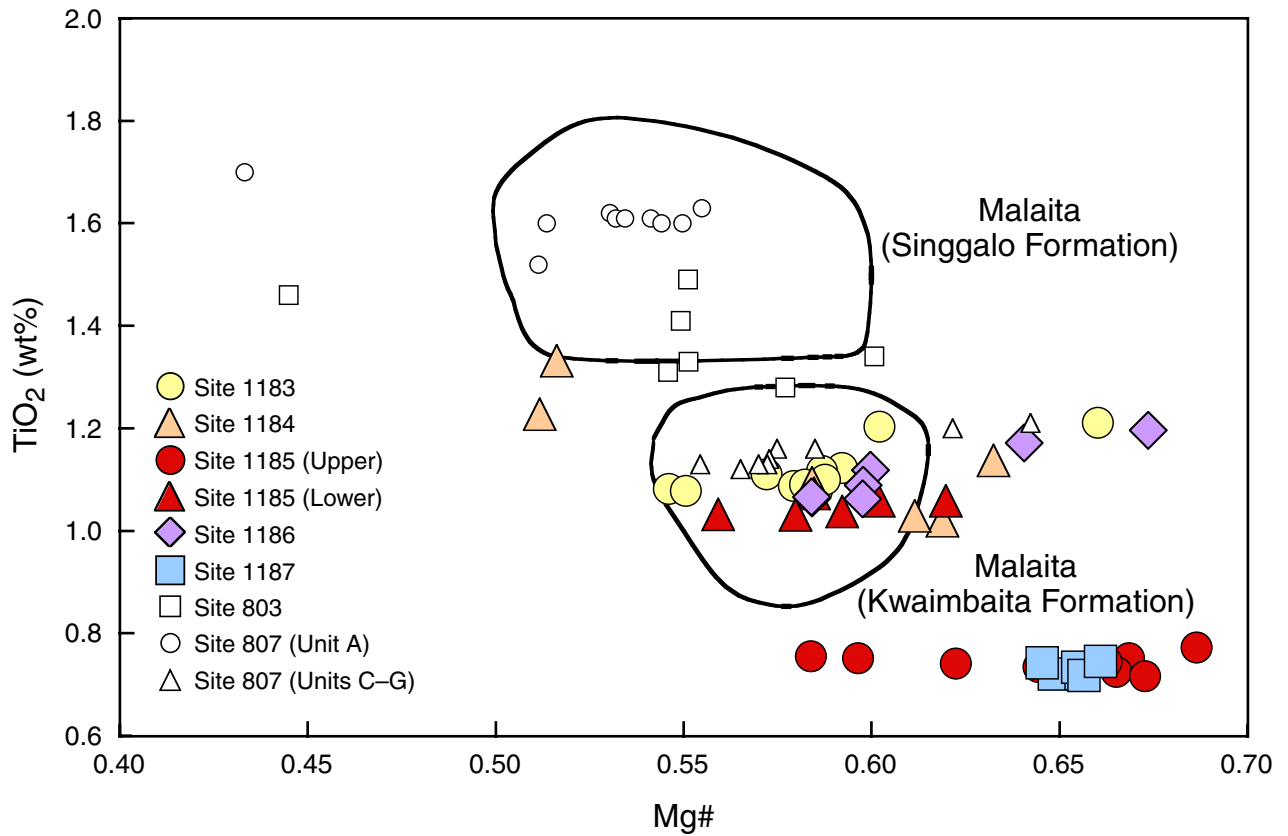


Figure F12. Zr vs. TiO_2 for basement rocks recovered at all Leg 192 sites, and ODP Sites 803 and 807. Data for Sites 803 and 807 are from Mahoney et al. (1993). The fields for the Kwaimbaita Formation and the overlying Singgalo Formation on Malaita (Tejada et al., 1996, in press) are shown for comparison.

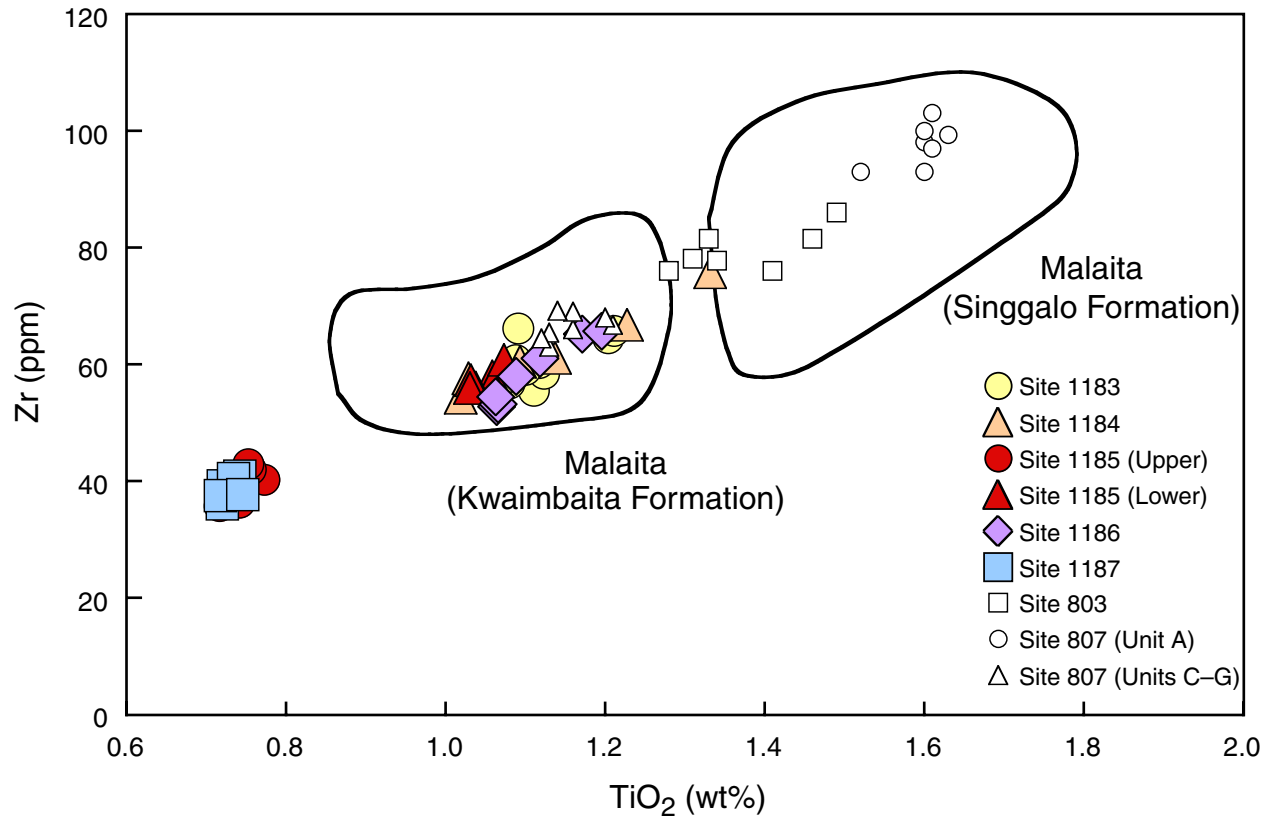


Figure F13. Cr vs. TiO_2 for basement rocks recovered at all Leg 192 sites, and ODP Sites 803 and 807. Data for Sites 803 and 807 are from Mahoney et al. (1993). The fields for the Kwaimbaita Formation and the overlying Singgalo Formation on Malaita (Tejada et al., 1996, in press) are shown for comparison.

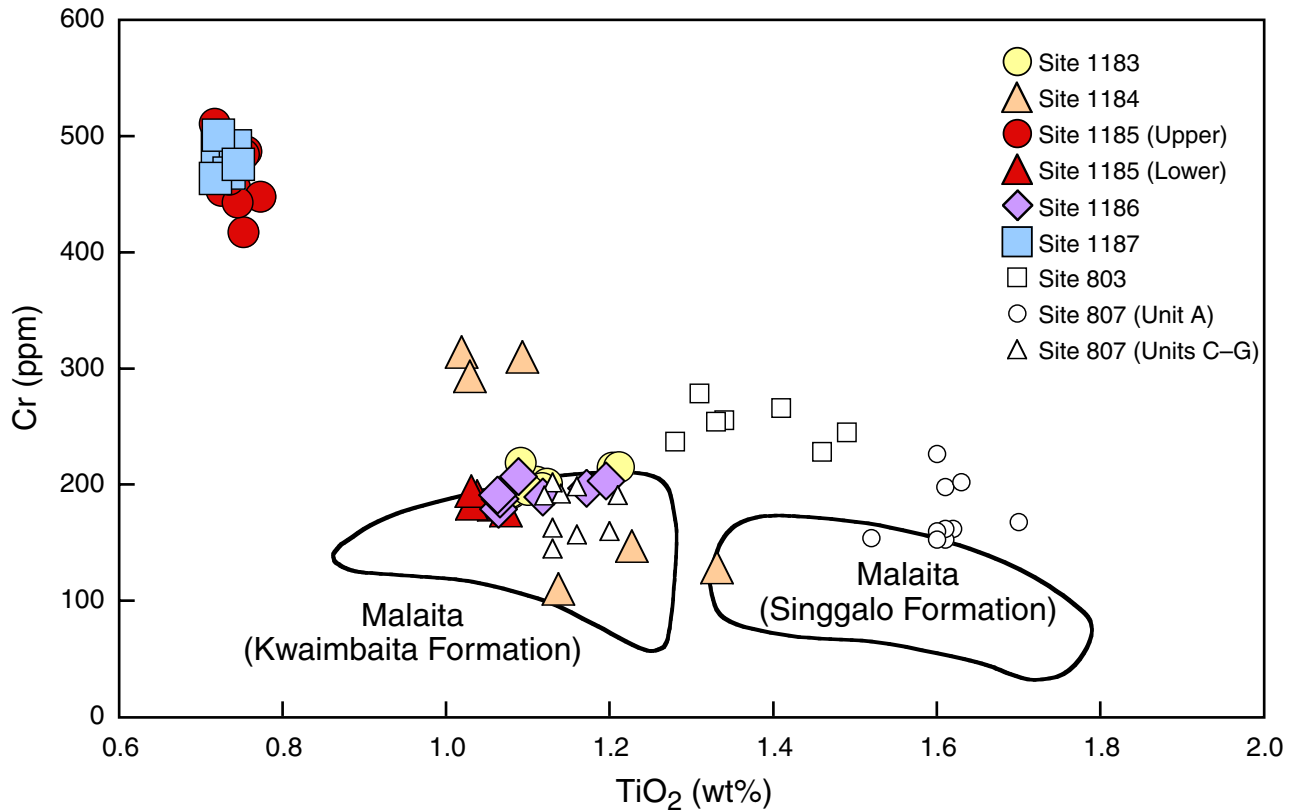


Figure F14. Close-up photograph showing a 1.5 cm × 3 cm plagioclase-rich xenolith on the outer surface of the core (interval 192-1183A-59R-2 [Piece 10A, 112–119 cm]).



Figure F15. Paleolatitude, calculated from paleomagnetic inclination, for cores from Hole 1183A. Data are plotted against biostratigraphic age.

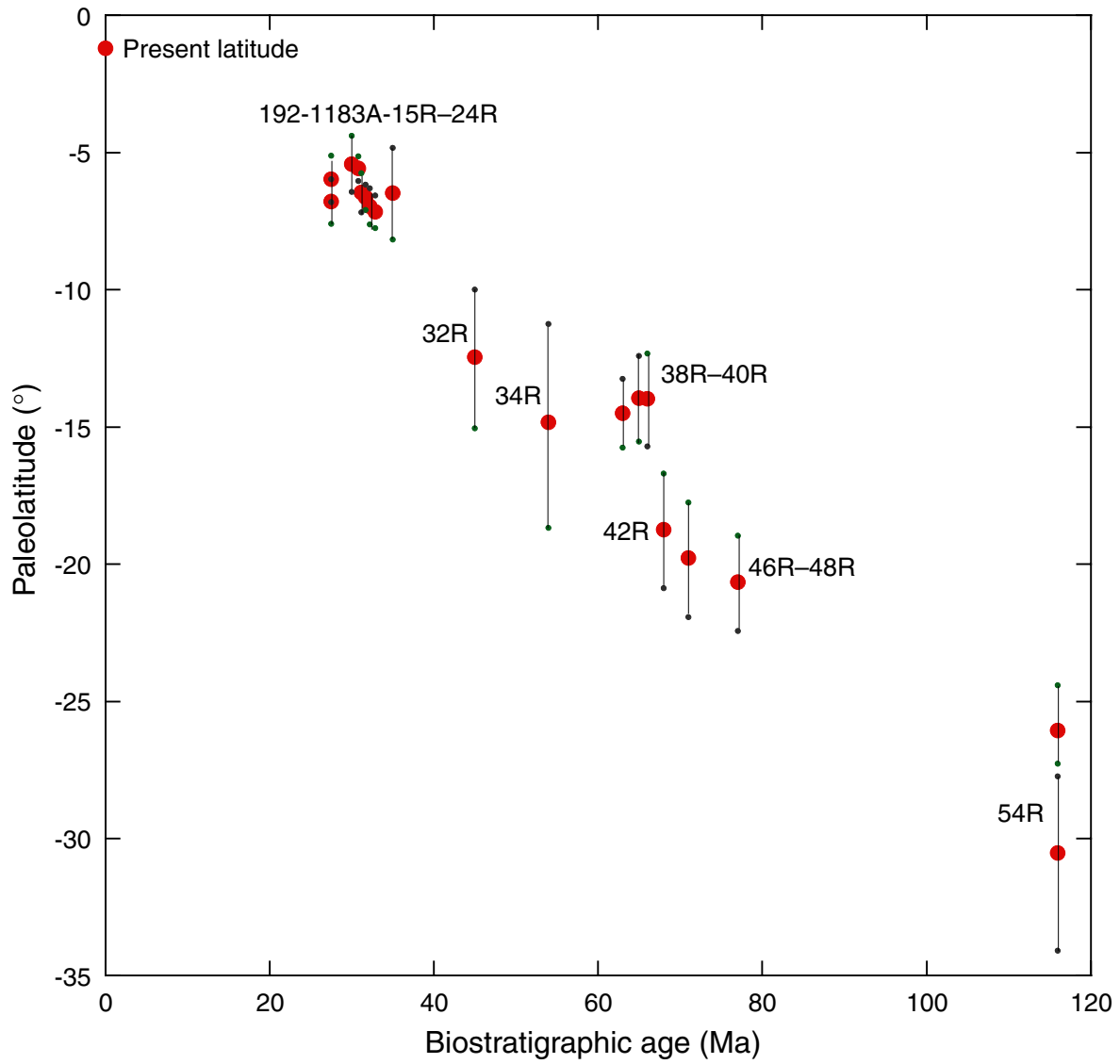


Figure F16. Seismic reflection record for Site 1184. *Hakuho Maru* KH98-1 Leg 2, Line 101, multichannel seismic reflection profile across Site 1184 (see Fig. F2, p. 37, for location). Vertical exaggeration = ~4.2 at seafloor. UTC = Universal Time Coordinated.

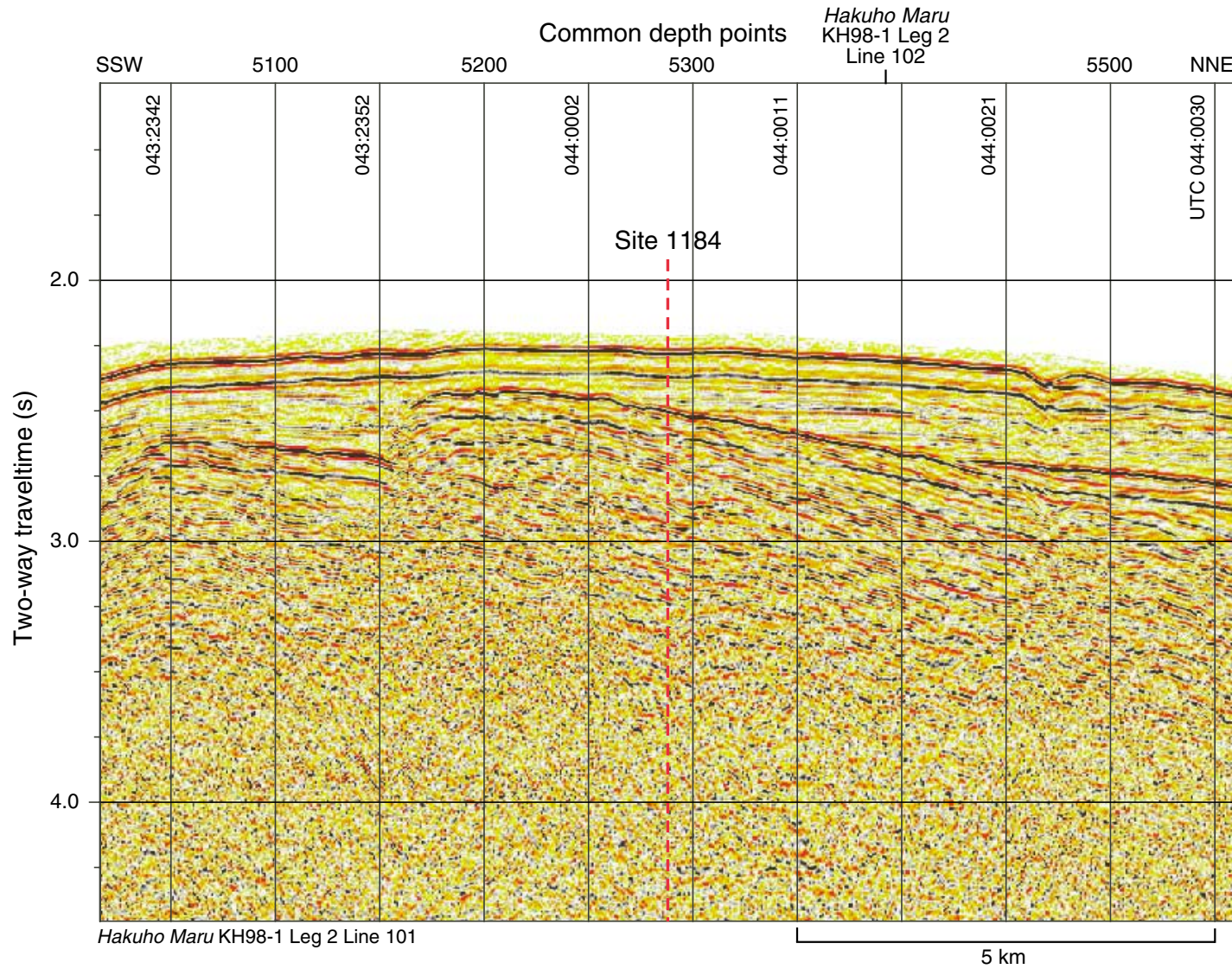


Figure F17. Summary of lithologic characteristics of the subunits of Unit II at Site 1184, based on the facies defined in Table T2, p. 75. "Wood" indicates approximate intervals in which pieces of wood were found. The uppermost interval is represented by two pieces, 1–2 cm long and <2 mm thick. At the other three wood-bearing levels, pieces of wood are as long as 6 cm. Red shading in the Graphic lithology column indicates red or yellow oxidized intervals. In the chromaticity plot, a = the variation between green (negative) and red (positive), and b = the variation between blue (negative) and yellow (positive) (Blum, 1997). See legend in Figure F10 in the "Site 1184" chapter.

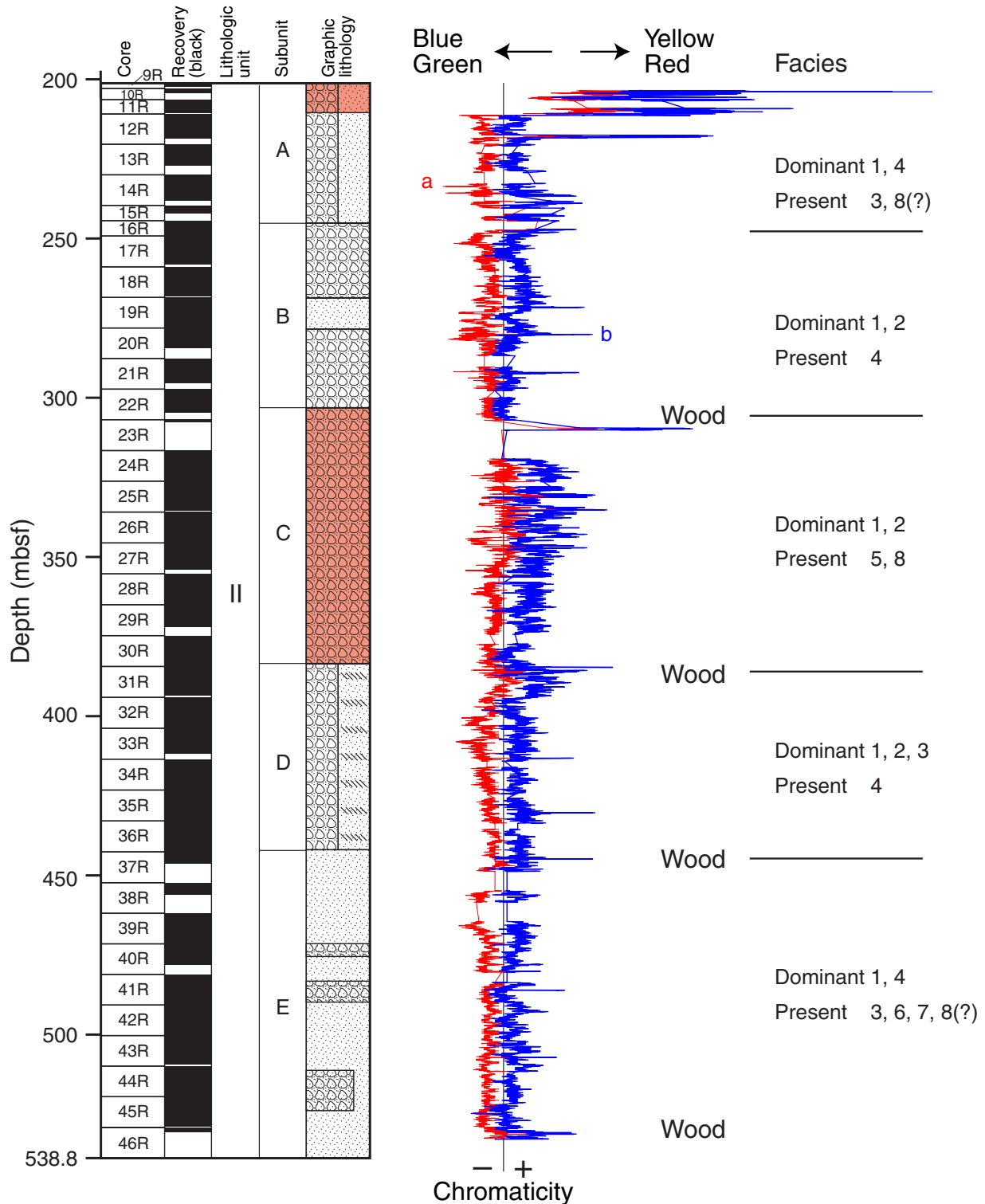


Figure F18. Close-up photograph of wood fragments in lithic vitric tuff near the base of Subunit IIE (interval 192-1184A-45R-7, 48–65 cm).

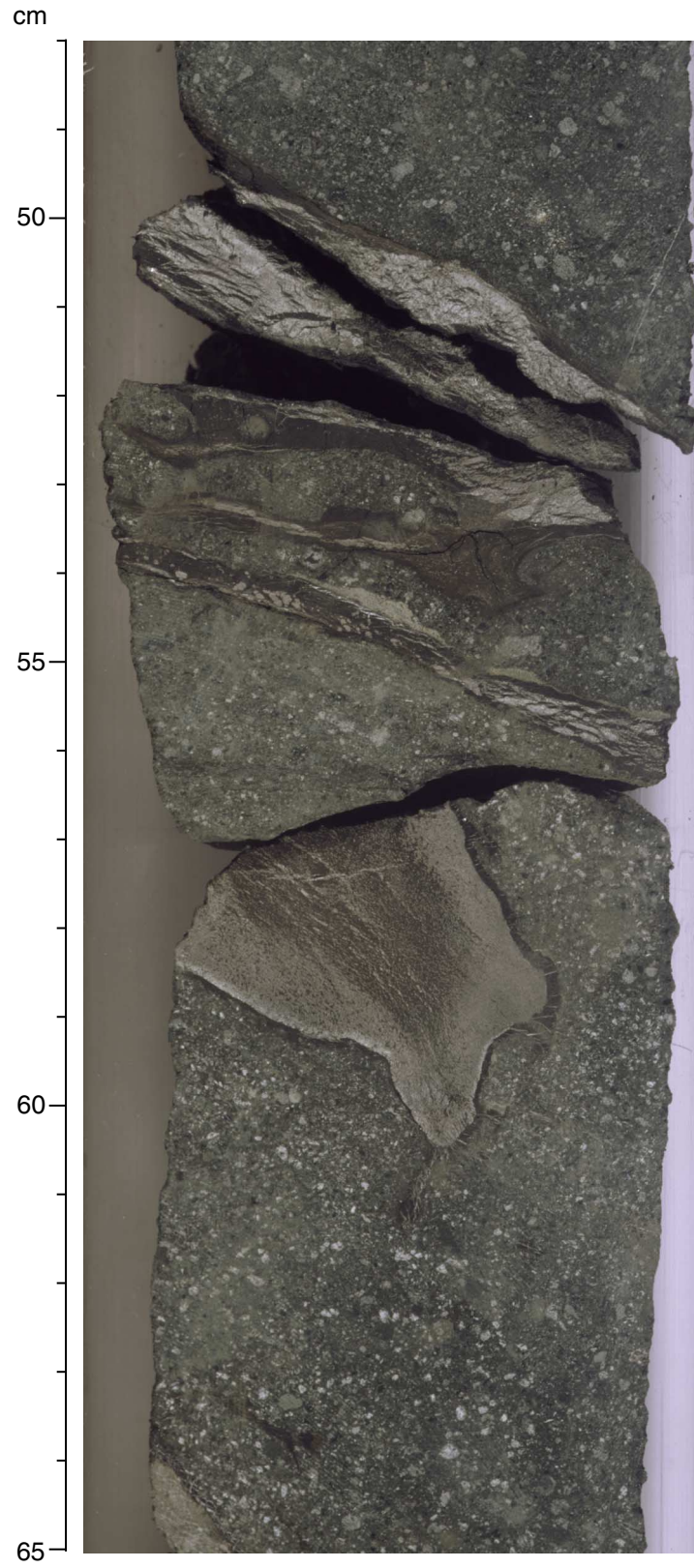


Figure F19. Photomicrograph showing a wide range of lithic and vitric clast types present in a lithic vitric tuff from Subunit IID (**Sample 192-1184A-31R-7, 40–43 cm**). The clasts include glass shards (light brown), basalt, and tachylite (black). The glass is completely altered to smectite, and the matrix is composed mainly of zeolite (plane-polarized light; photomicrograph ID# 1184A_076).

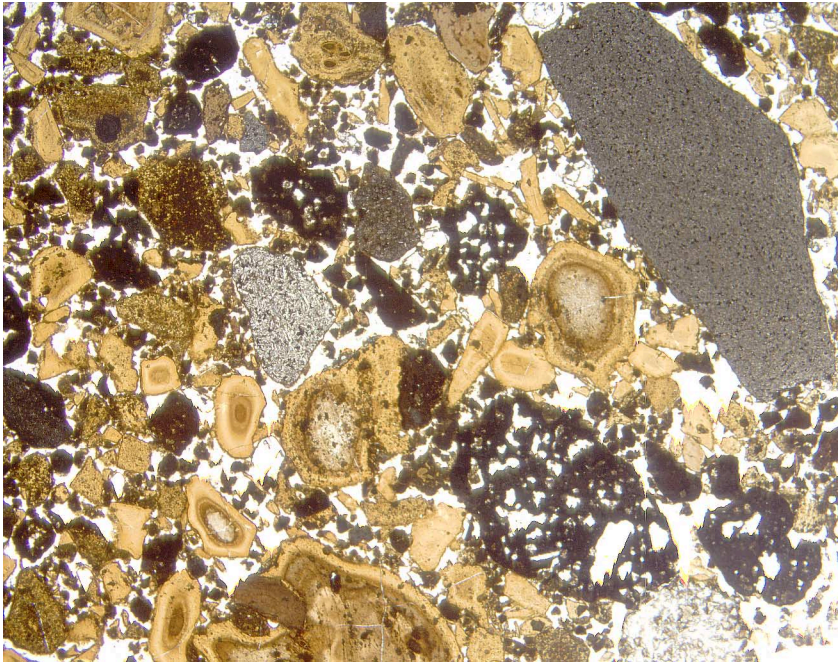


Figure F20. Close-up photograph of accretionary lapilli, both whole (round) and fragmented, in gray lithic vitric tuff, Subunit IIA (interval 192-1184A-14R-1, 58–66 cm).

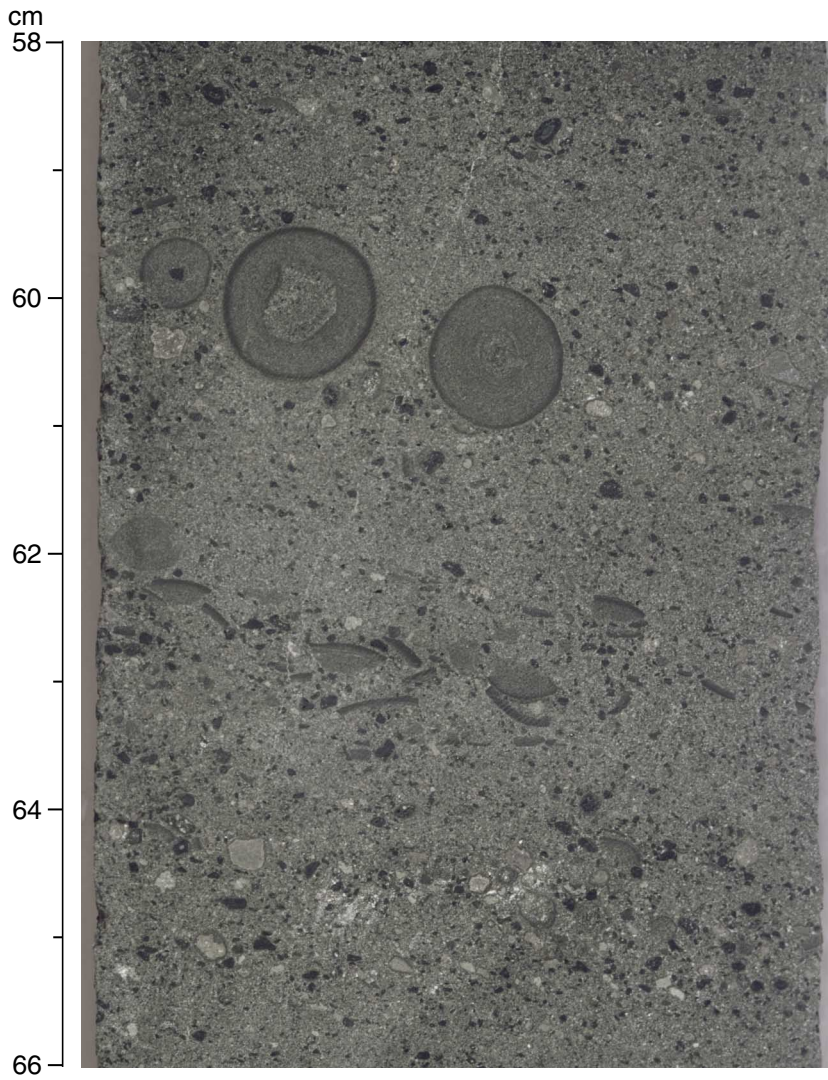


Figure F21. Close-up photograph of coarse (≤ 2 cm) angular clasts in lapilli tuff, Subunit IIB (interval 192-1184A-21R-6, 68–80 cm). The large pale clast is diabase.

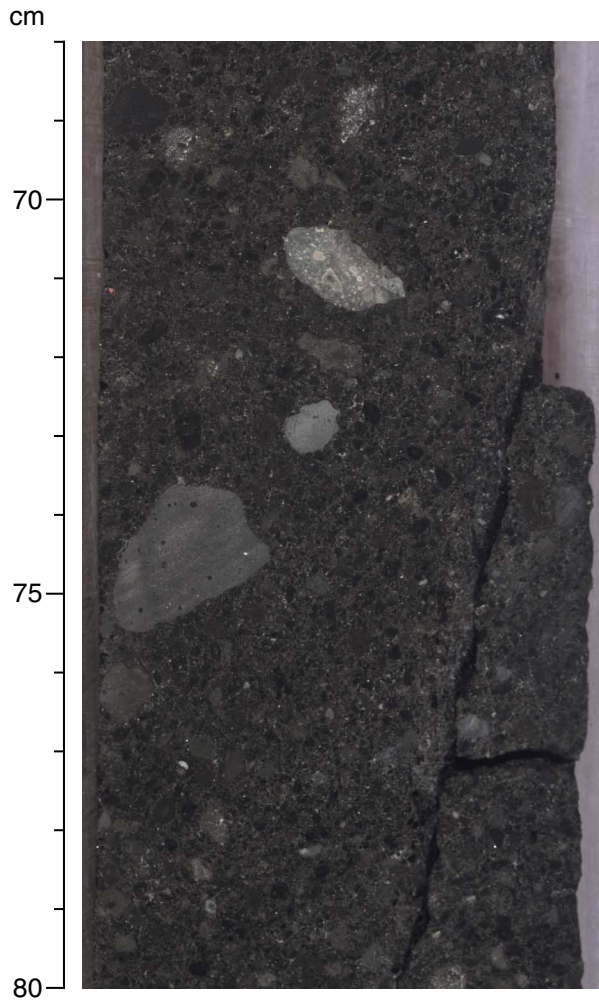


Figure F22. Schematic interpretation of the eruptive setting of the volcaniclastic rocks at Site 1184. These reworked pyroclastic deposits probably formed on top of a large seamount as it grew to within ~200 m of the sea surface. The presence of basalt at depth is conjectural. Letters A through F identify features for which we have evidence in the volcaniclastic rocks. A: The presence of blocky, nonvesicular glass shards suggests fragmentation of rapidly quenched magma in hydromagmatic eruptions under shallow water; abundant tachylite clasts in parts of the succession suggest that this process occurred in an environment that was at times subaerial. B: Accretionary and armored lapilli form in the atmosphere, in steam-rich columns of volcanic ash. C: The absence of blocks, bombs, or lapilli >20 mm suggests that the primary pyroclastic deposits formed several kilometers from the eruption center(s). D: Wood fragments found at the bases of four of the five subunits indicate proximity to land. E: Deposition or redeposition of the volcaniclastic material in a marine setting is indicated by the presence of nannofossils throughout the unit. F: Redeposition by turbidity currents is suggested by the presence of rip-up clasts and broken accretionary lapilli and by the absence of the layering that would be expected from material settling through water.

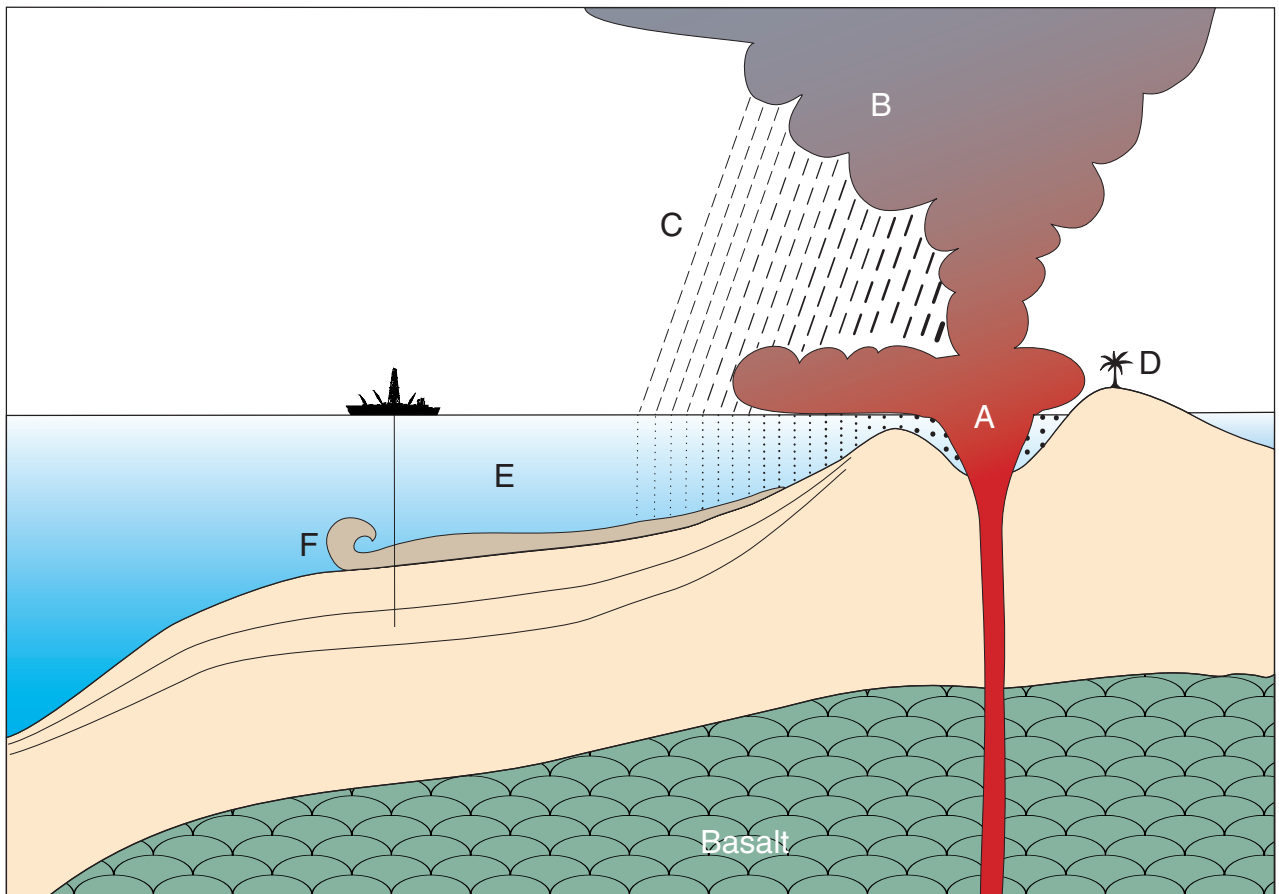


Figure F23. Lithic vitric tuff from Subunit IIE ([Sample 192-1184A-42R-1, 147–150 cm](#)). Rims of glass shards are altered to smectite (plane-polarized light; photomicrograph ID# 1184A_082).

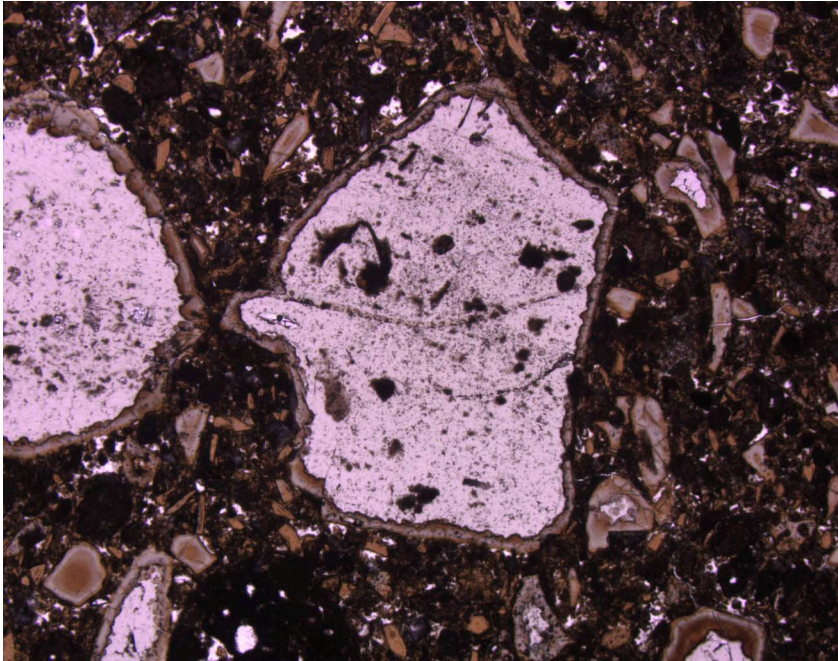


Figure F24. *Hakuho Maru* KH98-1 Leg 2, Line 401, multichannel seismic reflection profile across Site 1185 (see Fig. F2, p. 37, for location). Vertical exaggeration = ~4.2 at seafloor. UTC = Universal Time Coordinated.

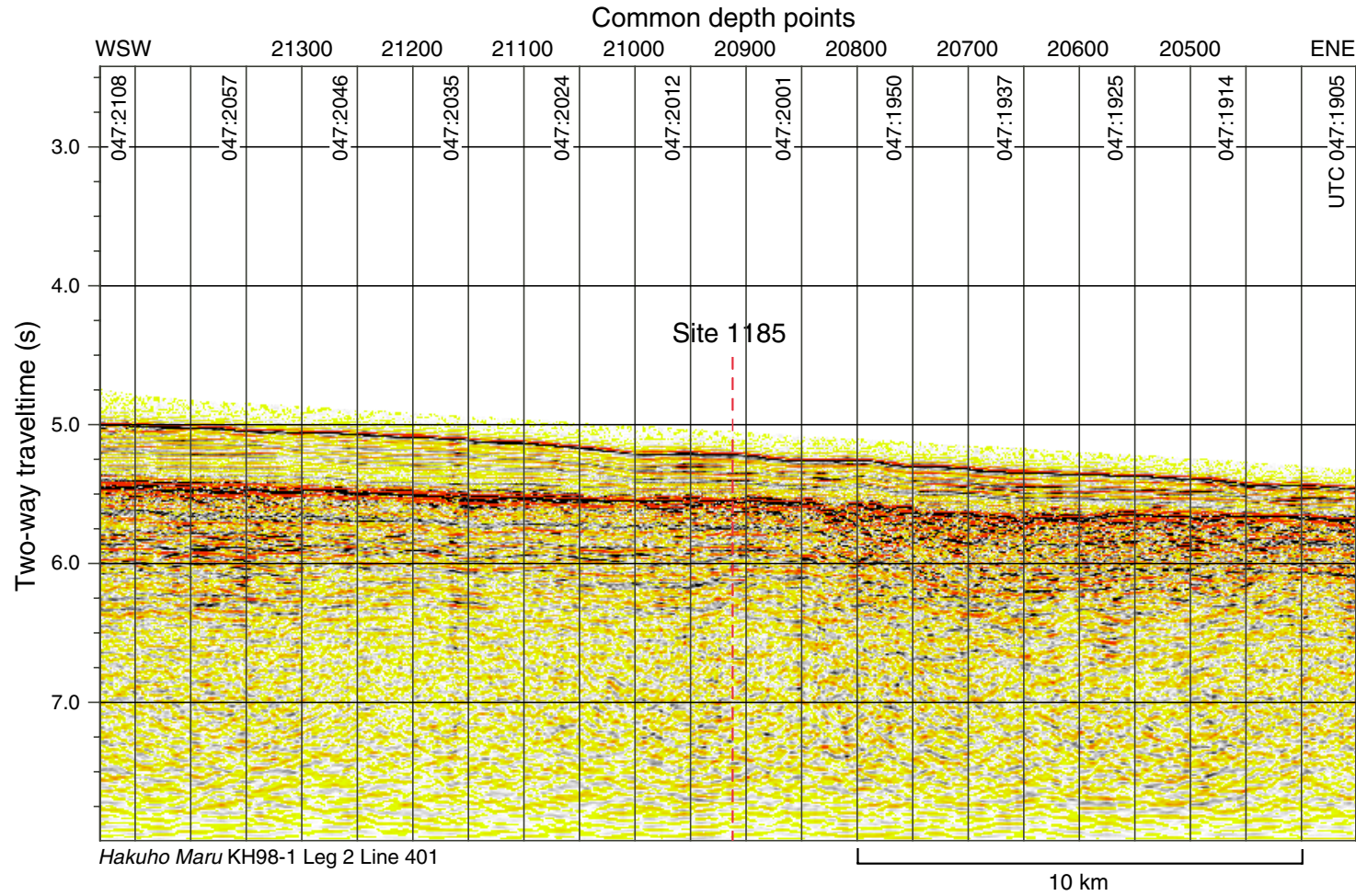


Figure F25. Hole 1185A log showing core recovery, lithostratigraphic divisions, schematic lithology, color reflectance, carbonate content, and components of sediments. In the color column, L = the total reflectance and indicates lighter shades to the right; a and b quantify the hue as chromaticity, where a = variation between green (low percent values) and red (high percent values) and b = variation between blue (low percent values) and yellow (high percent values) (Blum, 1997). Component percentages are from observation of smear slides and thin sections.

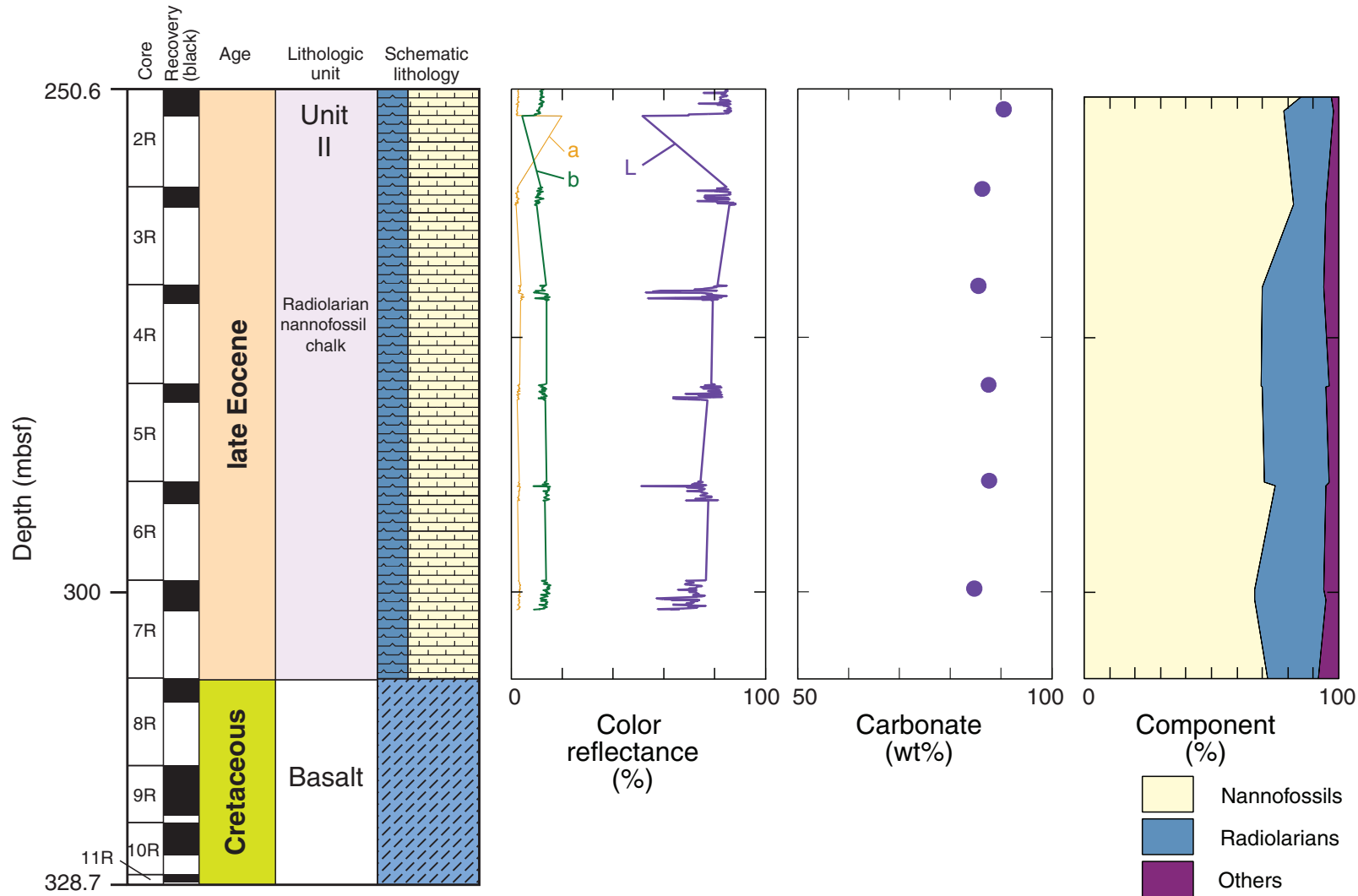


Figure F26. Lithologic log of basement units at Site 1185. The upper and lower groups of units in Hole 1185B are distinct in their petrography, composition, state of alteration, and biostratigraphic age.

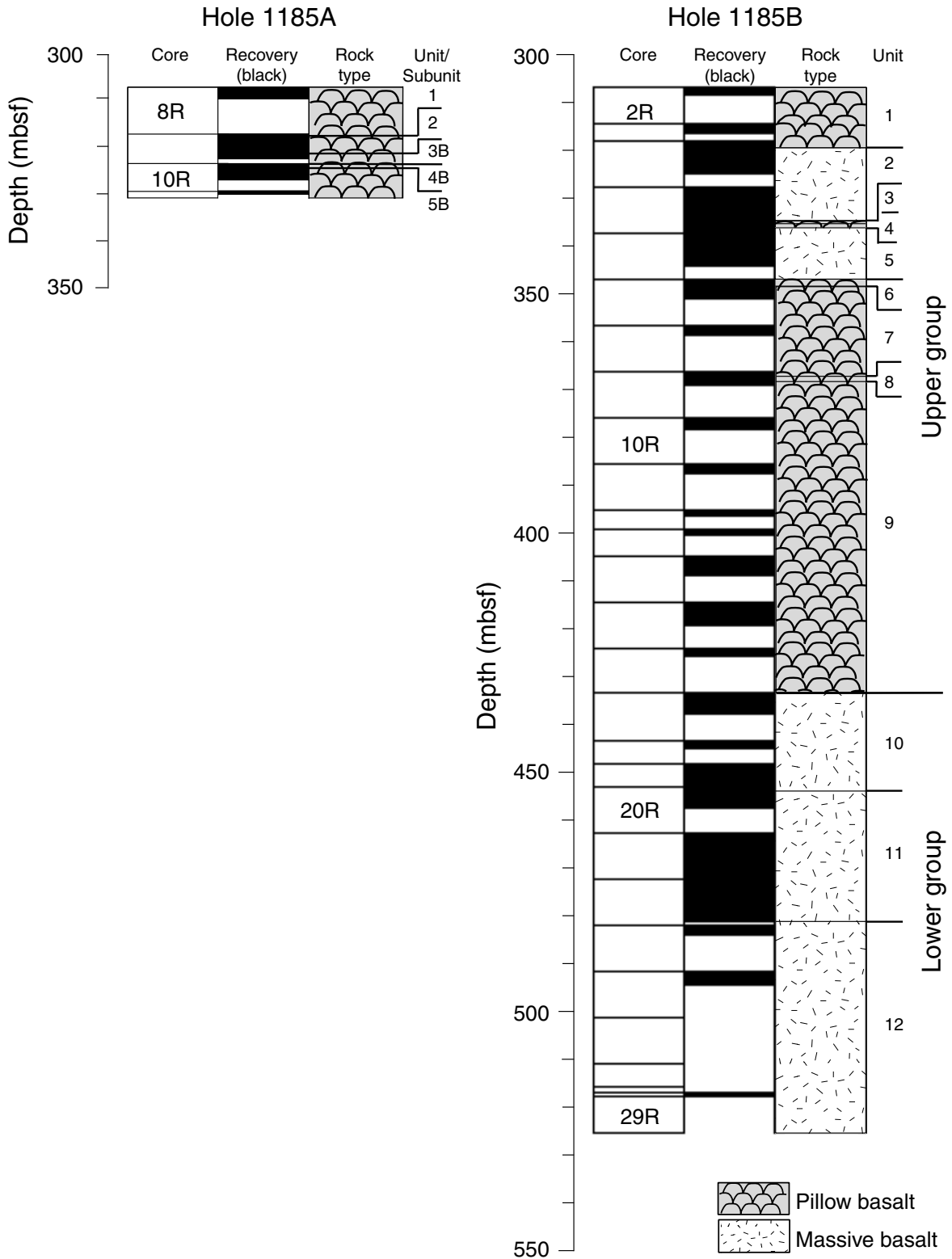
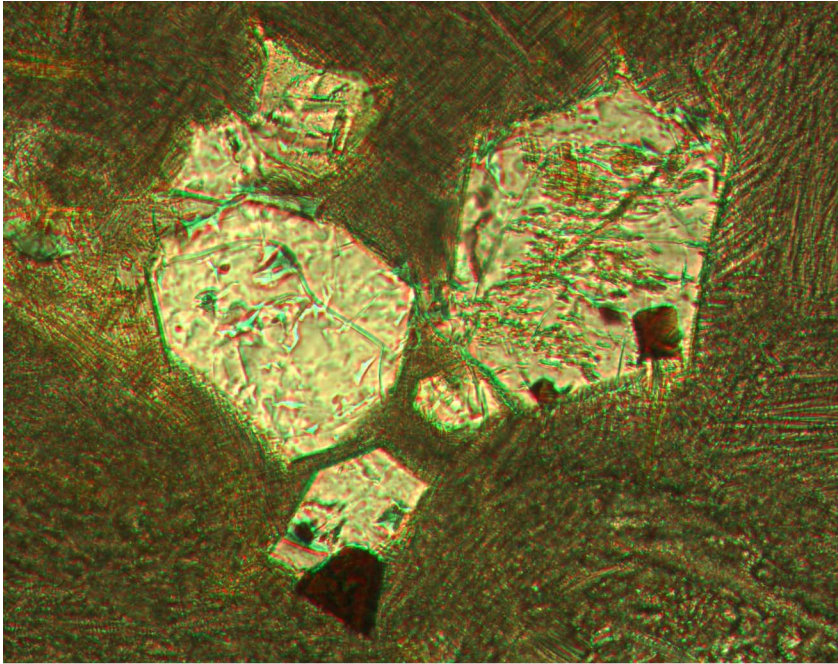


Figure F27. Photomicrograph of olivine phenocrysts and tiny octahedral crystals of chrome spinel in a quenched pillow margin (Sample 192-1185A-8R-1 [Piece 2, 15–18 cm]). The groundmass consists of glass with dendritic microlites (plane-polarized light; photomicrograph ID# 1185A_118).



0.1 mm

Figure F28. Close-up photograph showing spherulitic texture in an aphanitic pillow margin, basement Unit 1 (interval 192-1185B-3R-1, 54–63 cm). The spherulites are highlighted by alteration.

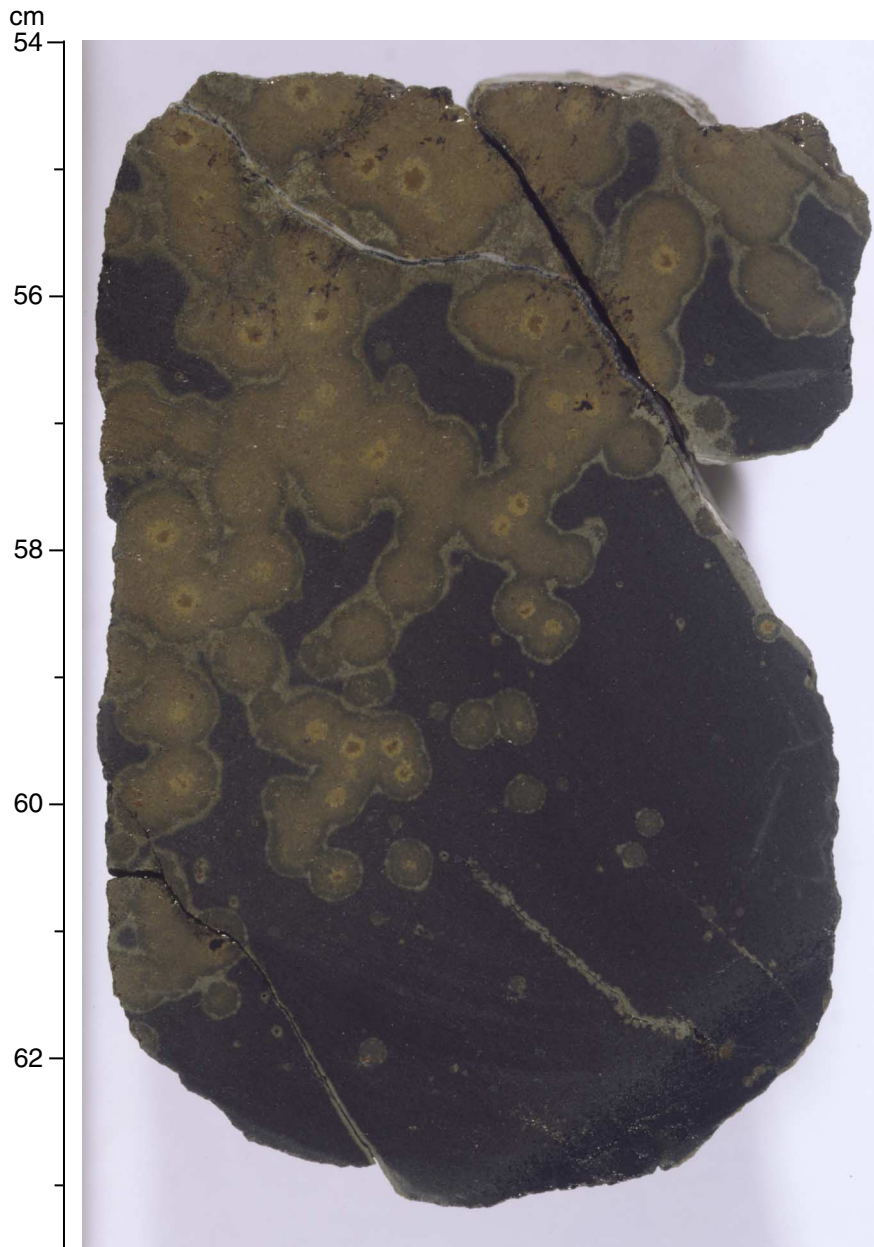


Figure F29. *Hakuho Maru* KH98-1 Leg 2, Line 403, multichannel seismic reflection profile across Site 1186 (see Fig. F2, p. 37). Vertical exaggeration = ~4.2 at seafloor. UTC = Universal Time Coordinated.

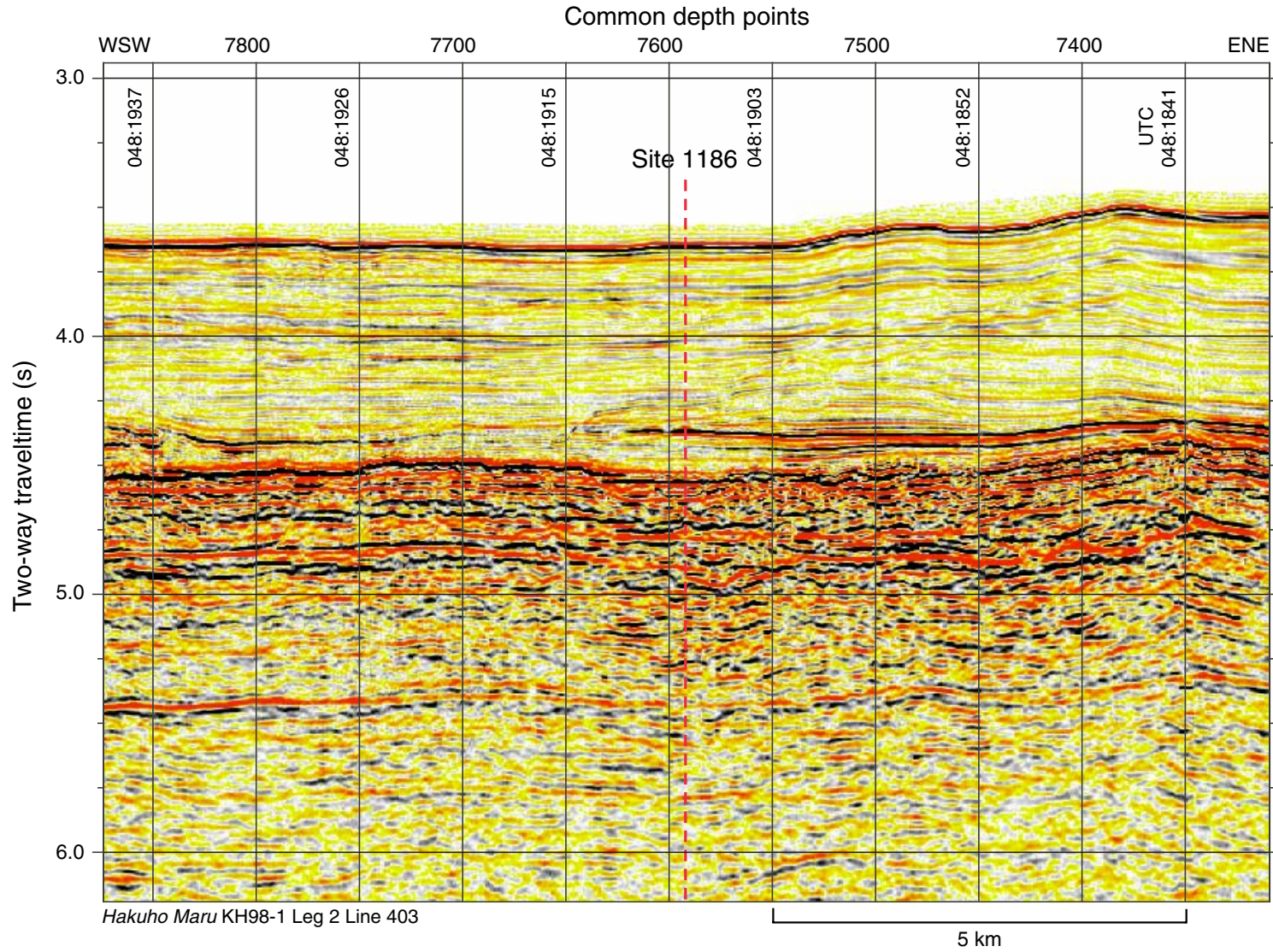


Figure F30. Lithologic log and selected properties of sediments at Site 1186. The interval from 0 to 697.4 mbsf was not cored. In the color column, L = the total reflectance and indicates lighter shades to the right; a and b quantify the hue as chromaticity, where a = the variation between green (low percent values) and red (high percent values) and b = the variation between blue (low percent values) and yellow (high percent values) (Blum, 1997). Higher values of magnetic susceptibility generally correlate with bands rich in volcanic ash (e.g., Core 192-1186A-13R) or with claystone (e.g., Core 192-1186A-26R and base of sedimentary sequence in Core 192-1186A-30R). Natural gamma radiation intensity is from the Formation MicroScanner tool run; medium-penetration resistivity and caliper of borehole diameter are from the geophysical tool run. ([Figure shown on next page.](#))

Figure F30. (Caption shown on previous page.)

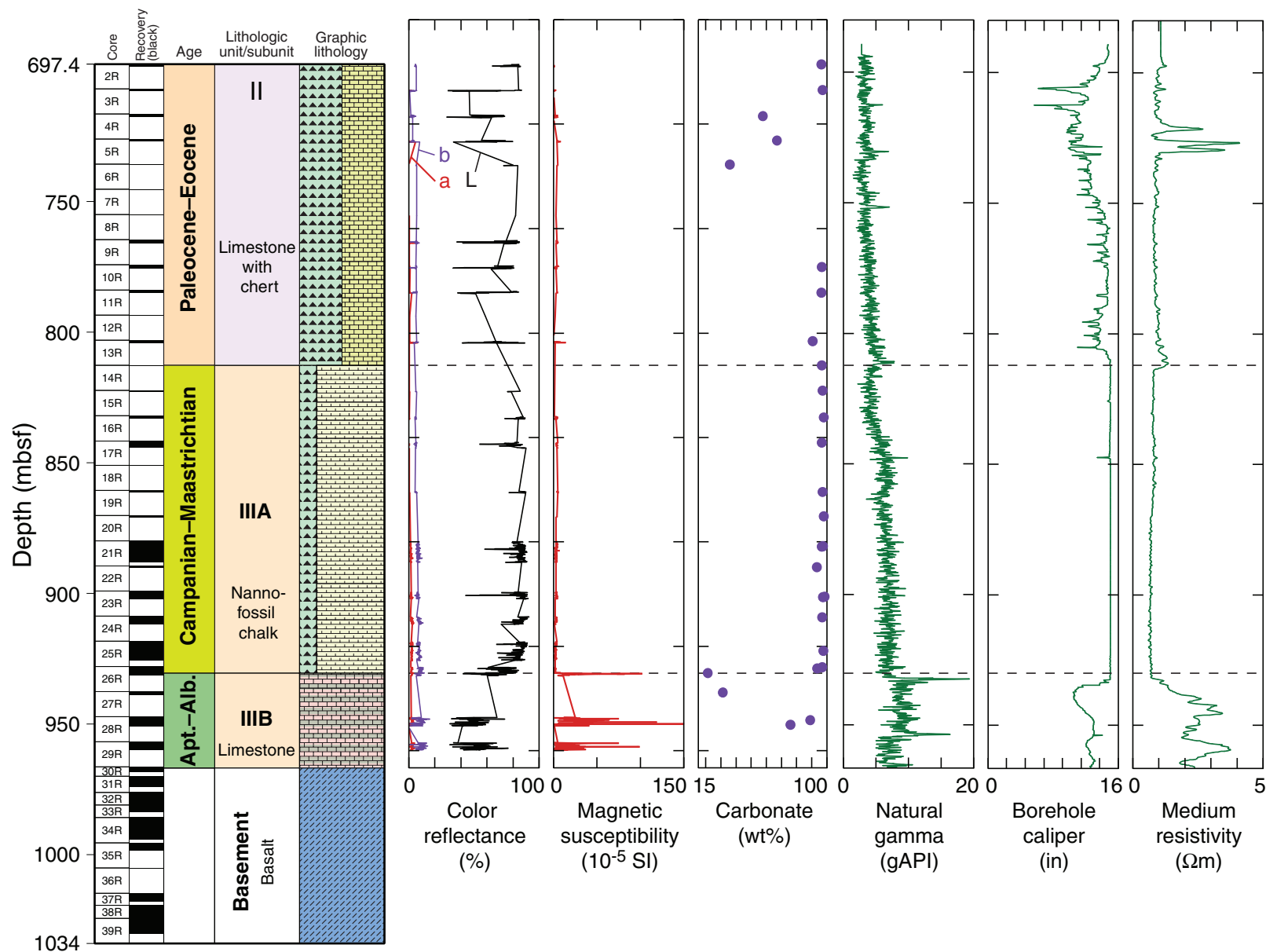


Figure F31. Close-up photograph of limestone conglomerate between lava flows in Hole 1186A (interval 192-1186A-32R-3, 65–93 cm).



Figure F32. Lithologic log of basement units at Site 1186 showing the distribution of plagioclase-rich xenoliths, glassy pillow rims, and vesicles. Dashed line = unit boundary. The location of the Unit 3/Unit 4 boundary is uncertain because of poor recovery. However, Formation MicroScanner logging tool images suggest that the top of Unit 4 consists of ~9 m of pillow basalt.

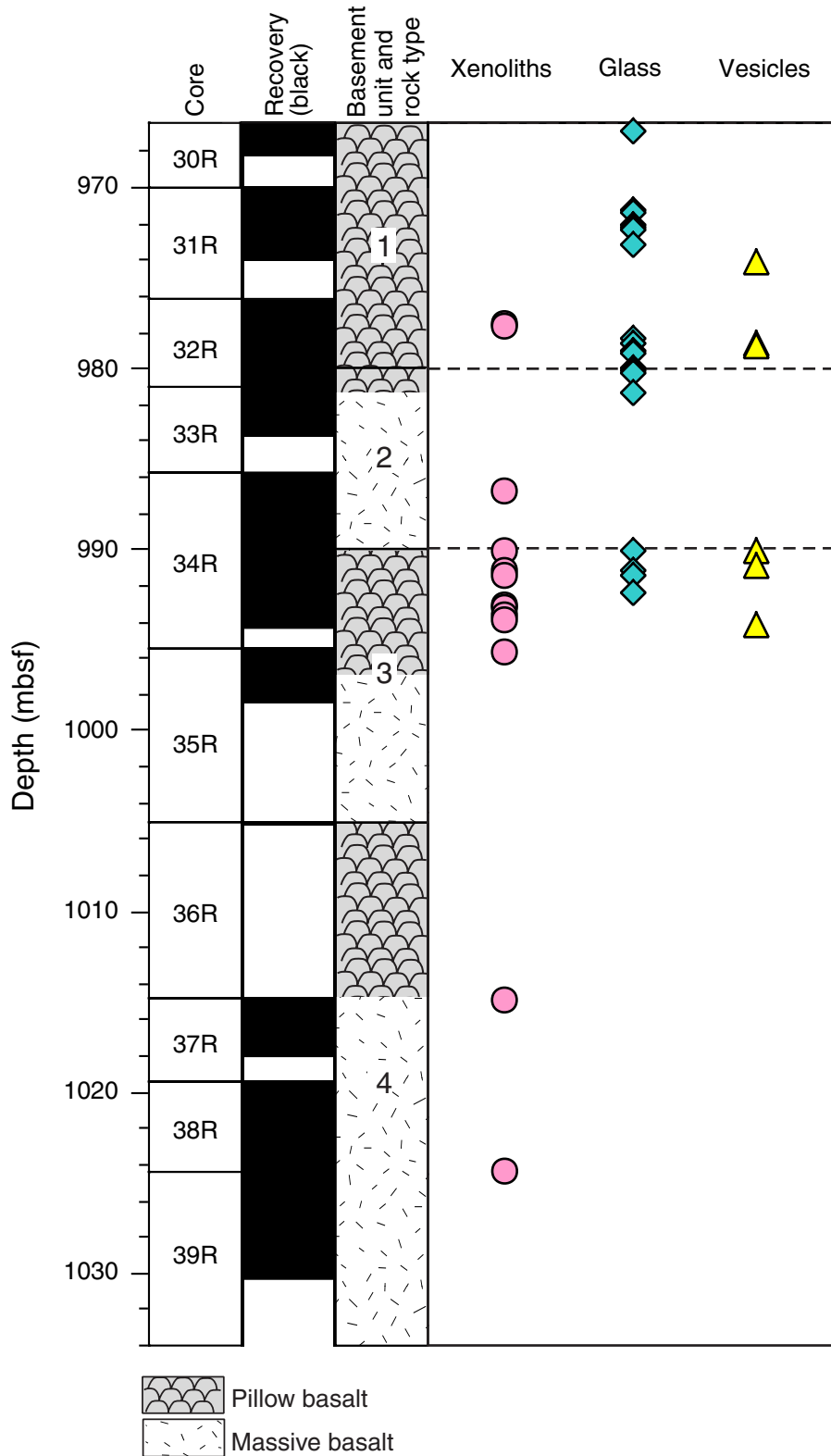


Figure F33. Photomicrograph of plagioclase laths and sprays of clinopyroxene crystals in basalt from the interior of massive flow Unit 2 (see Fig. F32, p. 68) (Sample 192-1186A-34R-2, 143-146 cm) (crossed polars; photomicrograph ID# 1186A_247).

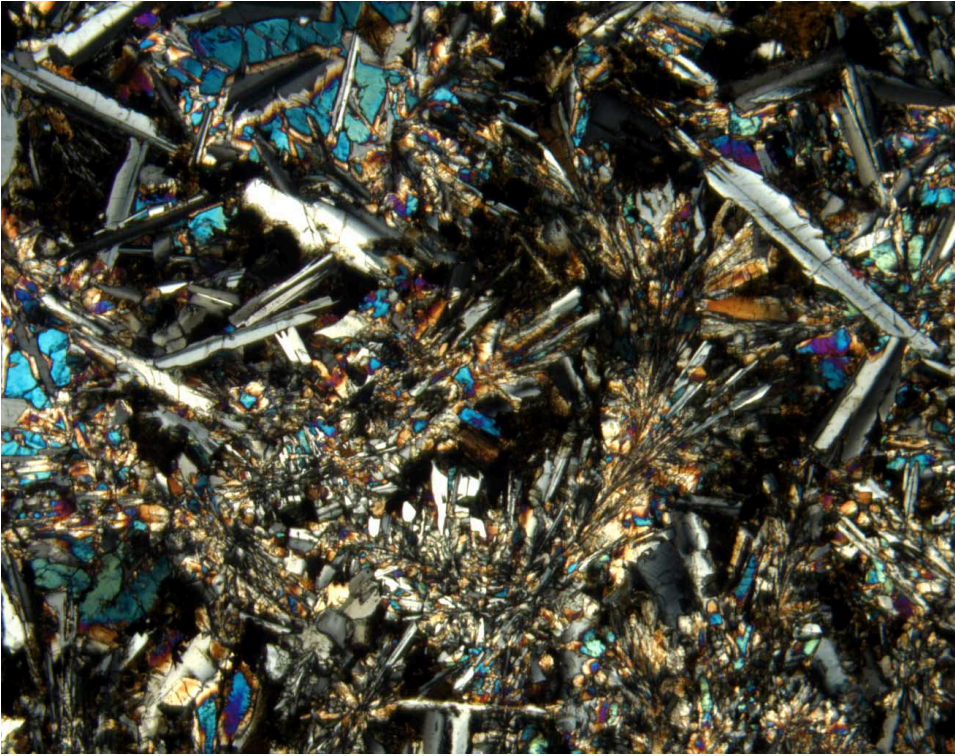
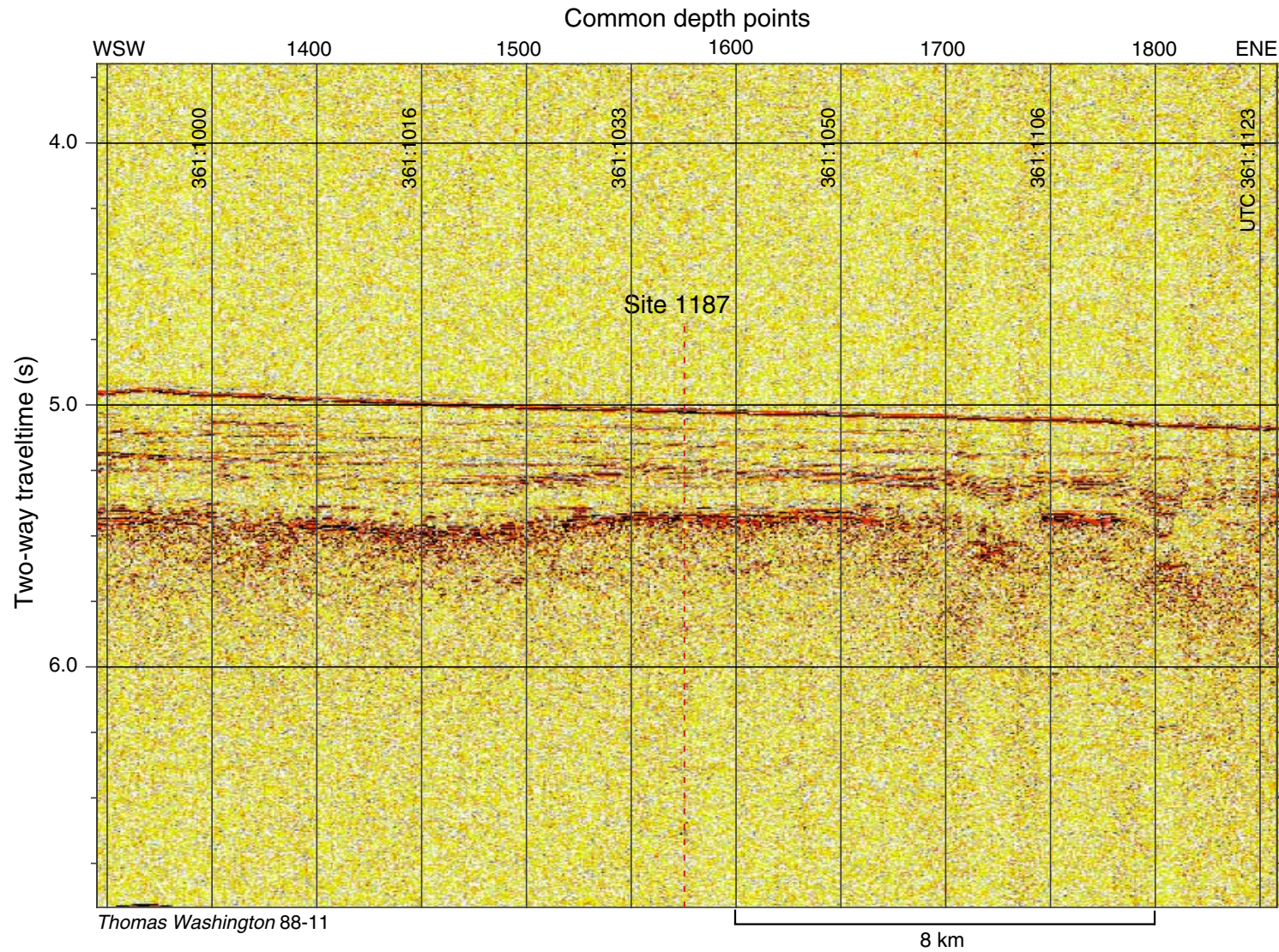


Figure F34. *Thomas Washington* 88-11 single-channel seismic reflection profile across Site 1187 (see Fig. F2, p. 37, for location). Vertical exaggeration = ~6.67 at seafloor. UTC = Universal Time Coordinated.



Thomas Washington 88-11

8 km

Figure F35. Lithologic log of basement units at Site 1187 showing the thickness of individual cooling units defined by the presence of glassy or aphanitic margins. Cooling units <1.5 m thick are probably pillows, but the four units that are 2–3 m thick could be thin massive flows.

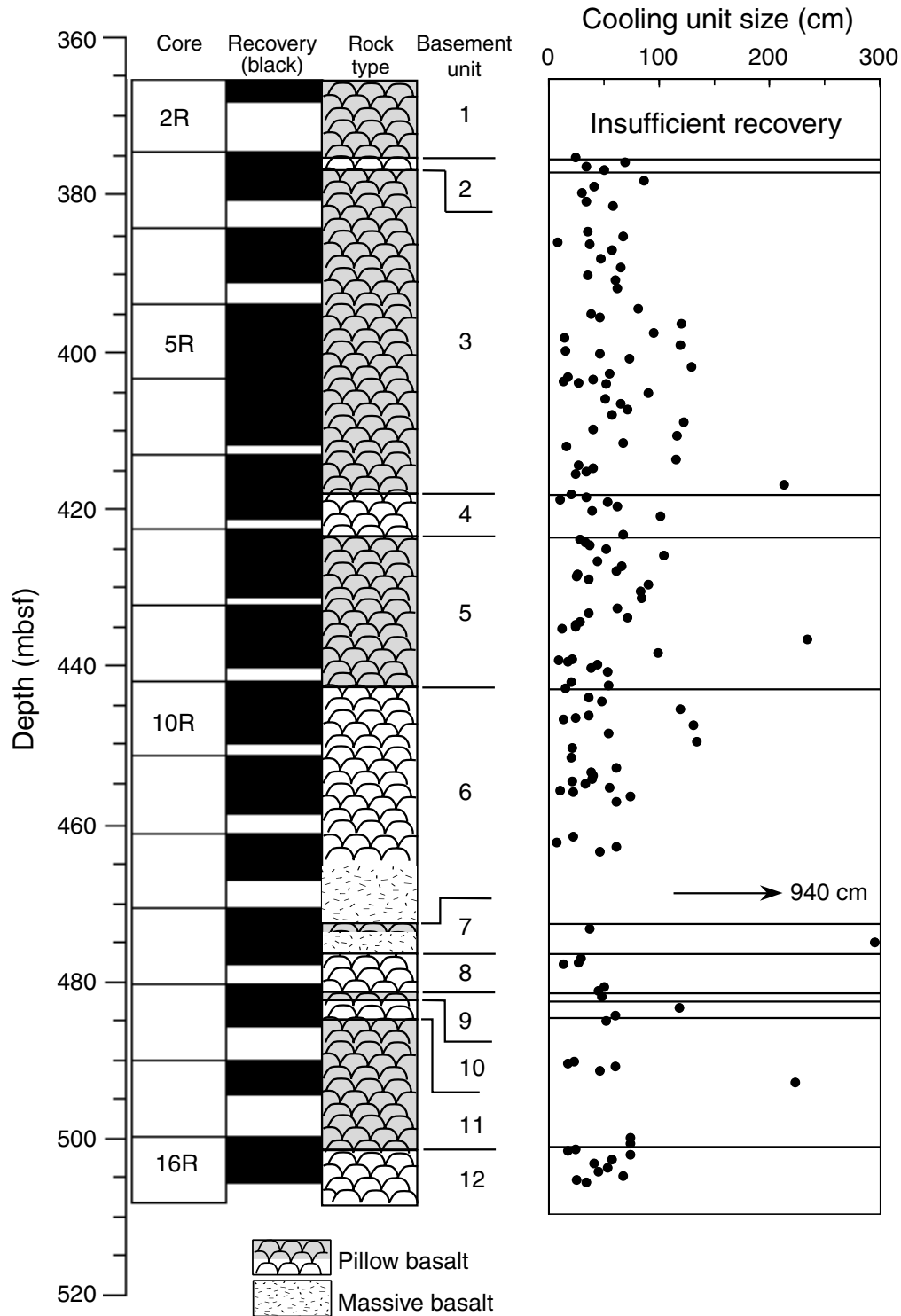


Figure F36. Stratigraphic sections drilled during Leg 192 and at the three previous DSDP and ODP Ontong Java Plateau basement sites. Seven sites are arranged on a transect from the crest of the main plateau (Site 1183) eastward to the plateau rim (Site 1185) and then north and northwestward to Site 807 on the northern flank. Site 1184 lies off the transect, 586 km to the southeast of Site 1185. Basement ages for the previously drilled sites are from ^{40}Ar - ^{39}Ar dating of basalt (Mahoney et al., 1993). For the Leg 192 sites, basement ages are estimated from biostratigraphic evidence.

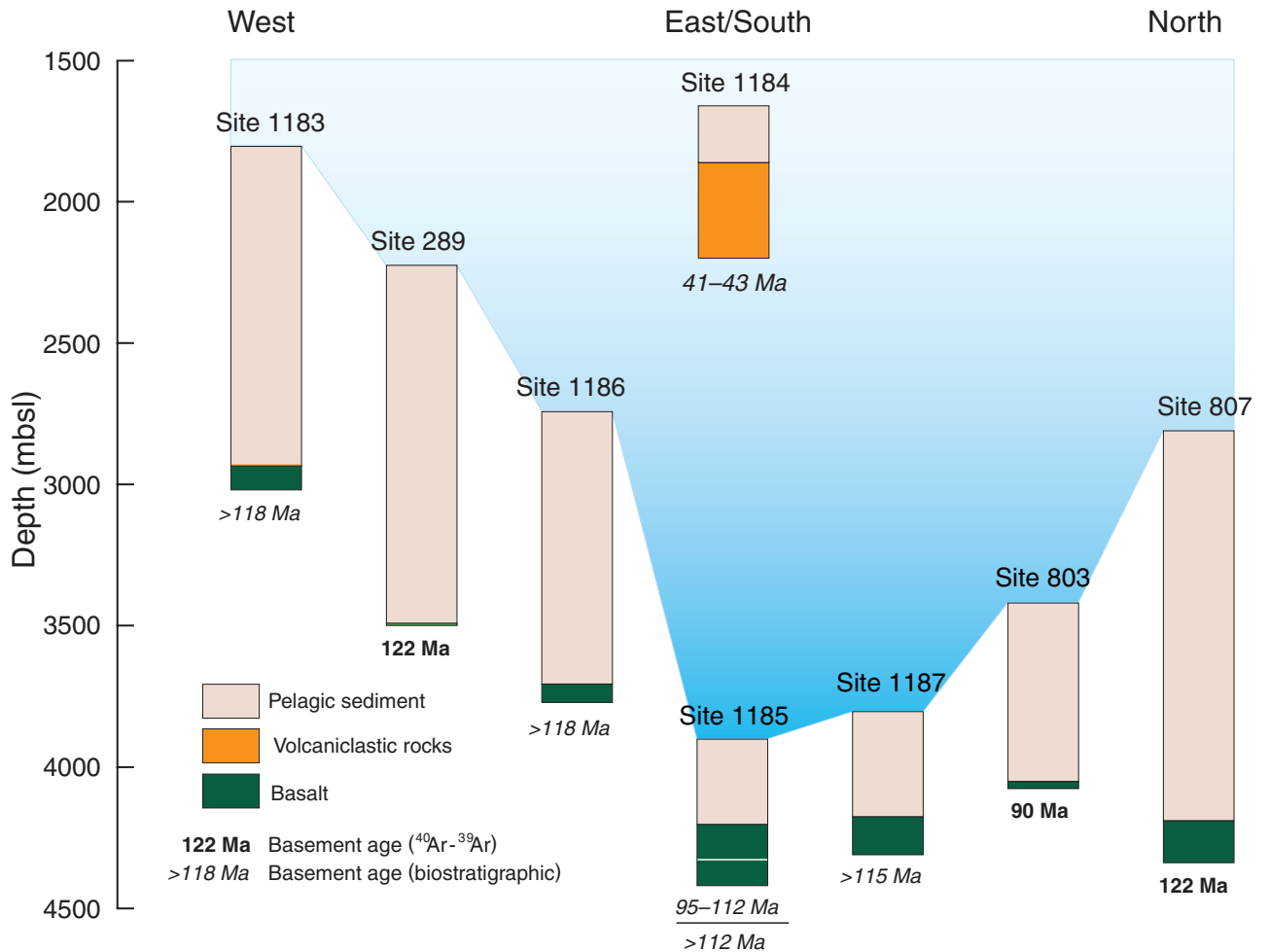


Figure F37. Basement sections drilled during Leg 192 and at the three previous DSDP and ODP Ontong Java Plateau basement sites (as in Fig. F36, p. 72), with water depths corrected to remove the effect of sediment loading. The corrected basement depth (D_c) is obtained from the equation of Crough (1983): $D_c = d_w + t_s (\rho_s - \rho_m) / (\rho_w - \rho_m)$, in which d_w is water depth in meters, t_s is sediment thickness in meters, ρ_s is average sediment density (1.90 g/cm³), ρ_m is upper mantle density (3.22 g/cm³), and ρ_w is seawater density (1.03 g/cm³).

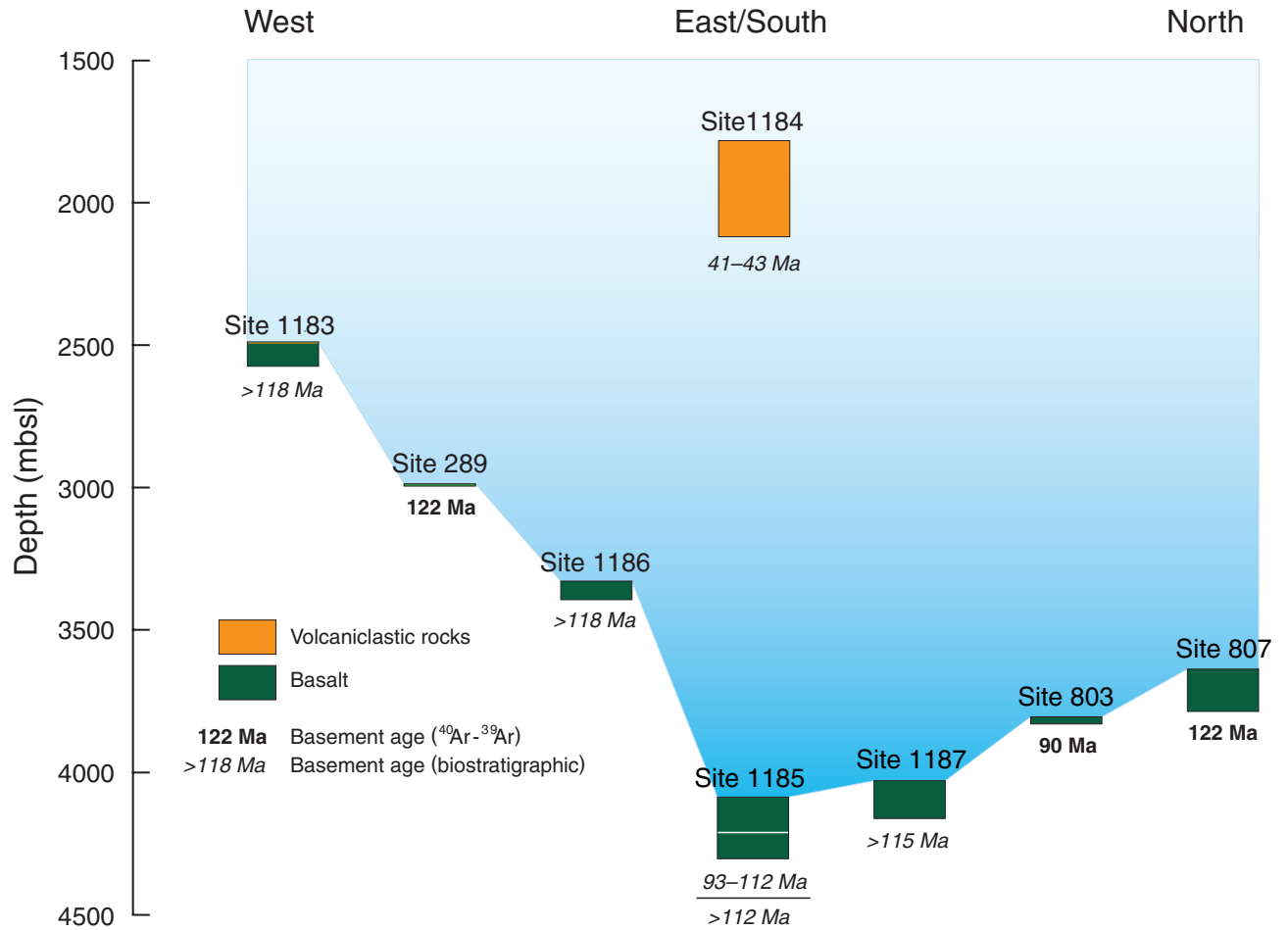


Table T1. Hole summary for Leg 192.

Hole	Latitude	Longitude	Water depth (m)	Sediment thickness (m)	Sediment cored (m)	Sediment recovery (m)	Basement depth (mbsf)	Basement penetration (m)	Basement recovery (m)	Total penetration (m)	Oldest sediment (Ma)*
1183A	1°10.6189'S	157°0.8988'E	1804.7	1130.37	503.1	216.50	1130.37	80.7	44.20	1211.1	118
1184A	5°0.6653'S	164°13.9771'E	1661.5	201.10	66.7	49.80	201.10	337.7	278.90	538.8	41-43
1185A	0°21.4560'S	161°40.0619'E	3898.9	312.0	57.9	14.08	308.54/312.0 [†]	16.7	11.17	328.7	93-112
1185B	0°21.4559'S	161°40.0511'E	3898.9	309.51	<7.5	1.51	309.51	216.6	90.68	526.1	112
1186A	0°40.7873'S	159°50.6519'E	2728.7	968.6	271.2	49.33	966.82/968.6 [‡]	65.4	39.36	1034.0	118
1187A	0°56.5518'N	161°27.0784'E	3803.6	372.5	7.0	1.47	366.97/372.5 [†]	135.8	100.87	508.3	115

Notes: * = timescales of Berggren et al. (1995) and Gradstein et al. (1995). † = depths of basement contact noted by the driller; all other depths are curated depths. ‡ = driller noted basement at 969 m; however, 1.4 m of basalt was recovered from a cored interval that bottomed at 970 mbsf, yielding a basement depth of 968.6 mbsf. Depth, penetration, and recovery of volcaniclastic rock (Unit II) at Hole 1184A are given in the respective "basement" columns.

Table T2. Volcaniclastic facies in Unit II, Site 1184.

Facies	Sedimentary structure	Grain size	Sorting	Thickness	Lithology	Interpretation
1	Massive with some subtle gradations in grain size; includes thin layers of very coarse sand to granules	Very fine sand to pebble	Very poor	20 cm to >10 m	Lithic vitric lapilli tuff	Muddy debris flow deposit
2	Massive, grain size oscillations	Coarse sand to pebble	Very poor	2-30 m	Lithic vitric lapilli tuff to lapillistone	Stony debris flow deposit
3	Inclined granule lamination	Medium sand to granule	Poor	2-5 m	Lithic vitric lapilli tuff	Current-reworked deposit
4	Grading, parallel lamination, traction carpet	Fine to very coarse sand	Moderate	5-200 cm	Lithic vitric tuff	Turbidite
5	Massive, clast supported	Granule to pebble	Moderate	20 cm to 10 m	Tachylitic lapillistone	Quenched subaerial eruptive products
6	Chaotic bedding	Fine sand to pebble	Very poor	>3 m	Lithic vitric lapilli tuff	Slump deposit
7	Inverse grading, mud drape	Clay, very fine to coarse sand	Good	~20 cm	Lithic vitric tuff and mudstone	Fluvial deposit?
8	Massive	Silt to very fine sand	Good	5 cm	Lithic vitric tuff	Air-fall ash